

Regulation of receptor kinase-mediated immune signalling by dynamic phosphorylation

Daniel Couto

A thesis submitted to the University of East Anglia for the degree of Doctor of Philosophy

The Sainsbury Laboratory

Norwich Research Park

Norwich, UK

December 2015

This copy of the thesis has been supplied on condition that anyone who consults it is understood to recognise that its copyright rests with the author and that use of any information derived there from must be in accordance with current UK Copyright Law. In addition, any quotation or extract must include full attribution.

Abstract

Plants recognize pathogen-associated molecular patterns (PAMPs) via cell surface-localized pattern recognition receptors (PRRs), initiating a broad-spectrum defense response against pathogens, known as PRR-triggered immunity (PTI). However, immunity comes at a cost; and immune responses need to be tightly regulated. How PTI signalling is negatively regulated in plants is not fully understood. PRRs are present at the plasma membrane in dynamic kinase complexes that heavily rely on trans-phosphorylation to initiate signaling. The *Arabidopsis* cytoplasmic kinase BIK1 associates with different PRRs and plays a central role in the activation of downstream immune signaling.

In this study, we identify the protein phosphatase PP2C38 as a negative regulator of BIK1 activity and BIK1-mediated immunity. PP2C38 dynamically associates with BIK1, as well as with the PRRs FLS2 and EFR, but not with the regulatory receptor kinase (RK) BAK1. PP2C38 regulates PAMP-induced BIK1 phosphorylation and impairs the phosphorylation of the NADPH oxidase RBOHD by BIK1, leading to reduced oxidative burst and stomatal immunity. Notably, upon PAMP perception, PP2C38 is phosphorylated on serine 77, most likely by BIK1, and dissociates from the PRR-BIK1 complex. We suggest that this mechanism relieves the negative regulation imposed by PP2C38 to enable efficient BIK1 activation. This study uncovers an important regulatory mechanism of this central immune component, and extends our knowledge on how plant immunity is appropriately controlled.

Table of Contents

Abstract	2
List of Tables	6
List of Figures	7
List of publications arising from the work in this thesis	9
Acknowledgements	10
Abbreviations	11
Chapter 1: Regulation of surface-mediated innate immunity in plants	15
1.1. Introduction	15
1.2. Formation and activation of PRR complexes.....	17
1.2.1. Recruitment of regulatory RKs	20
1.2.2. Recruitment of RLCKs	23
1.3. Downstream events and signalling pathways	24
1.4. Negative regulation of RK-mediated immunity	27
1.4.1. Regulation of PRR complex formation by pseudokinases	30
1.4.2. Regulation of PRR complex phosphorylation status.....	31
1.4.3. Regulation of the PRR complex by protein turn-over.....	35
1.4.4. Negative regulation of MAPK signalling cascades.....	36
1.4.5. Negative regulation at the transcriptional level	38
1.4.6. Negative regulation by hormones and endogenous peptides.....	40
1.5. Manipulation of plant immunity by bacterial effectors	43
1.6. Thesis objectives and overview	45
Chapter 2: Material and Methods	47
2.1. Plant material and growth conditions	47
2.1.1. <i>Arabidopsis thaliana</i> lines	47
2.1.2. Plants grown on soil	47
2.1.3. Plants grown on plates	48
2.1.4. Plants grown on liquid media	48
2.1.5. <i>Arabidopsis</i> seed sterilization.....	48
2.1.6. Generating stable transgenic <i>Arabidopsis</i> lines.....	48
2.1.7. Crossing of <i>Arabidopsis</i> plants.....	48
2.2. Bacterial Strains	49
2.3. Culture media and reagents.....	49
2.3.1. Reagents and elicitors.....	49
2.3.2. Culture media recipes	49
2.3.3. Antibiotics	50
2.4. Biological assays	50

2.4.1. PAMP-induced ROS assay	50
2.4.2. Bacterial spray infection	50
2.4.3. Stomatal closure.....	51
2.5. Molecular biology	51
2.5.1. DNA Methods	51
2.5.2. PCR methods	53
2.5.3. RNA methods	56
2.5.4. Molecular cloning	58
2.6. Protein work	61
2.6.1. Protein separation by polyacrylamide gel electrophoresis.....	61
2.6.2. Wet blotting	62
2.6.3. Immunodetection.....	62
2.6.4. Coomassie brilliant blue (CBB) staining.....	63
2.6.5. Expression of recombinant proteins in <i>N. benthamiana</i>	63
2.6.6. Isolation and transfection of <i>Arabidopsis</i> protoplasts.....	64
2.6.7. Protein extraction from <i>N. benthamiana</i> and <i>Arabidopsis</i>	65
2.6.8. Protein immunoprecipitation.....	66
2.6.9. α -GFP and α -HA immunoprecipitation	66
2.6.10. α -FLAG immunoprecipitation	66
2.6.11. Submission of immunoprecipitated protein samples for mass spectrometry analysis.....	67
2.6.12. Identification of phosphosites by mass spectrometry	67
2.6.13. Expression of GST- and MBP-tagged recombinant of proteins in <i>E. coli</i>	67
2.6.14. Purification of GST-tagged proteins	68
2.6.15. Purification of MBP-tagged proteins.....	68
2.7. Enzymatic assays	69
2.7.1. Phosphatase treatment	69
2.7.2. PP2C activity assays.....	70
2.7.3. Trans-phosphorylation assays	70
2.7.4. IP-kinase assays	70
2.8. Cell biological assays.....	71
2.9. Yeast two-hybrid screen	71
2.10. Statistical analysis.....	72

Chapter 3: The *Arabidopsis* protein phosphatase PP2C38 controls the phosphorylation status of the central immune kinase BIK1 73

3.1. Prologue.....	73
3.2. Results	74
3.2.1. PP2C38 associates dynamically with the EFR-BIK1 and FLS2-BIK1 complexes	74
3.2.2. PP2C38 is an active PM-localized phosphatase	79
3.2.3. PP2C38 regulates BIK1 phosphostatus and activity.....	83

Chapter 4: PP2C38 is a negative regulator of PRR-triggered immunity 87

4.1. Prologue.....	87
4.2. Results	88
Chapter 5: Phosphorylation of PP2C38 on serine 77 leads to its dissociation from BIK1	95
5.1. Prologue.....	95
5.2. Results	96
Chapter 6: Discussion	103
6.1. PP2C38 is a novel regulator of BIK1 activity	103
6.2. Multi-level regulation of PRR complexes	105
6.3. PP2C38 and BIK1: a ‘phospho-standoff’	107
Chapter 7: Conclusions and outlook	110
References	112

List of Tables

Table 2.1. List of <i>Arabidopsis thaliana</i> lines.	47
Table 2.2. Bacterial strains.	49
Table 2.3. Program for cloning and genotyping PCRs.	53
Table 2.4: Primers used in this study.	54
Table 2.5. Program for colony PCR.	55
Table 2.6. PCR program for site-directed mutagenesis.....	56
Table 2.7. Program used for qRT-PCR.	57
Table 2.8. Vector backbones used in this study.	58
Table 2.9. Constructs used in this study.	59
Table 2.10. Antibodies used in this study.	63
Table 3.1. List of proteins interacting with EFR-CD in Y2H screen.....	75

List of Figures

Figure 1.1. Recruitment of regulatory RKs and RLCKs by PRRs in <i>Arabidopsis</i> and rice.....	19
Figure 1.2. Negative regulation of PTI signalling by a multi-layered system.....	29
Figure 1.3. Negative regulation at the PRR complex level.	34
Figure 3.1. PP2C38 associates dynamically with EFR and FLS2 <i>in planta</i>	76
Figure 3.2. PP2C58 does not associate with EFR <i>in planta</i>	76
Figure 3.3. Characterization of <i>PP2C38</i> over-expression and mutant lines.....	77
Figure 3.4. PP2C38 dynamically associates with FLS2 in <i>Arabidopsis</i> plants.	78
Figure 3.5. PP2C38 dynamically associates with BIK1 but not BAK1... ..	79
Figure 3.6. Phylogenetic analysis of <i>Arabidopsis</i> PP2C clade D and PP2C38 orthologs.....	80
Figure 3.7. PP2C38 is an active PP2C.	82
Figure. 3.8. PP2C38 localizes to the plasma membrane.....	83
Figure 3.9. PP2C38 does not regulate EFR activation.	84
Figure 3.10. PP2C38 regulates BIK1 activation.	85
Figure 4.1 Overexpression of <i>PP2C38</i> impairs the PAMP-induced ROS burst.	88
Figure 4.2. PAMP-induced ROS burst on <i>PP2C38</i> over-expression and mutant lines.	89
Figure 4.3. PP2C38 negatively regulates stomatal immunity.	91
Figure 4.4. Characterization of PP2C48 mutant lines.....	92
Figure 4.5. Loss of <i>PP2C38</i> and <i>PP2C48</i> enhances PAMP-induced ROS production.....	93
Figure 4.6. PP2C38 negatively regulates chitin-triggered ROS burst.	93
Figure 5.1. PAMP perception induces PP2C38 band shift.	96
Figure 5.2. PP2C38 band shift is caused by phosphorylation.	97
Figure 5.3. PP2C38 is phosphorylated on S77 <i>in vivo</i>	98

Figure 5.4. BIK1 over-expression results in constitutive PP2C38 phosphorylation.	98
Figure 5.5. BIK1 phosphorylates PP2C38 on S77.....	100
Figure 5.6. S77 phosphorylation is required for PAMP-induced PP2C38-BIK1 complex dissociation.....	101
Figure 5.7. EFR and FLS2 kinase activities are not required for PAMP-induced dissociation of PP2C38.....	102
Figure 6.1. Model: PP2C38 dephosphorylates BIK1 to attenuate innate immune signaling.	109

List of publications arising from the work in this thesis

Chapter 1 will be the basis for the following manuscript:

Couto, D. and Zipfel, C. Regulation of surface-mediated innate immunity in plants.
Nat. Rev. Immunol. *In preparation.*

Chapters 3, 4 and 5 have been compiled into the following manuscript:

Couto D.*, Niebergall R.*, Liang, X., Bücherl, C. A., Sklenar, J., Macho, A. P.,
Ntoukakis, V., Altenbach, D., Robatzek, S., Uhrig, J., Menke, F., Zhou, J. M. and
Zipfel, C. The Arabidopsis protein phosphatase PP2C38 negatively regulates the
central immune kinase BIK1. *Under revision in PLoS Pathogens.*

*Co-first authors

Acknowledgements

I am extremely grateful to my supervisor Cyril Zipfel for accepting me in his lab and giving me the opportunity to pursue my PhD. Thank you for all the advice, knowledge and guidance, and perhaps most importantly, thank you for giving me the freedom and pushing me to find my own way.

I would like to thank the Portuguese government and Fundação para a Ciência e Tecnologia (FCT) for funding my PhD.

I would like to thank Lars Østergaard, my secondary supervisor, for his advice and support during my PhD.

Thank you Cécile Segonzac and Alberto Macho for being my lab mentors, I've learnt so much from you!

Thank you Xiangxiu and Jian-Min Zhou for such a fruitful collaboration.

Thank you to all my lab mates, those who have already left and those who are still around. You make our lab such a fun place to work! Some of you have had to put up with me just a little bit too much: Yasu, Cécile, Alberto, Rosa, Jacqui, Christoph, Nick, Martin, Freddy, Artemis, Jorge, Diew, Shushu, Susanne, Roda, and of course, Lena. You have helped me countless times and taught me a lot! Thank you!

My office mates (and the occasional visitors): Andy, Will, Jan, Seb, Laura, Matt, Simon, Jelle, Moira, Rooney... Thank you for all the good times!

Thanks to the TSL support teams and JIC horticultural services. Thanks Tim!

Thank you Porto for always being there despite the distance, and giving me a reason to carry on.

Thank you Humberto. Thank you Manuela.

Thank you SuperBock, I couldn't do it without you.

Thank you Henry for making me dream when life becomes too serious.

Thank you Sara for your love, patience and support.

Thank you to my parents, my sister and my uncles for their unconditional love and support. Without you I wouldn't be here.

Abbreviations

ABA	Abcisic acid
AHA	Arabidopsis H ⁺ -ATPase
Ala (A)	Alanine
Asn (N)	Asparagine
Asp (D)	Aspartate
ASR3	Arabidopsis SH4-related3
ATP	Adenosine triphosphate (
Avr	Avirulence protein/ gene
BAK1	BR11-associated kinase 1
BIK1	Botrytis-induced kinase 1
BIR	BAK1-interacting RLK
BKI1	Bri1 kinase inhibitor 1
BKK1	BAK1-like 1
BL	Brassinolide
BON	BONZAI
BR	Brassinosteroid
BR11	Brassinosteroid insensitive 1
BSK1	BR-signaling kinase 1
BZR1	Brassinazole-resistant 1
CBB	Coomassie Brilliant Blue
CC	Coiled-coil
CD	Cytoplasmic domain
CDKC	Cyclin-dependent kinase C
CDPK	Calcium-dependent protein kinase
CeBIP	Chitin elicitor binding protein
CERK1	Chitin elicitor binding protein 1
CK	Cytokinin
COR	Coronatin
CTD	C-terminal domain
DCL	Dicer-like protein
DNA	Deoxyribonucleic acid
dNTPs	Deoxynucleotide
dpi	Days post-inoculation
EDS	Enhanced disease susceptibility
EDTA	Ethylenediaminetetraacetic acid
EFR	EF-Tu receptor
EF-Tu	Elongation factor Tu
EGF	Epidermal growth factor
EGTA	Ethylene glycol tetraacetic acid
EIL	EIN3-like
EIN	ET-insensitive
ERF	ET response factor
ET	Ethylene
EV	Empty vector
FLS2	Flagellin-sensing 2

FRK1	Flg22-induced kinase 1
GA	Gibberellin
GFP	Green fluorescent protein
HBI1	Homolog of BEE2 interacting with IBH 1
Hop	Hrp outer protein
Hpa	Hyaloperonospora arabidopsidis
HR	Hypersensitive response
IL	Interleukin
IP	Immunoprecipitation
IRAK	IL-1-associated receptor kinase
JA	Jasmonic acid
JAZ	Jasmonate ZIM domain
KAPP	Kinase associated protein phosphatase
LPS	Lipopolysaccharide
LRR	Leucine-rich repeat
LYK	Lysin motif RLK
LYP	Lysin motif-containing proteins
Lys (K)	Lysine
LysM	Lysine motif
MAPK	Mitogen-activated protein kinase
MBP	Maltose binding protein
MES	2-(N-morpholino)ethanesulfonic acid
miRNA	MicroRNA
MKP	MAPK phosphatase
MKS1	MAPK substrate 1
MS	Mass spectrometry
MVQ	MPK3/6-targeted VQPs
MyD88	Myeloid differentiation primary response gene 88
NBS	Nucleotide-binding site
Nep	Necrosis- and ET-inducing protein
NLP	Nep-like protein
NLR	NOD-like receptor
NLS	Nuclear localization sequence
NO	Nitric oxide
OG	Oligogalacturonides
O/N	Over night
PAD4	Phytoalexin deficient 4
PAGE	Polyacrylamide gel electrophoresis
PAMP	Pathogen-associated molecular pattern
PAR	poly(ADP-ribose)
PARG	PAR glycohydrolase
PARP	PAR polymerase
PBL	PBS-like
PBS1	AvrPphB susceptible 1
PCD	Programmed cell death
PCR	Polymerase chain reaction
PCRK1	PTI compromised receptor-like cytoplasmic kinase 1

PDF	Plant defensin
PEG	Polyethylene glycol
PEPR	AtPep receptor
PGN	Peptidoglycan
PLL	POL-like
PM	Plasma membrane
POL	Poltergeist
PP2A	Protein phosphatase type 2A
PP2C	Protein phosphatase type 2C
PR	Pathogenesis-related
PRR	Patter recognition receptor
PSK	Phytosulfokine
PSKR	PSK receptor
Pto	<i>Pseudomonas syringae</i> pv. tomato
PTI	PRR-triggered immunity
PTP	Protein tyrosine phosphatase
PUB	Plant U-box
pv.	pathovar
PVDF	Polyvinylidene fluoride
PVX	Potato virus X
R	Resistance protein/ gene
RACK1	Receptor for Activated C-kinase 1
RBOH	Respiratory burst oxidase homolog
RIP	Receptor-interacting protein
RIPK	RPM1-induced kinase
RK	Receptor kinase
RLCK	Receptor-like cytoplasmic kinase
RLP	Receptor-like protein
RNA	Ribonucleic acid
ROS	Reactive oxygen species
RPM1	Resistance to <i>P. maculicola</i> protein 1
RPS	Resistant to <i>P. syringae</i>
RT	Reverse transcriptase
SA	Salicylic acid
SCN1	Suppressor of npr1, constitutive 1
SE	Standard error
Ser (S)	Serine
SERK	Somatic embryogenesis related kinase
SGI	Seedling growth inhibition
SID2	SA induction deficient 2
SOBIR1	Suppressor Of BIR1 1
SsE1	<i>Sclerotinia sclerotiorum</i> elicitor 1
SUMM	Suppressor of MKK1 MKK2
T3SS	Type III secretion system
Thr (T)	Threonine
TIR	Toll/Interleukin receptor
TLR	Toll-like receptor

TM	Transmembrane
TRIS	Tris(hydroxymethyl)aminomethane
Ub	Ubiquitin
VQP	VQ domain-containing protein
WRKY	WRKY DNA binding protein
XB	XA21-binding protein
Xoo	Xanthomonas oryzae pv. oryzae
ZAR1	Hopz-activated resistance 1

Chapter 1: Regulation of surface-mediated innate immunity in plants

1.1. Introduction

The plant innate immune system relies on the capacity of each cell to initiate defence responses against potential pathogenic microbes. To achieve this, plants employ a multi-tier surveillance system that recognizes non-self or modified-self by means of plasma membrane (PM)-localized and intracellular immune receptors (Zipfel, 2014). At the cell surface, receptor kinases (RKs) or receptor-like proteins (RLPs) function as pattern-recognition receptors (PRRs) to perceive conserved microbe-derived molecules, classically known as pathogen-associated molecular patterns (PAMPs), or host-derived damage-associated molecular patterns (DAMPs). Structurally, plant RKs possess a ligand-binding ectodomain, a single trans-membrane domain, and an intracellular kinase domain; RLPs share the same basic conformation, except they lack a kinase domain or any other recognizable intracellular signalling domain. For this reason, RLPs are thought to depend on regulatory RKs to transduce ligand perception into intracellular signalling. PRRs may be distinguished based on the type of ectodomain, which determines the nature of the respective ligands. Leucine-rich repeat (LRR)-containing PRRs preferentially bind proteins or peptides, such as bacterial flagellin or EF-Tu, and endogenous AtPep peptides (Gomez-Gomez *et al.*, 2001; Chinchilla *et al.*, 2006; Yamaguchi *et al.*, 2006; Zipfel *et al.*, 2006; Sun *et al.*, 2013b; Tang *et al.*, 2015). In turn, PRRs containing lysine motifs (LysM) bind carbohydrate-based ligands, such as fungal chitin or bacterial peptidoglycan (PGN) (Kaku *et al.*, 2006; Iizasa *et al.*, 2010; Willmann *et al.*, 2011; Liu *et al.*, 2012a; Hayafune *et al.*, 2014). Furthermore lectin-PRRs bind extracellular ATP or bacterial lipopolysaccharides (LPS), and epidermal growth factor (EGF)-like domains recognize plant cell-wall derived

oligogalacturonides (OGs) (Brutus *et al.*, 2010; Choi *et al.*, 2014; Ranf *et al.*, 2015). Given the diverse and conserved nature of PAMPs, PRR-triggered immunity (PTI) effectively repels most non-adapted pathogens, while contributing to basal immunity during infection.

Inside the cell, nucleotide-binding site and leucine-rich repeat (NBS-LRR) proteins represent a second group of immune receptors that is classically associated with the recognition of pathogen-secreted virulence effectors. Adapted pathogens evolved these effectors to suppress host immunity and/or manipulate the host metabolism in their favour. In turn, recognition by NBS-LRRs betrays the pathogen in what has been described as an evolutionary arms race between plants and pathogens (Jones & Dangl, 2006). Effector recognition may occur through direct binding or by sensing the perturbing activity of an effector on host components (Dodds & Rathjen, 2010). Plants have evolved a 'guard strategy', where critical immune components are guarded by NBS-LRRs, which become activated upon effector-triggered modification of their 'gardees'. Plants may also use a 'decoy' strategy. In this case, NBS-LRRs guard non-functional mimics (or decoys) of key immune components that are normally targeted by effectors (van der Hoorn & Kamoun, 2008). Additionally, motifs of immune components targeted by effectors may be fused to NBS-LRRs ('integrated decoys' or 'integrated sensors'). Effector-triggered modification of such sensor (or decoy) motifs, which may or not retain their original function, activates a partner NBS-LRR to initiate immune signalling (Cesari *et al.*, 2014; Wu *et al.*, 2015).

An additional intracellular detection system, specific for viruses, involves binding and processing of dsRNA by ribonuclease Dicer-like proteins (DCLs) to trigger RNA-based antiviral immunity (Ding, 2010). Interestingly, NBS-LRRs are also involved in anti-viral immunity through recognition of viral proteins or by sensing virus-mediated host manipulation. Although no viral PAMPs have yet been identified

to elicit plant defences, recent reports point towards a potential role of LRR-RKs during anti-viral immunity (Korner *et al.*, 2013; Zorzatto *et al.*, 2015).

PAMP perception appears to occur exclusively at the cell surface in plants, thus contrasting with the mammalian innate immune system, where PAMPs are perceived both outside and inside the cell, for example by surface-localized Toll-like receptors (TLRs) and NOD-like receptors (NLRs), respectively. Nevertheless, several parallels can be observed between both innate immune systems (Ausubel, 2005; Ronald & Beutler, 2010; Maekawa *et al.*, 2011), as discussed throughout this chapter. Here, an overview of the main signalling events triggered during PTI in plants is provided, while expanding on the negative regulatory mechanisms employed by plant cells to keep innate immune responses under control.

1.2. Formation and activation of PRR complexes

PAMP recognition by TLRs plays a crucial role in the initiation of innate immunity in mammals (Medzhitov, 2001). TLRs are transmembrane receptors composed of an LRR-containing ectodomain and a cytoplasmic Toll/interleukin-1 (IL-1) receptor (TIR) domain. Upon ligand binding, TLRs form multimeric complexes with a variety of co-receptor proteins and use their TIR domain as docking platforms for different TIR-containing adaptor proteins (O'Neill & Bowie, 2007). TLRs show selectivity for adaptor proteins, enabling the activation of specific immune responses according to the perceived molecules. MyD88 was the first identified TIR adaptor and is used by all mammalian TLRs (except TLR3) (O'Neill & Bowie, 2007). Agglomeration of adaptors into higher-order complexes, such as the 'Myddosome', creates a signalling platform where IRAK/Pelle kinases, or other receptor interacting-protein (RIP) kinases, are activated to initiate a signalling cascade that leads to transcriptional reprogramming and production of pro-inflammatory cytokines (Gay *et al.*, 2014; Kawasaki & Kawai, 2014).

In plants, PRRs recruit regulatory RKs upon ligand binding and signal through receptor-like cytoplasmic kinases (RLCKs), which provide a link between extracellular ligand perception and activation of cytoplasmic signalling components. Interestingly, the kinase domain of plant RKs and RLCKs is phylogenetically related to IRAK/Pelle kinases (Shiu & Bleecker, 2001). However, no direct equivalent of TIR-adaptor proteins has been identified in plants, suggesting that plant PRRs bypass this need by directly forming kinase complexes that readily undergo trans-phosphorylation. While different adaptor proteins provide TLR signalling with flexibility and with the possibility of activating different downstream pathways, similar properties may be achieved by differential recruitment of regulatory RKs, and most importantly of distinct RLCKs (Fig. 1.1).

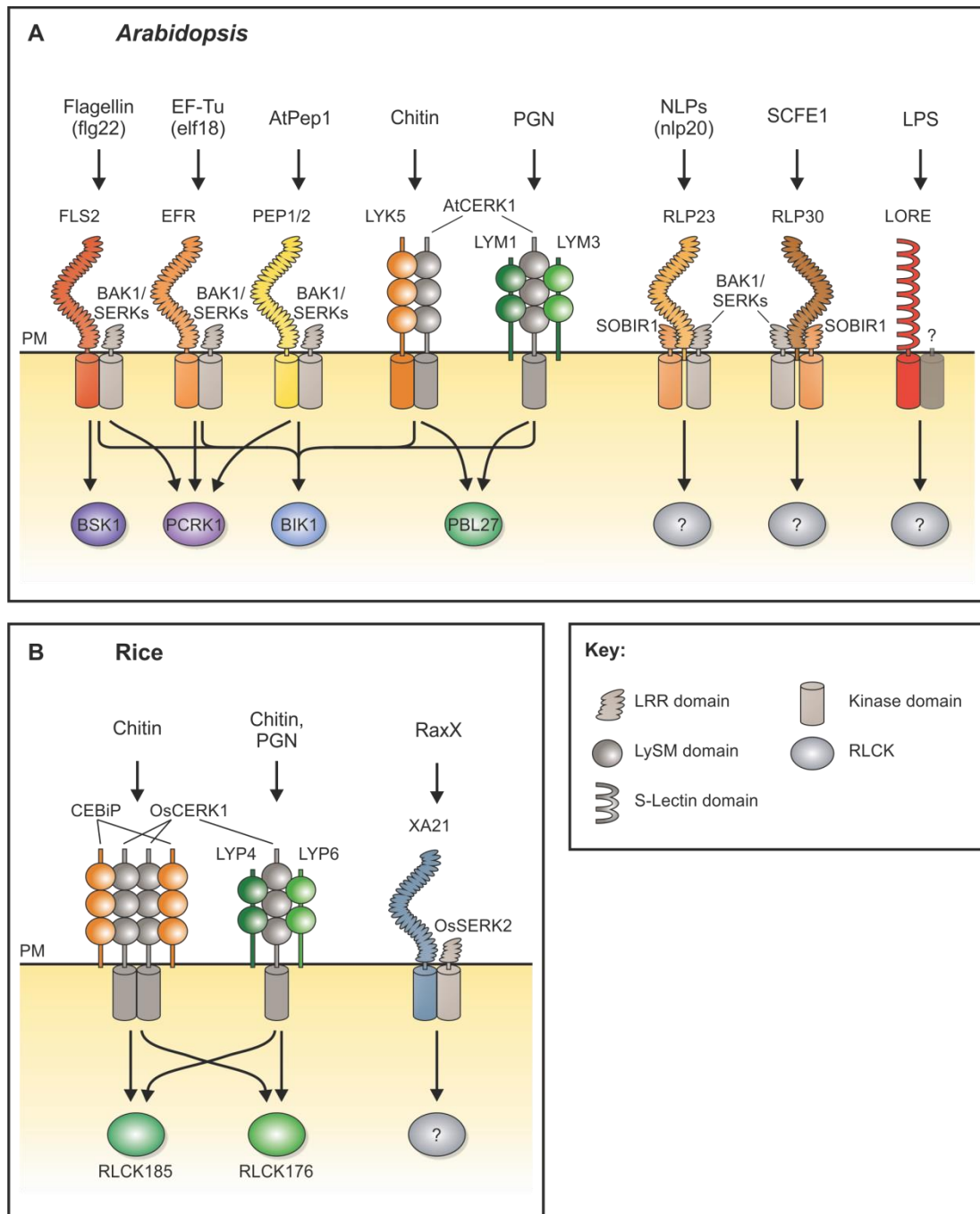


Figure 1.1. Recruitment of regulatory RKs and RLCKs by PRRs in *Arabidopsis* and rice.

PRRs recruit different regulatory RKs according to their ectodomain. In addition, RLCKs are specifically recruited to the different PRR complexes.

(A) In *Arabidopsis*, BAK1 (and related SERKs) and AtCERK1 are recruited upon ligand perception by LRR-RKs and LysM-RKs/ RLPs, respectively. Constitutive bimolecular LRR-RLP/SOBIR1 complexes recruit BAK1/SERKs upon ligand binding. No regulatory RKs interacting with the LPS-perceiving LORE S-Lectin-RK have yet been identified. BIK1 is a convergent point for multiple PRR pathways.

(B) In rice, OsCERK1 is recruited by the RLPs CEBiP and LYP4/6 upon ligand perception. XA21 constitutively associates with the BAK1 ortholog OsSERK2.

1.2.1. Recruitment of regulatory RKs

Both RKs and RLPs form dynamic complexes with regulatory RKs at the PM to activate immune signalling. For example, the *Arabidopsis* LRR-RKs FLS2, EFR and PEPR1/2, which recognize bacterial flagellin (or the epitope flg22), EF-Tu (or the epitopes elf18 or elf26), and the endogenous AtPep1 (an related peptides), respectively, all associate with the regulatory LRR-RK BAK1/SERK3 (and related SERKs) in a ligand-dependent manner (Gomez-Gomez *et al.*, 2001; Yamaguchi *et al.*, 2006; Zipfel *et al.*, 2006; Chinchilla *et al.*, 2007; Krol *et al.*, 2010; Yamaguchi *et al.*, 2010; Roux *et al.*, 2011; Sun *et al.*, 2013b; Tang *et al.*, 2015). Additionally, BAK1 regulates plant growth by interacting with the receptor LRR-RK BRI1 upon perception of the growth-promoting brassinosteroid hormones (BRs) (Kim & Wang, 2010). Although the presence of BAK1 is not strictly necessary for flg22 binding *in vivo* (Chinchilla *et al.*, 2007), it acts as a co-receptor for flg22 that is critical to activate signalling (Sun *et al.*, 2013b). Co-crystallization of FLS2 and BAK1 ectodomains together with flg22, revealed that the C-terminus of FLS2-bound flg22 clenches onto BAK1 ectodomain to stabilize the FLS2-BAK1 heterodimer (Sun *et al.*, 2013b). Modelling and mutagenic analysis suggested that BAK1 is recruited to the PEPR1-AtPep1 complex in an identical manner (Tang *et al.*, 2015). Similarly, BAK1 and SERK1 directly interact with BRI1-bound brassinolide (BL, the most active BR) (Santiago *et al.*, 2013; Sun *et al.*, 2013a). In these examples, ligand binding to the receptor creates new surfaces for SERK interaction and/or acts as a 'molecular glue' that stabilizes the receptor-SERK complex. In contrast, crystal structure of the growth-promoting peptide phytosulfokine (PSK) bound to its receptor PSKR1 revealed that SERK1 does not participate in PSK binding (Wang *et al.*, 2015b). Instead, PSK induces allosteric modifications on PSKR surface that allow subsequent recruitment of SERK1 (Wang *et al.*, 2015b). Because it is not clear whether SERKs participate in ligand binding with other PRRs (and thus

behaving as true co-receptors), the more comprehensive term 'regulatory RK' is favoured in this study.

FLS2-BAK1 heteromerization occurs almost instantly following flg22 perception (Chinchilla *et al.*, 2007; Schulze *et al.*, 2010), suggesting these RKs might be already present in pre-assembled complexes at the PM. However, a study relying on multiparameter fluorescence imaging spectrometry (MFIS) did not find evidence for FLS2-BAK1 pre-assembled complexes or for FLS2 homomerization (Somssich *et al.*, 2015), which in the latter case could be detected by co-immunoprecipitation (Sun *et al.*, 2012). Intriguingly, FLS2 and BAK1 re-organized in multimeric complexes several minutes after the initial flg22-triggered heterodimerization (Somssich *et al.*, 2015), but the biological relevance of these larger complexes is not yet understood.

LRR-RLPs, which lack a signalling kinase domain, constitutively associate with SOBIR1 or SOBIR1-like LRR-RKs to form the bimolecular equivalent of a genuine RK (Gust & Felix, 2014; Liebrand *et al.*, 2014). BAK1 or other SERKs seem to be only recruited to the RLP-SOBIR1 complex upon ligand binding, as recently shown for the *Arabidopsis* RLP23 and tomato Cf-4 (Albert *et al.*, 2015; Postma *et al.*, 2015). Consistently, *Arabidopsis* requires BAK1 and SOBIR1, as well as RLP30, to recognize a partially purified elicitor from the fungal pathogen *Sclerotinia sclerotiorum* (SCFE1), although biochemical characterization is still missing (Zhang *et al.*, 2013). BAK1 recruitment to PRRs may not be ligand-dependent in all plant species, as the rice (*Oryza sativa*, Os) LRR-RK XA21 was found to constitutively associate with the BAK1 ortholog OsSERK2 (Chen *et al.*, 2014). Whether this association is further enhanced upon ligand binding can now be tested since the *Xanthomonas oryzae* pv. *oryzae* (Xoo)-derived PAMP RaxX was recently identified as the XA21 ligand (Pruitt *et al.*, 2015).

Analogous to BAK1, the LysM-RK CERK1 appears to act as a regulatory RK that associates with different LysM-containing PRRs to activate immune signalling. In rice, the LysM-RLP CEBiP forms a homodimer upon chitin binding that is followed by heteromerization with OsCERK1, creating a signalling-active sandwich-type receptor system (Shimizu *et al.*, 2010; Hayafune *et al.*, 2014). Two other LysM-RLPs, LYP4 and LYP6, act as dual-specificity receptors for both chitin and PGN, associating with CERK1 in a ligand-dependent manner (Liu *et al.*, 2012a; Ao *et al.*, 2014). Although LYP4 associates with LYP6, as well as with CEBiP, these complexes partially dissociate following ligand perception (Ao *et al.*, 2014). Further studies, including structural analysis of ligand-bound complexes, will be required to consolidate these data and improve our understanding of chitin perception in rice.

In *Arabidopsis*, AtCERK1 was thought to be the unique receptor responsible for chitin responsiveness, as it was shown to homodimerize upon direct chitin binding (Miya *et al.*, 2007; Petutschnig *et al.*, 2010; Liu *et al.*, 2012b). However, a recent study demonstrated that the LysM-RK LYK5 displays higher chitin-binding affinity than AtCERK1 (Cao *et al.*, 2014). Notably, LYK5 (and to a lesser extent its closest homolog LYK4) is genetically required for chitin responsiveness, and forms a complex with CERK1 only upon chitin perception (Wan *et al.*, 2012; Cao *et al.*, 2014). Whether LYK5 and AtCERK1 organize into a sandwich-type receptor system similar to rice CEBiP and OsCERK1 remains to be shown. Furthermore, AtCERK1 is also recruited by the LYP4 and LYP6 paralogs in *Arabidopsis*, LYM1 and LYM3, during PGN recognition to mediate anti-bacterial immune responses (Gimenez-Ibanez *et al.*, 2009a; Gimenez-Ibanez *et al.*, 2009b; Willmann *et al.*, 2011). Intriguingly, LYM1 and LYM3 do not seem to play a role in chitin-mediated responses (Willmann *et al.*, 2011).

Recruitment of regulatory RKs seems to be specified by the type of PRR ectodomain. Accordingly, BAK1 is dispensable for chitin-triggered responses,

whereas CERK1 does not participate in flg22-mediated signalling (Wan *et al.*, 2008; Gimenez-Ibanez *et al.*, 2009a). Remarkably, neither BAK1 or CERK1 are required to mediate signalling by the novel S-lectin-RK LORE, recently identified as the *Arabidopsis* receptor for bacterial LPS (Ranf *et al.*, 2015), suggesting the latter may interact with yet unknown regulatory RKs.

1.2.2. Recruitment of RLCKs

The *Arabidopsis* and rice genomes code for over 160 and 280 RLCKs, respectively (Lehti-Shiu *et al.*, 2009). Most remain uncharacterized, but in recent years several RLCKs were reported to play important roles in PTI. BIK1, a member of *Arabidopsis* RLCK subfamily VII, is the best-studied example. Under resting conditions, BIK1 associates with FLS2, and likely with BAK1 (although, in some cases, FLS2 or EFR co-expression was required for detection of BIK1-BAK1 complexes) (Lu *et al.*, 2010; Zhang *et al.*, 2010). Upon flg22 elicitation, BAK1 associates with FLS2 and phosphorylates BIK1 (Lu *et al.*, 2010; Zhang *et al.*, 2010). In turn, BIK1 phosphorylates both BAK1 and FLS2 before dissociating from the PRR complex to activate downstream signalling components (Lu *et al.*, 2010; Zhang *et al.*, 2010). BIK1 and other closely-related PBL proteins are also required to activate immune responses triggered by elf18, AtPep1 and chitin (Lu *et al.*, 2010; Zhang *et al.*, 2010; Liu *et al.*, 2013; Ranf *et al.* 2014; Monaghan *et al.* 2015), thus representing an early convergence point for distinct PRR-mediated pathways.

Another RLCK from family VII, PCRK1, was reported to mediate BAK1-dependent PTI responses (Sreekanta *et al.*, 2015). Furthermore, OsRLCK176 and OsRLCK185, members of rice RLCK family VII, both interact with CERK1 and positively regulate responses to PGN and chitin (Yamaguchi *et al.*, 2013; Ao *et al.*, 2014). Similarly, PBL27, the OsRLCK185 ortholog in *Arabidopsis*, specifically mediates immune responses triggered by chitin, but not by flg22 (Shinya *et al.*, 2014). Interestingly, BSK1, an RLCK from subfamily XII, previously associated with

BR signalling, dynamically associates with FLS2 to regulate specific subsets of flg22-, but not elf18-, induced responses (Shi *et al.*, 2013). This raises the possibility that plants may, in part, owe the robustness and flexibility of their immune system to their large repertoire of RLCKs. In turn, these vary on their affinity to the different PRRs and ability to activate distinct signalling pathways, and are possibly subjected to different regulatory constraints.

1.3. Downstream events and signalling pathways

Once ligand recognition occurs and PRR complexes are activated, a branched signalling cascade is initiated within minutes to promote defence responses that can last up to days. Rapid ion-flux changes at the PM, accompanied by rise of cytosolic Ca²⁺ levels, and production of apoplastic reactive oxygen species (ROS), are amongst the first outputs recorded after P/DAMP perception (Boller & Felix, 2009). In turn, activation of Ca²⁺-dependent protein kinase (CDPK) and mitogen-activated protein kinase (MAPK) cascades conveys immune signalling to the nucleus, resulting in transcription reprogramming to establish PTI (Boller & Felix, 2009).

A direct link between PRR complex activation and ROS production was demonstrated by the finding that AtRBOHD, the NADPH oxidase responsible for PRR-triggered ROS burst in *Arabidopsis*, associates with the PRR complex and is directly phosphorylated by BIK1 and related PBLs upon PRR elicitation (Kadota *et al.*, 2014; Li *et al.*, 2014b). BIK1-mediated AtRBOHD phosphorylation, which is independent of Ca²⁺, is critical for initiation of the ROS burst that in turn acts as a key messenger to promote closure of stomata (natural openings on the leaf epidermis for gaseous exchanges) and limit entry of bacterial pathogens into the apoplast (Kadota *et al.*, 2014; Li *et al.*, 2014b). Other RLCKs, such as BSK1 and PCRK1, are genetically required for PAMP-triggered ROS burst and may also

directly phosphorylate AtRBOHD (Shi *et al.*, 2013; Sreekanta *et al.*, 2015). In turn, phosphorylation of AtRBOHD by PBL13 was recently proposed to negatively impact ROS production (Lin *et al.*, 2015). The activity of RBOH enzymes is further regulated by Ca²⁺ binding to conserved EF-hand motifs and by CDPK-mediated phosphorylation (Kobayashi *et al.*, 2007; Ogasawara *et al.*, 2008; Oda *et al.*, 2010; Dubiella *et al.*, 2013). This is in line with a synergistic model where initial BIK1-mediated phosphorylation primes RBOH activation by enhancing its sensitivity to subsequent Ca²⁺-dependent regulation (Kadota *et al.*, 2014; Kadota *et al.*, 2015). In addition, the rice small GTPase OsRac1, which is directly phosphorylated by OsCERK1 upon chitin perception, is a positive regulator of OsRBOHB (AtRBOHD ortholog) (Wong *et al.*, 2007; Oda *et al.*, 2010; Akamatsu *et al.*, 2013).

Besides controlling RBOHD, BIK1 and PBL1 are also required for the P/DAMP-triggered cytosolic Ca²⁺ burst that precedes ROS production (Li *et al.*, 2014b; Ranf *et al.*, 2014; Monaghan *et al.*, 2015); however, the molecular mechanisms and identity of the channel(s) responsible for the Ca²⁺ burst remain a mystery. The Ca²⁺ burst activates CDPKs, which not only regulate RBOHs, but are also important regulators of transcriptional reprogramming during PTI. Multiple knockout of *Arabidopsis* CPK4,5,6 and 11 impaired flg22-induced transcription of specific sets of genes (Boudsocq *et al.*, 2010), as well as flg22- and OG-induced ethylene production and resistance to the necrotrophic fungus *Botrytis cinerea* (Gravino *et al.*, 2015). These CDPKs phosphorylate a group of WRKY transcription factors (WRKY8/28 and 48) during NBS-LRR-mediated immunity (Gao *et al.*, 2013). Whether these or other transcription factors are directly phosphorylated by CDPKs during PTI remains to be shown.

MAPKs represent a second vehicle used by PRRs to mediate transcriptional changes into the nucleus. At least two distinct cascades lead to the activation of four MAPKs in *Arabidopsis* within a few minutes of P/DAMP treatment. MPK3 and MPK6

are activated by the MAPK kinases (MKKs or MEKs) MKK4/5, but their corresponding MAPK kinase kinase (MP3K or MEKK) remains unknown (Asai *et al.*, 2002; Suarez-Rodriguez *et al.*, 2007). A second cascade comprised by MEKK1 and MKK1/2 activates MPK4, and likely its closely related homolog MPK11 (Meszaros *et al.*, 2006; Suarez-Rodriguez *et al.*, 2007; Gao *et al.*, 2008; Bethke *et al.*, 2012). MPK4 was initially characterized as a negative regulator of plant immune signalling, as mutations associated with this MAPK cascade were accompanied by severe autoimmune phenotypes, including over-accumulation of salicylic acid (SA) and spontaneous cell death (Petersen *et al.*, 2000; Suarez-Rodriguez *et al.*, 2007). It was later found that the integrity of MPK4 cascade is guarded by the NBS-LRR SUMM2, in a process that involves MPK4-dependent phosphorylation of MEKK2/SUMM1 and PAT1, a component of the mRNA decapping machinery (Kong *et al.*, 2012; Zhang *et al.*, 2012; Roux *et al.*, 2015). Although MPK4 is required for flg22-induced gene transcription (Frei dit Frey *et al.*, 2014), expression of constitutively-active MPK4 versions negatively impacted *Arabidopsis* immune responses (Berriri *et al.*, 2012), which complicates our views on the exact role of MPK4 in PTI signalling. One cannot exclude that while conveying PAMP-triggered signalling, MPKs may activate downstream substrates that are themselves negative regulators of PTI, as part of a feedback loop to maintain cellular homeostasis (discussed below). Accordingly, a negative role in PTI was recently proposed for MPK3 (Frei dit Frey *et al.*, 2014).

The link between PRR and MAPK cascade activation remains an unsolved riddle. None of the RLCKs known to play a role in PTI, neither the above-mentioned CDPKs are involved in flg22-dependent MAPK activation (Boudsocq *et al.*, 2010; Feng *et al.*, 2012). However, disruption of *PBL27* or *OsRLCK185* specifically impaired MAPK activation in response to chitin but not to flg22 (Yamaguchi *et al.*, 2013; Shinya *et al.*, 2014). Whether these RLCKs directly activate MPKs, or act

themselves as MPKKs to directly phosphorylate MPKs, remains to be shown. Interestingly, neither PBL27 nor OsRLCK185 are required for chitin-triggered ROS burst (Yamaguchi *et al.*, 2013; Shinya *et al.*, 2014), suggesting that RLCKs have pathway- and PAMP-specific roles, and that signalling starts to branch at the level of the PRR complex.

A recent study revealed that protease IV secreted by the bacterial pathogen *Pseudomonas aeruginosa*, with homologs in other bacterial genera, triggered immune responses in *Arabidopsis* (Cheng *et al.*, 2015). Protease IV activated MPK3 and MPK6 via a G-protein pathway, where RACK1 acts as a scaffold linking G-protein subunits to all tiers of the MAPK cascade (Cheng *et al.*, 2015). Importantly, activation of MPK3/6 by flg22 did not follow the same pathway. How this protease triggers plant immunity, and whether RLCKs are involved in activation of the G-protein-RACK1-MAPK complex, remains to be shown.

Downstream of MAPKs and CDPKs, a number of transcription factors are responsible for a transcriptional reprogramming that prioritizes immunity, resulting in production of anti-microbial compounds/enzymes, reinforcement of extracellular barriers, for example by deposition of callose at the cell wall, and synthesis of hormones that may induce secondary transcriptional waves (Meng & Zhang, 2013). Collectively, these responses lead to the establishment of PTI at the expense of plant growth inhibition.

1.4. Negative regulation of RK-mediated immunity

Excessive or untimely activation of immune responses lead to development of autoimmune and inflammatory diseases in mammals (Goldszmid & Trinchieri, 2012; Murray & Smale, 2012). This is equally the case for plants, where growth and immunity are finely balanced, and dictate their developmental and reproductive

success (Wang & Wang, 2014; Lozano-Duran & Zipfel, 2015). Plants employ different strategies to prevent unnecessary immune responses, and to adjust their amplitude and duration accordingly, in order to maintain cellular homeostasis. These include limiting the ability of PRRs to recruit their cognate regulatory RKs, regulation of signalling initiation and amplitude at the level of PRR complexes, monitoring of cytoplasmic signal transducing pathways and control of the transcriptional reprogramming process (Fig. 1.2). In addition, signalling is integrated into a complex network of hormones and endogenous peptides, which act in a cell-autonomous manner, as well as at the tissue and organ levels, providing a communication system throughout the plant (Fig. 1.2). In the next sections, we address in more detail the molecular mechanisms that control PTI signalling at these different steps.

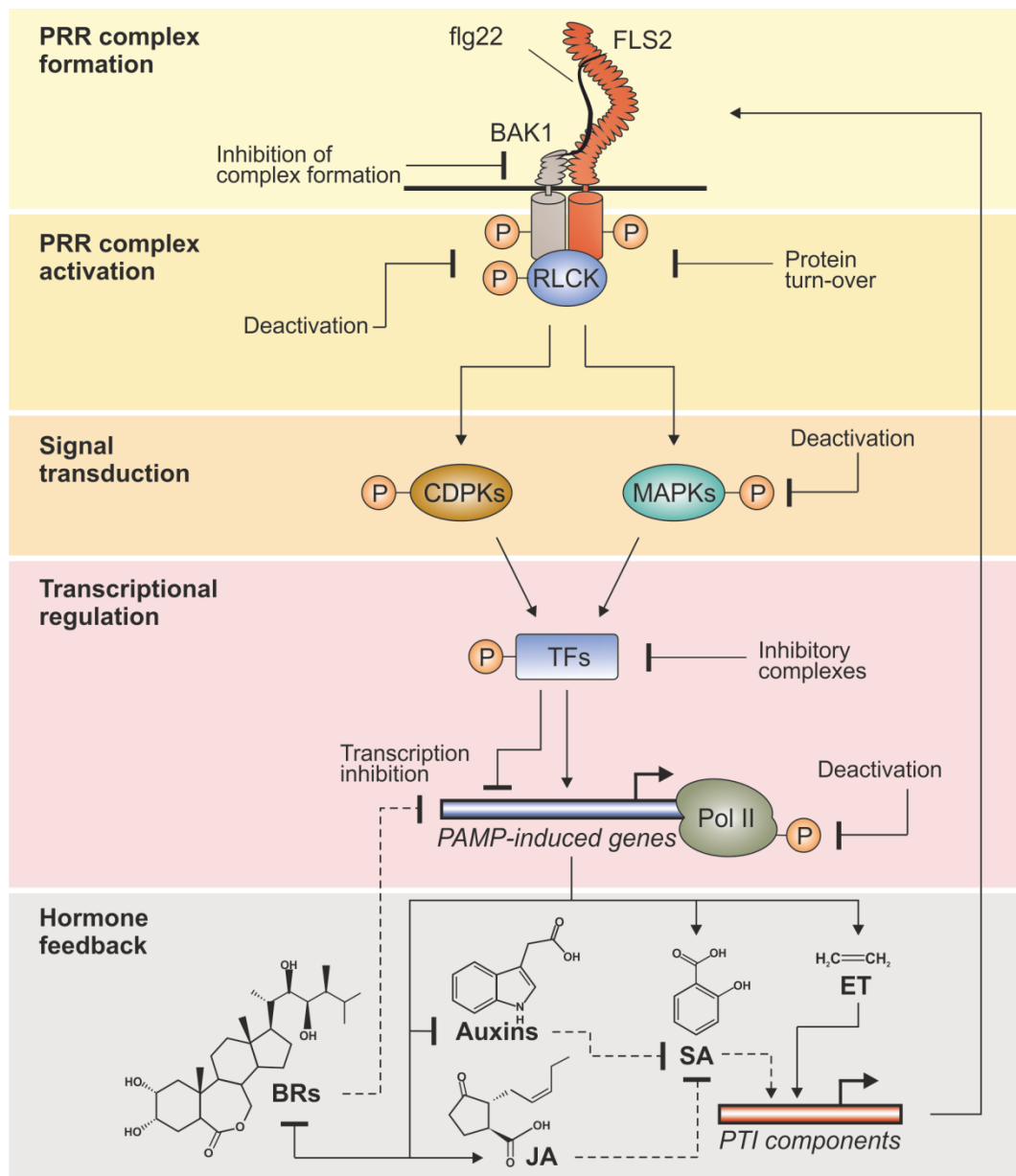


Figure 1.2. Negative regulation of PTI signalling by a multi-layered system.

The *Arabidopsis* FLS2-dependent pathway is used to illustrate PTI signalling. At the cell surface, formation of the FLS2-BAK1 heterodimer can be inhibited by the action of pseudokinases, such as BIR2. In the cytoplasm, the signalling output of the PRR complex is modulated through regulation of its phosphorylation status and by protein turnover. Downstream signalling transducers, such as MAPKs, have their activity modulated by several phosphatases; mechanisms negatively regulating CDPKs are currently unknown. Transcriptional reprogramming is mediated by transcription factors (TFs). For example, WRKY TFs may be kept in inhibitory complexes by VQPs. In turn, negatively-acting TFs are activated by MAPKs to repress transcription of defence-related genes, in a negative feedback that fine-tunes signalling. The CTD domain of RNA polymerase II (Pol II) is phosphorylated upon PAMP recognition, an action that can be reversed by phosphatases to modulate the polymerase activity. PTI signalling is integrated in a network of plant hormones that regulates the transcription of defence-related genes and of key PTI

signalling components (eg. *FLS2*). The biosynthesis of these hormones is repressed or enhanced by the PTI signalling pathway.

1.4.1. Regulation of PRR complex formation by pseudokinases

Pseudokinases account for at least 10% of all human and *Arabidopsis* kinases (Castells & Casacuberta, 2007; Zeqiraj & van Aalten, 2010). However, their role and mode of action has only recently started to be understood in mammals (Boudeau *et al.*, 2006), whereas in plants they remain, for the most part, enigmatic. Canonical kinases may act as signalling enzymes through ATP hydrolysis and protein phosphorylation. In turn, pseudokinases, which retain the overall kinase structure but are unable to hydrolyse ATP due to loss of key catalytic residues, may represent important signalling regulators by acting as allosteric activators of other kinases, or by promoting or preventing protein-protein interactions (Shaw *et al.*, 2014). IRAK-M (also known as IRAK3) is a prime example of a pseudokinase that negatively regulates mammalian TLR signalling by controlling the dynamics of TLR-adaptor complexes. During stimulation of TLR4 or TLR9, IRAK-M binds to MyD88-IRAK4 complexes, preventing IRAK1 phosphorylation and subsequent interaction with TRAF6 (Kobayashi *et al.*, 2002). Expression of IRAK-M is mostly confined to immune cells and is induced during TLR signalling, which is thought to be necessary for restricting inflammation and cytokine production (Hubbard & Moore, 2010).

In *Arabidopsis*, BIR2, and other members of the same LRR-RK subfamily, were found to associate with BAK1 under resting conditions (Gao *et al.*, 2009; Halter *et al.*, 2014). Several residues required for kinase activity are not conserved within this subfamily, and structural analysis revealed that the nucleotide-binding site of BIR2 is not accessible for ATP binding, confirming that it is a pseudokinase (Blaum *et al.*, 2014). Silencing or deletion of *BIR2* increased flg22- (and also elf18-) triggered responses, which was linked to enhanced FLS2-BAK1 complex formation (Halter *et al.*, 2014). In contrast, *BIR2* over-expression constrained FLS2-BAK1 interaction

and reduced PAMP responsiveness (Halter *et al.*, 2014). Moreover, BIR2 was shown to dissociate from BAK1 upon flg22 treatment and was not part of the FLS2-BAK1 complex (Halter *et al.*, 2014). This suggests that BIR2 negatively regulates BAK1 by competing with other interactors. Binding of flg22 by FLS2 is likely to enhance its affinity to BAK1 in detriment of BIR2. With the deletion of BIR2 and absence of competition, the threshold required for FLS2-BAK1 interaction is expected to be lower, facilitating complex formation. BIR2 is phosphorylated by BAK1 kinase domain *in vitro* (Blaum *et al.*, 2014; Halter *et al.*, 2014); whether phosphorylation by BAK1 or other kinase accounts for BIR2 dissociation remains to be shown. Of note, the FLS2-BAK1 complex in *BIR2*-silencing lines could still not be detected in the absence of flg22 stimulus, indicating that even in the absence of a competitor flg22-binding is a strict requirement, or that additional negative regulators may still be present. Indeed, BIR1 was previously proposed to negatively regulate plant immunity (Gao *et al.*, 2009). However, the role of BIR1 was not assessed after PAMP elicitation, and the elevated salicylic acid (SA) levels of *bir1* mutants may complicate the interpretation of the contributions of BIR1 to immune signalling.

1.4.2. Regulation of PRR complex phosphorylation status

Recruitment of TIR-adaptor proteins upon ligand perception by TLRs creates a platform where kinases, such as IRAK1 and IRAK4, are brought into close proximity, allowing their trans-phosphorylation and activation (Li *et al.*, 2002; Ferrao *et al.*, 2014). In plants, PRR activation follows a different approach. The kinase domains of RKs or RLP-SOBIR1 bimolecular PRRs function themselves as platforms for interaction and phosphorylation of regulatory RKs and RLCKs. These kinases form complexes even under resting conditions; nevertheless, signalling is generally only initiated upon ligand recognition. This suggests the presence of tight inhibitory mechanisms (Fig. 1.3), especially since kinases like BAK1 and BIK1

possess strong enzymatic activity (Lu *et al.*, 2010; Schwessinger *et al.*, 2011; Lin *et al.*, 2014).

It has long been suspected that protein phosphatases were important regulators of plant immunity, as treatment of cell cultures with phosphatase inhibitors was sufficient to initiate responses similar to those triggered by pathogen-derived elicitors (Felix *et al.*, 1994; Chandra & Low, 1995). Yet, the molecular and genetic basis for such observations was only recently uncovered by the identification of a specific *Arabidopsis* protein phosphatase type 2A (PP2A) holoenzyme, composed of subunits A1, C4, and B η , that constitutively associates with and negatively regulates BAK1 activity (Segonzac *et al.*, 2014). Mutants for any of these subunits exhibited enhanced PAMP-induced responses dependent on BAK1, but not on CERK1 (Segonzac *et al.*, 2014). The activity of the BAK1-associated PP2A was transiently reduced following PAMP perception (Segonzac *et al.*, 2014), suggesting that PP2A itself is negatively regulated to allow PRR complex activation. Importantly, treatment with cantharidin, a PP2A-specific inhibitor, was sufficient to induce BAK1 hyper-phosphorylation (Segonzac *et al.*, 2014). This is consistent with previous reports of phosphatase inhibitors spontaneously triggering ROS bursts (Chandra & Low, 1995), and demonstrates that a tight regulation of BAK1 is crucial to prevent unintended activation of downstream RLCKs in the absence of PAMPs.

PRRs are themselves under regulation by protein phosphatases, namely by members of the type 2C (PP2C) family. The rice PP2C XB15 dephosphorylates XA21 *in vitro* and negatively regulates XA21-mediated immune responses (Park *et al.*, 2008). XA21 phosphorylates XB15 *in vitro* (Park *et al.*, 2008), but whether this represents a regulatory mechanism remains to be tested. XA21 is further regulated by the ATPase XB24, which is thought to promote auto-phosphorylation of specific XA21 phosphosites to inhibit its kinase activity (Chen *et al.*, 2010). The XB15 orthologs in *Arabidopsis*, PLL4 and PLL5, associate with EFR and play a negative role in EFR-mediated responses (Holton *et al.*, 2015), demonstrating that, at least

some PRR regulatory mechanisms are conserved between distantly-related plant species. Another *Arabidopsis* PP2C, KAPP, interacts with the FLS2 cytoplasmic domain in yeast two-hybrid assays and its over-expression inhibits flg22 responsiveness (Gomez-Gomez *et al.*, 2001). However, the specificity of this action was questioned when KAPP was shown to interact with a number of unrelated RKs (Ding *et al.*, 2007).

The prominence of kinases within PRR complexes dictates that their phosphorylation status must be kept under tight regulation, namely by protein phosphatases (Fig. 1.3). The reversible nature of this regulation allows plant cells not only to prevent unintended signalling activation, but also to modulate signalling amplitude and fine-tune immune responses.

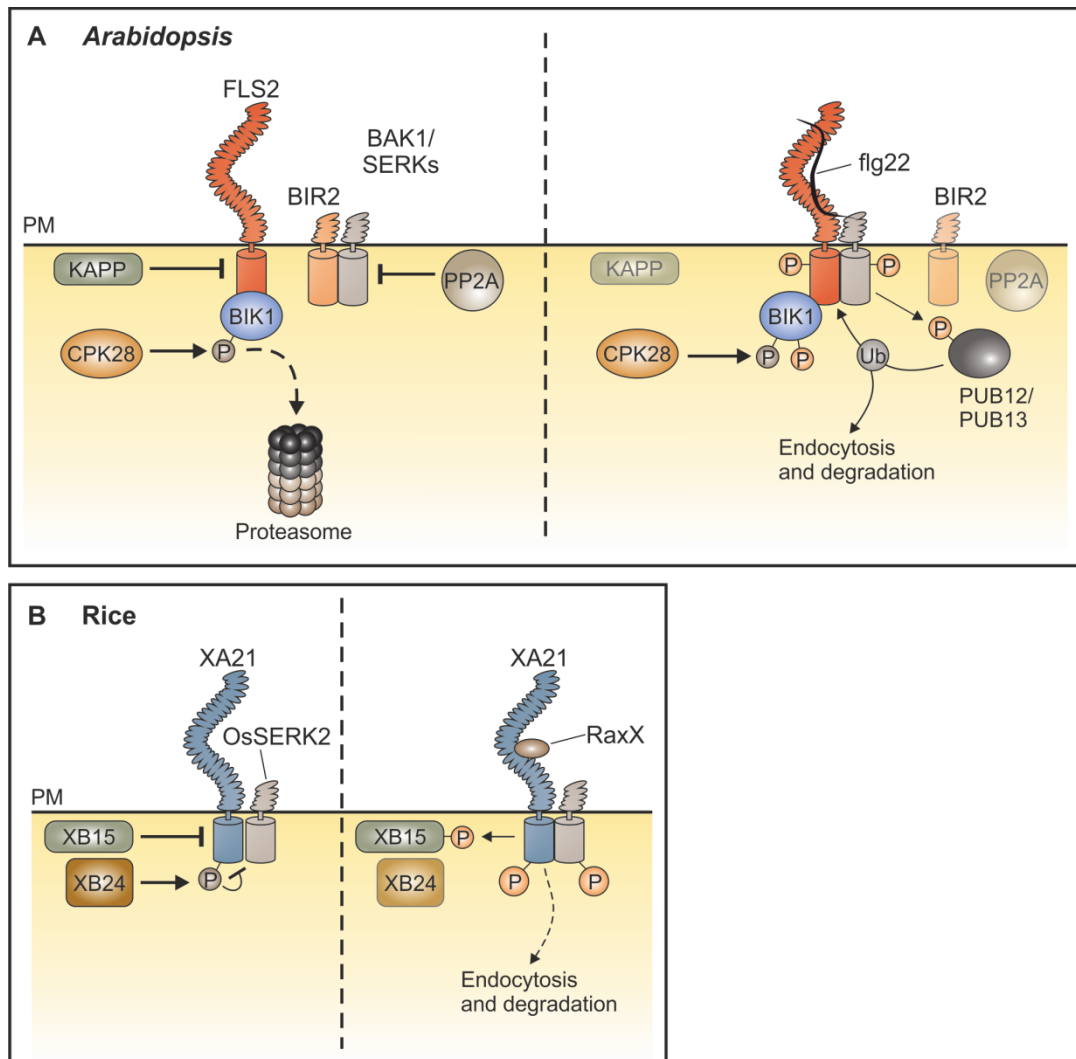


Figure 1.3. Negative regulation at the PRR complex level.

The *Arabidopsis* FLS2-flg22 and rice XA21-RaxX systems are used as representative models for plant PRR regulation.

(A) The pseudokinase BIR2 blocks BAK1 interaction with FLS2; upon flg22 perception BIR2 dissociates from BAK1. In the absence of stimuli, the phosphorylation status of PRR complex components is regulated by different phosphatases: the PP2C KAPP negatively regulates FLS2; PP2A holoenzyme controls BAK1. Following flg22 perception, PP2A is transiently inactivated by an unknown mechanism. Basal BIK1 levels are controlled by CPK28-mediated phosphorylation of BIK1 residues that facilitate its proteasomal degradation. BAK1 phosphorylates the E3 ligases PUB12 and PUB13 in a flg22-dependent manner, which in turn ubiquitinate and target FLS2 for degradation, likely via the endocytic route; whether FLS2 degradation contributes to PTI negative regulation remains a matter of debate.

(B) In rice, the PP2C XB15 dephosphorylates XA21 and the ATPase XB24 promotes autophosphorylation of inhibitory XA21 residues. During *Xoo* infection, XB24 dissociates from XA21. XB15 is phosphorylated by XA21, but the relevance of is not clear.

1.4.3. Regulation of the PRR complex by protein turn-over

Attachment of K48-linked poly-ubiquitin chains is a universally conserved mechanism amongst eukaryotes to selectively mark proteins for proteasomal degradation, and an effective way to control the levels of signalling components in the cell (Kondo *et al.*, 2012). A number of E3 ubiquitin ligases mediate ubiquitination and degradation of TLR signalling components in order to attenuate or shut down immune signalling (Kondo *et al.*, 2012). Similarly, modulation of PTI signalling amplitude in *Arabidopsis* can be achieved by fine-tuning of BIK1 protein levels. CPK28 constitutively associates with BIK1 to control its proteasome-dependent turnover (Monaghan *et al.*, 2014). The mechanism by which this is achieved is not entirely understood, but it is likely to involve CPK28-dependent phosphorylation of specific BIK1 residues that may facilitate the recruitment of a yet unknown E3 ligase. The role of CPK28 in PTI was identified in a suppressor screen of the *bak1-5* mutant, which carries a *BAK1* allele with a point mutation that specifically impaired in PTI signalling, but not plant growth (Roux *et al.*, 2011; Schwessinger *et al.*, 2011; Monaghan *et al.*, 2014). Due to the dominant-negative effect of this point mutation, these plants exhibit extremely low responsiveness to PAMPs triggering BAK1-dependent responses (Schwessinger *et al.*, 2011). Strikingly, loss-of-function mutants of *CPK28* (*mob1* and *mob2*) could partially restore PAMP responsiveness by causing BIK1 to accumulate (Monaghan *et al.*, 2014), suggesting that BIK1 is a rate-limiting factor during PTI signalling, and that BIK1 protein levels dictate the amplitude of PTI responses. Manipulating BIK1 levels by deleting or over-expressing *CPK28* in wild-type plants resulted in significant enhancement or impairment of PTI responses, respectively, further supporting this hypothesis (Monaghan *et al.*, 2014).

Members of the *Arabidopsis* Plant U-box (PUB) family of ubiquitin E3 ligases are known to negatively regulate PTI responses. Successive disruption of *PUB22*,

PUB23 and *PUB24* into higher-order mutants results in a gradual increase of PTI responses, such as ROS production and immune marker gene expression (Trujillo *et al.*, 2008). *PUB22* is stabilized upon flg22 perception and mediates proteasomal degradation of Exo70B2, a subunit of the exocyst complex that is required for PTI responses (Stegmann *et al.*, 2012). How the exocyst complex affects early immune signalling, and whether these ligases have additional substrates required for PTI remains to be addressed. Two other partially redundant members of the same E3 ligase family, *PUB12* and *PUB13*, have been implicated in the degradation of *FLS2*. Upon flg22 treatment, *BAK1* phosphorylates *PUB12/13* promoting their association with *FLS2*, which is then ubiquitinated (Lu *et al.*, 2011). Degradation of integral PM proteins typically follows the endocytic route, which can also be regulated in an ubiquitin-dependent manner. *FLS2* and other PRRs undergo ligand-dependent endocytosis, but whether this process is required for sustaining or terminating PRR-mediated signalling, or to allow replenishment of the PM with newly-synthesized PRRs is still a matter of debate (Ben Khaled *et al.*, 2015). Mutation of *DRP2b*, a dynamin required for scission and release of clathrin-coated vesicles during endocytosis, partially compromised flg22-induced *FLS2* endocytosis (Smith *et al.*, 2014). In addition, it enhanced flg22-induced ROS production, while rendering plants more susceptible to bacterial infection (Smith *et al.*, 2014). Mutants on other components of the endocytic machinery produced similar bacterial susceptibility phenotypes (Ben Khaled *et al.*, 2015). However, the conclusions taken from these experiments must be carefully considered, as interference with general endocytic regulators may affect trafficking of various components that may be equally involved in PTI signalling and plant immunity (Ben Khaled *et al.*, 2015).

1.4.4. Negative regulation of MAPK signalling cascades

MAPKs are activated in response to PAMP perception and are instrumental for transcriptional reprogramming by directly or indirectly controlling the activity of

transcription factors (Arthur & Ley, 2013; Meng & Zhang, 2013; Tsuda & Somssich, 2015). Thus, the actions of MAPKs are likely to be kept under tight control. Phosphorylation of both Tyr and Thr residues in the activation loop is critical for MAPK activation; consequently, dephosphorylation of any of these residues renders them inactive (Caunt & Keyse, 2013). Dual-specificity protein phosphatases [DUSPs, also known as MAPK phosphatases (MKPs)] dephosphorylate both these residues and are important modulators of MAPK activity during innate immunity in mammals (Arthur & Ley, 2013; Caunt & Keyse, 2013).

In *Arabidopsis*, DUSPs, as well as protein Tyr phosphatases (PTPs) and protein Ser/Thr phosphatases (in particular PP2Cs) were shown to target PRR-activated MAPKs. The closely-related PP2Cs AP2C1 and PP2C5 regulate PRR-dependent MPK3 and MPK6 activation. Single or double mutations of *AP2C1* and *PP2C5* enhanced MPK3 and MPK6 phosphorylation in response to elf26 (Brock *et al.*, 2010), while *AP2C1* over-expression abolished their activation in response to flg22 and OGs, compromising MPK3/6-dependent gene induction and induced resistance to the necrotrophic fungus *Botrytis cinerea* (Galletti *et al.*, 2011). In addition to its roles on MPK3 and MPK6, AP2C1 was shown to inactivate MPK4 *in vivo* (Schweighofer *et al.*, 2007).

The DUSP MKP1 and PTP1 regulate MPK3 and MPK6 in a partially redundant manner. Mutation of *MPK1* increased elf26-dependent responses and decreased bacterial susceptibility, which correlated with enhanced MPK3 and MPK6 activation (Anderson *et al.*, 2011). Intriguingly, *MKP1* mutation in *Arabidopsis* ecotypes possessing the NBS-LRR SCN1 produces a stunted phenotype, consistent with over-activation of immune responses, which is further aggravated by mutation of *PTP1* (Bartels *et al.*, 2009). This dramatic phenotype can be partially rescued by mutating *MPK3*, *MPK6* or *SCN1*, suggesting that the effects of MAPK activation and/ or the integrity of the MKP1 pathway may be monitored by a SCN1-dependent pathway (Bartels *et al.*, 2009). In addition, MPK2 could dephosphorylate both MPK3

and MPK6 *in vitro* (Lee & Ellis, 2007); however, *MKP2* over-expression only strongly affected activation of MPK3, but not of MPK6, during the early stages of *B. cinerea* infection (Lumbreras *et al.*, 2010). This collection of data demonstrates the importance of protein phosphatases in the regulation of MAPKs and immune responses, but a more systematic biochemical and functional characterization will be required to fully address their role in PTI signalling.

1.4.5. Negative regulation at the transcriptional level

Establishment of PTI ultimately relies on a massive transcriptional reprogramming that entails large energetic costs for the cell (Lozano-Duran & Zipfel, 2015). Several mechanisms are in place that negatively regulate transcription factors and the transcriptional machinery to ensure timely and adequate activation of immune-related genes. The plant-specific WRKY family of transcription factors has been particularly associated with plant immunity. WRKY33 is a well-characterized member of this family, and is responsible for PAMP-induced activation of the phytoalexin camalexin biosynthetic genes, among others (Tsuda & Somssich, 2015). WRKY33 is maintained in an inhibitory complex by MPK4 and the VQ motif-containing protein (VQP) MKS1 (Qiu *et al.*, 2008). Upon flg22 perception, MPK4 phosphorylates MKS1 and releases the MKS1-WRKY33 complex (Qiu *et al.*, 2008), allowing WRKY33 to be phosphorylated and activated by MPK3 and MPK6 (Mao *et al.*, 2011; Rasmussen *et al.*, 2012). Interestingly, several other VQPs interact with different WRKYs and are substrates of MPK3/6, suggesting these proteins are a widespread mechanism that regulates WRKY-dependent gene transcription (Cheng *et al.*, 2012; Pecher *et al.*, 2014; Weyhe *et al.*, 2014). Consistently, over-expression of the MPK3/6-targeted VQP1 (MVQ1) inhibited the PAMP-induced and WRKY-dependent expression of *NHL10*, and abolished PAMP-induced resistance to *Pseudomonas syringae* (Pecher *et al.*, 2014). Importantly, phosphorylation by MPK3/6 upon flg22 treatment destabilized MVQ1 proteins, thus releasing WRKYs

from MVQ1-imposed inhibition. Interestingly, other VQPs, such as SIB1 and SIB2, were shown to stimulate the DNA binding affinity of WRKY33 (Lai *et al.*, 2011). How different combinations of VQPs and WRKYs interact with MAPKs to regulate transcription during PTI is a challenge to be addressed in the future.

ASR3 is a plant-specific trihelix transcription factor that acts as a transcriptional repressor during PTI (Li *et al.*, 2015). Accordingly, *asr3* mutants showed enhanced flg22-induced gene expression and increased resistance to *P. syringae*, while early PTI outputs, such as ROS production or MAPK activation were unaffected. Remarkably, phosphorylation of ASR3 by MPK4 upon flg22 elicitation enhances its DNA affinity. With this action, MPK4 promotes binding of ASR3 to the promoter regions of flg22-upregulated genes, such as *FRK1*, initiating a negative feedback mechanism to fine-tune immune gene expression.

Transcriptional regulation during PTI may also be achieved by direct regulation of the C-terminal domain (CTD) of the largest RNA polymerase II subunit. The CTD is composed of several repeats and is subject to post-translational modifications that ultimately determine its activity. The CTD is phosphorylated in response to different PAMPs by cyclin-dependent kinases C (CDKCs), which are activated by MAPK cascades (Li *et al.*, 2014a). In turn, the CTD phosphatase-like protein CPL3, which was identified in a mutant screen as a negative regulator of early PAMP-induced gene expression, dephosphorylates the CDKC-activated CTD to repress transcription (Li *et al.*, 2014a). How CPL3 activity is regulated in the context of PTI signalling remains to be addressed; nonetheless this study elegantly demonstrated that coordination between the MAPK-CDKC module and CPL3 dictates the CTD phosphorylation status, and underpins gene activation during PTI.

Attachment of poly(ADP-ribose) (PAR) chains to target proteins is a common post-translational modification catalysed by PAR polymerases (PARPs) in eukaryotes. This modification is known to regulate important cellular processes, such as DNA repair, gene transcription and chromatin remodelling, particularly during stress, including inflammatory responses in mammals (Gibson & Kraus, 2012). PARP2 accounts for most of *Arabidopsis* PARylation activity in response to DNA damage-inducing agents (Song *et al.*, 2015), and its activity is enhanced following flg22 treatment (Feng *et al.*, 2015). Consistent with a positive role of PARylation in PTI signalling, *parp1/parp2* double mutants were compromised in flg22-induced gene induction and immunity against *P. syringae*, but not in early PTI responses (Feng *et al.*, 2015; Song *et al.*, 2015). PARylation can be reverted by the action of PAR glycohydrolases (PARGs). PARG1 was found to negatively regulate PAMP-induced gene transcription in the same mutant screen that identified CPL3 (Feng *et al.*, 2015). Although their targets remain elusive, it is now evident that the combination of PARP and PARG activities determines the outcome of transcriptional reprogramming during PTI.

1.4.6. Negative regulation by hormones and endogenous peptides

The plant immune system is highly regulated by a complex network of hormones that integrates both external and internal cues to maintain homeostasis and coordinate immune responses at the spatial and temporal levels. Hormones may act downstream of immune-recognition events and/or modulate immune signalling by controlling the basal levels of signalling components in the cell. Salicylic acid (SA) and jasmonic acid (JA) represent the two major immune-related hormones, and often act antagonistically (Pieterse *et al.*, 2012). SA positively regulates basal FLS2 levels, and activation of SA signalling, either by exogenous treatment or by the use of SA-overproducing plants, induces FLS2 protein accumulation and consequently enhances flg22-triggered responses (Tateda *et al.*, 2014; Yi *et al.*, 2014).

Conversely, JA application has a negative impact on FLS2-mediated responses, such as ROS burst and callose deposition (Yi *et al.*, 2014). Whether this effect is due to perturbation of FLS2 accumulation and/or a reflection of the JA-SA antagonism remains to be shown. Remarkably, several *P. syringae* strains produce the phytotoxin coronatine (COR), a structural mimic of a bioactive JA conjugate, as well as effector proteins that directly activate JA signalling (Geng *et al.*, 2014). Consequently, this suppresses SA signalling and inhibits typical PTI responses, such as stomatal closure and cell wall reinforcement (Geng *et al.*, 2014).

A third hormone produced by plants during pathogen attack, ethylene (ET), is essential for *FLS2* transcription by controlling the activation of its promoter through the ET-responsive transcription factor EIN3 (Boutrot *et al.*, 2010). ET plays both antagonistic and synergistic roles in its relationship with SA, while mostly being synergistic to JA (Pieterse *et al.*, 2012).

Surprisingly, biosynthesis of all three hormones is increased following flg22 perception (Felix *et al.*, 1999; Mishina & Zeier, 2007; Flury *et al.*, 2013). JA production seems to be required for flg22-dependent induction of the AtPep1-PEPR1/2 pathway (Flury *et al.*, 2013), which further strengthens PTI responses. In turn, this pathway is synergistically activated by ET and SA during elf18-triggered responses (Tintor *et al.*, 2013).

Several growth-promoting hormones have been associated with plant immunity. For example, auxin is known to antagonize SA signalling, and some plant pathogens have evolved to hijack and use auxin signalling to their advantage (Robert-Seilaniantz *et al.*, 2011a). Although concrete data is still missing, such an effect on SA signalling is likely to negatively influence the levels of PTI signalling components. Accordingly, the microRNA *miR393* is induced upon flg22 perception and targets the auxin receptors to inhibit auxin signalling and alleviate its antagonism on SA signalling (Navarro *et al.*, 2006; Robert-Seilaniantz *et al.*, 2011b).

In turn, cytokinins (CKs) may stimulate SA signalling and boost immunity (Robert-Seilaniantz *et al.*, 2011a); however, many pathogens are known to tamper with CK signalling and to secrete their own CKs in order to induce susceptibility (Naseem *et al.*, 2014). The most remarkable example is perhaps *Agrobacterium*, which manipulates CK and auxin signalling to induce nutrient re-allocation and tumour formation (Gohlke & Deeken, 2014). Moreover, it was recently shown that activation of CK signalling by the *Pto* effector HopQ1, or by exogenous CK application, suppressed PTI via repression of *FLS2* transcription (Hann *et al.*, 2014). This contradicted a previous report showing that CK treatment enhanced resistance against *Pto* (Choi *et al.*, 2010), a conflict that may lie on the CK dosage.

Importantly, brassinosteroids (BRs) have been shown to suppress PTI responses and prioritize growth over immunity (Albrecht *et al.*, 2012; Belkhadir *et al.*, 2012), in a process that is mainly mediated by the transcription factor BZR1 (Lozano-Duran *et al.*, 2013). Furthermore, the transcription factor HBI1, which is itself a transcriptional target of BZR1, was shown to negatively regulate immune signalling, while being a positive regulator of BR signalling (Fan *et al.*, 2014; Malinovsky *et al.*, 2014). A model has been proposed where BZR1 integrates BR and gibberellin (GA) signalling, as well as environmental cues, such as light or darkness, to suppresses PTI via activation of a set of WRKY transcription factors that negatively regulate immunity (Lozano-Duran & Zipfel, 2015). Interestingly, transcription of BR biosynthetic genes is rapidly inhibited following PAMP perception (Jiménez-Góngora *et al.*, 2015), revealing a complex bi-directional negative crosstalk between PTI and BR signalling.

An additional layer of complexity is brought about by the growth-promoting endogenous tyrosine-sulfated PSK α and PSY1 peptides, which negatively regulate several PTI responses (Igarashi *et al.*, 2012; Mosher *et al.*, 2013). Perception of PSK α and PSY1 is mainly attributed to the LRR-RKs PSKR1 and PSY1R, respectively, which are both transcriptionally up-regulated upon PAMP perception

(Igarashi *et al.*, 2012; Mosher *et al.*, 2013), generating a feedback loop that opposes immunity and promotes growth.

Plant hormones make up a flexible and robust system, which feedbacks, either positively or negatively, on immune signalling, and is capable of responding against pathogenic threats, while maintaining homeostasis. A parallel could be drawn between plant hormones and pro- and anti-inflammatory cytokines that regulate inflammatory responses during mammalian innate immunity, and are critical to avoid autoimmunity. In particular, IL-10 negatively regulates TLR signalling primarily by controlling transcription of TLR-induced genes (Murray, 2005). In plants, such a role could be attributed to BRs and to the endogenous peptides PSK α and PSY1.

1.5. Manipulation of plant immunity by bacterial effectors

A common feature of Gram-negative pathogenic bacteria is the use of the type III secretion system (T3SS) to inject effector proteins (virulence factors) directly into host cells. These effectors manipulate host cells to the pathogen advantage, and can suppress plant immunity by targeting key signalling components (Macho & Zipfel, 2015).

Similar to host phosphatases that negatively regulate PRR complexes, bacterial effectors interfere with the phosphorylation status of PRR complexes to block the early steps of PTI signalling. The *P. syringae* effector AvrPto acts as a general kinase inhibitor, targeting RKs, such as FLS2 and EFR, to inhibit PTI responses triggered by multiple PAMPs (Shan *et al.*, 2008; Xiang *et al.*, 2008). Another *P. syringae* effector, HopAO1, displays tyrosine phosphatase activity and inhibits elf18-triggered immunity by dephosphorylating EFR tyrosine residues (Macho *et al.*, 2014). The *Xanthomas campestris* pv. *campestris* effector AvrAC possesses a previously uncharacterized uridylyl transferase activity, and uridylylates key phosphosites of several RLCKs, including BIK1, to block PTI signalling (Feng *et al.*,

2012). Remarkably, *Arabidopsis* detects AvrAC virulence by using the decoy substrate PBL2, which is guarded by the NBS-LRR ZAR1 (Wang *et al.*, 2015a). Additionally, the *Xoo* effector Xoo1418, a protein of unknown function, interacts with several rice RLCKs and prevents CERK1-dependent phosphorylation of OsRLCK185, suppressing both PGN- and chitin-triggered immune responses (Yamaguchi *et al.*, 2013).

HopAI1 from *P. syringae* permanently inactivates MAPKs by removing the phosphate group of phospho-threonines (Zhang *et al.*, 2007); however, its action on *Arabidopsis* MPK4 is recognized by the NBS-LRR SUMM2 (Zhang *et al.*, 2012).

Some bacterial effectors target immune signalling components for degradation: *P. syringae* cysteine protease AvrPphB cleaves BIK1 and other PBLs (Zhang *et al.*, 2010), and can be recognized by the NBS-LRR RPS5 (Shao *et al.*, 2003); whereas AvrPtoB functions as an ubiquitin E3 ligase to promote degradation of FLS2, EFR and CERK1 (Abramovitch *et al.*, 2006; Gohre *et al.*, 2008; Gimenez-Ibanez *et al.*, 2009a).

Several bacterial effectors manipulate JA signalling in order to suppress PTI. RIN4 is an intrinsically disordered protein conserved across plants and was recently found to play an important role in JA signalling and stomatal opening by regulating the H⁺-ATPase AHA1 (Lee *et al.*, 2015; Zhou *et al.*, 2015). Interestingly, a number of effectors have been found to target RIN4, but *Arabidopsis* RIN4 is guarded by two NBS-LRRs, RPS2 and RPM1 (Mackey *et al.*, 2002; Axtell & Staskawicz, 2003; Mackey *et al.*, 2003; Wilton *et al.*, 2010; Chung *et al.*, 2011; Liu *et al.*, 2011). In addition, the *P. syringae* effectors HopZ1a and HopX1 promote degradation of JAZ proteins, the key repressors of JA signalling (Jiang *et al.*, 2013; Gimenez-Ibanez *et al.*, 2014).

1.6. Thesis objectives and overview

As discussed in the previous sections, the different layers of the plant innate immune system are under tight regulation by a variety of mechanisms. Of particular interest for this thesis are the mechanisms that control activation of PRR complexes. It is becoming evident that protein phosphatases can play an important role in monitoring the phosphorylation status of such complexes, as demonstrated by the cases of KAPP and FLS2, XB15 and XA21, PLL4/PLL5 and EFR, and PP2A and BAK1. However, the molecular details underlying these relationships have not yet been fully elucidated, especially in terms of the potential mechanisms employed by the plant to relieve the phosphatase-imposed restrictions on PRR complexes. Moreover, it is likely that additional yet unidentified negative regulators may exist to control the phosphorylation status of PRRs and PRR-associated proteins. In particular, and although CPK28 has already been shown to modulate signalling amplitude by regulating BIK1 protein levels, no mechanism is currently known to control the phosphorylation status of this central immune regulator.

This thesis aims at identifying and characterizing the protein phosphatase PP2C38 as a novel negative regulator of PRR complexes. PP2C38 was initially found to interact with EFR cytoplasmic domain in a yeast two-hybrid screening. In Chapter 3, I describe the biochemical characterization of PP2C38 in regards to its association with EFR and FLS2, as well as with BIK1, *in planta*. Furthermore, I demonstrate that PP2C38 negatively regulates the phosphorylation status of BIK1, but not of EFR, during PAMP perception.

In Chapter 4, I reveal the biological relevance of PP2C38 during PTI signalling. I could show that PP2C38 negatively regulates the PAMP-induced ROS burst, most likely due to its effect on BIK1 phosphorylation. Consequently, PP2C38 also has a negative impact on stomatal immunity, a process known to be linked to ROS production.

In the last research Chapter (Chapter 5), I followed up on the observation that PP2C38 specifically dissociates from BIK1 after PAMP treatment. This dissociation correlated with the PAMP-induced phosphorylation of PP2C38, which occurs primarily at S77. I further demonstrated that S77 phosphorylation was required for PP2C38-BIK1 complex dissociation following PAMP perception, and proposed BIK1 as the most likely candidate to phosphorylate PP2C38. This led us to propose a model in which PP2C38 is phosphorylated by BIK1 upon PAMP perception, causing it to dissociate and relieving the regulatory constraint on BIK1. An expanded discussion of this model is provided in Chapter 6.

Chapter 2: Material and Methods

2.1. Plant material and growth conditions

2.1.1. *Arabidopsis thaliana* lines

In this study, all *Arabidopsis thaliana* genotypes used belong to the Columbia-0 (Col-0) ecotype. The full list of lines used in this study can be consulted in Table 2.1.

Table 2.1. List of *Arabidopsis thaliana* lines.

Lines	AGI code	Description	Reference/ SALK code
Col-0	-	Columbia-0, wild-type	-
<i>fls2 efr cerk1</i>	AT5G46330 AT5G20480 At3G21630	Triple T-DNA insertion mutant	Gimenez-Ibanez <i>et al.</i> (2009b)
<i>pp2c38-1</i>	AT3G12620	T-DNA insertion mutant	SALK_036920
<i>pp2c48-1</i>	AT3G55050	T-DNA insertion mutant	SALKseq_061058
<i>pp2c38-1 pp2c48-1</i>	AT3G12620 AT3G55050	Double T-DNA insertion mutant	-
Col-0/35S:PP2C38-GFP (pK7FWG2.0)	AT3G12620	Homozygous T3 transgenic line	-
<i>pp2c38-1/35S:PP2C38-GFP</i> #4.3 (pK7FWG2.0)	AT3G12620	Homozygous T3 transgenic line	-
<i>pp2c38-1/35S:PP2C38-GFP</i> #7.4 (pK7FWG2.0)	AT3G12620	Homozygous T3 transgenic line	-
<i>efr/pEFR:EFR-GFP</i>	AT5G20480	Homozygous T3 transgenic line	Nekrasov <i>et al.</i> (2009)

2.1.2. Plants grown on soil

For most applications, *Arabidopsis* plants were grown at 20 °C in a short-day photoperiod (10/14 hours) and 65 % humidity for 4-5 weeks. For seed bulking, plants were transferred to a long-day photoperiod (16/8 hour). *Nicotiana benthamiana* plants were grown at 24 °C with 45-65 % relative humidity under long-day conditions.

2.1.3. Plants grown on plates

Sterile *Arabidopsis* seeds were sown on plates containing Murashige-Skoog (MS) salts medium (Duchefa Biochemie) and 0.8 % agar, incubated for 2 days at 4 °C and then grown at 20-22 °C with a long-day photoperiod.

2.1.4. Plants grown on liquid media

Arabidopsis seedlings were grown in MS plates for 7-10 days as described above, and then transferred to liquid MS media in 6- or 24-well plates under sterile conditions, and grown at 22 °C with a long-day photoperiod.

2.1.5. *Arabidopsis* seed sterilization

Seeds were gas sterilized in a desiccator with a beaker containing 40 ml sodium hypochlorite solution (chlorine bleach) and 3 mL 37 % HCl. After a treatment time of 3-4 hours, seeds were dried in a sterile hood for 1 hour.

2.1.6. Generating stable transgenic *Arabidopsis* lines

Transgenic *Arabidopsis* lines were generated by floral dip method (Clough and Bent, 1998). All plant transformations were performed by the TSL Tissue Culture and Transformation support group. Transformants were then selected on MS agar plates supplemented with appropriated antibiotic.

2.1.7. Crossing of *Arabidopsis* plants

Individual flowers of mature *Arabidopsis* plants were emasculated using fine tweezers and fresh pollen from donor stamens was patted onto each single stigma. Mature siliques containing F1 seeds were harvested. Success of crossing was confirmed by genotyping, and plants containing desired alleles of both parents were grown as described above and allowed to self-pollinate.

2.2. Bacterial Strains

The bacterial strains used in this study are listed on Table 2.2.

Table 2.2. Bacterial strains.

Species	Strain	Use	Resistance	Reference
<i>Escherichia coli</i>	DH5 α	Molecular cloning	-	-
	BL21	Recombinant protein expression	-	-
<i>Agrobacterium tumefaciens</i>	GV3101	Plant transformation	Rifampicin, Gentamicin	-
<i>Pseudomonas syringae</i> pv. <i>tomato</i>	DC3000/ <i>hrcC</i>	Plant infection assay	Rifampicin, Chloramphenicol	Yuan and He (1996)

2.3. Culture media and reagents

2.3.1. Reagents and elicitors

Unless otherwise indicated, all reagents were purchased from Sigma-Aldrich.

Flg22 and elf18 peptides were purchased from EZ Biolab. Chitin was purchased from Sigma-Aldrich.

2.3.2. Culture media recipes

All recipes are for the scale of 1 L. Solutions were all sterilized by autoclaving.

LB (Lysogeny broth):

10 g tryptone, 5 g yeast extract, 10 g NaCl, pH 7.0. For solid medium, 10 g agar was included.

MS (Murashige Skoog):

4.3 g MS salts, 0.59 g MES, 0.1 g myo-inositol, 1 mL of 1000x MS vitamin stock, 10 g sucrose, pH=5.7 (with KOH). For solid medium, 8 g phytoagar.

2.3.3. Antibiotics

All antibiotics were used in the following final concentrations

Kanamycin: 50 µg/mL for bacteria and plants

Carbenicillin: 100 µg/mL for bacteria

Spectinomycin: 100 µg/mL for bacteria

Rifampicin: 50 µg/mL for bacteria

Gentamicin: 25 µg/mL for bacteria

Hygromycin: 40 µg/mL for plants and 100 µg/mL for bacteria

Nystatin: 10 µg/mL to prevent fungal contamination

2.4. Biological assays

2.4.1. PAMP-induced ROS assay

Leaf discs (4 mm diameter) of four 5-week-old plants were sampled using a biopsy punch tool and incubated O/N in 100 µL sterile water in a white 96-well plate (Greiner, Germany). The following day the water was replaced with 100 µL solution containing 17 µg/mL (m/v) luminol (Sigma-Aldrich), 10 µg/mL horseradish peroxidase (HRP, Sigma-Aldrich) and the indicated concentration of PAMP solution. Luminescence was measured using a Varioskan Flash (Thermo Scientific) multi plate reader or a Photek camera (East Sussex, UK).

2.4.2. Bacterial spray infection

Pseudomonas syringae pv. *tomato* (*Pto*) DC3000 *hrcC*⁻ strain was grown for 2 days in LB agar plates supplemented with appropriate antibiotics. A single colony was inoculated in a 200 mL LB cultures with appropriate antibiotics and grown ON at 28 °C with shaking. Cells were harvested by centrifugation for 5 min at 5.000 g and resuspended in sterile 10 mM MgCl₂ and OD_{600nm} adjusted to 1.0. Prior to spraying, 80 µL Silwett L-77 was added to 200 mL of bacterial solution. 4-8 soil grown plants

were sprayed with bacterial solution until all leaves were equally covered. Plants were covered with a dome for 1 day and bacterial growth assessed at 4 dpi. For this, three leaf discs (6 mm diameter) per plant were ground with a pestle in 10 mM MgCl₂, serially diluted and plated on LB agar plates with appropriate antibiotics (including nystatin to prevent fungal growth).

2.4.3. Stomatal closure

Leaf discs (4 mm) from soil-grown plants were incubated in stomatal opening buffer for 2-3 hours in a plant growth cabinet under white light. Subsequently, mock, ABA, flg22 or elf18 solutions with the indicated concentrations were added to the buffer, and samples incubated under the same conditions for 1-2 hours. Abaxial leaf surfaces were photographed under a light microscope (Leica DM 6000). Stomatal aperture was measured using ImageJ software as maximum width and length ratio.

Stomata opening buffer:

10 mM MES-KOH, pH 6.15; 50 mM KCl; 10 µM CaCl₂; 0.01 % Tween-20

2.5. Molecular biology

2.5.1. DNA Methods

2.5.1.1. Isolation of plant genomic DNA

Isolation of genomic DNA for genotyping and cloning purposes was performed using the 'Edward's buffer method' (Edwards *et al.*, 1991). One mature leaf or 2-4 ten-day-old *Arabidopsis* seedlings were ground in 400 µL extraction buffer [200 mM Tris-HCl (pH7.5), 250 mM NaCl, 25 mM EDTA, 0.5 % SDS] and centrifuged for 5 min at 16,000 *g*. Supernatant was transferred to new tubes and the same volume of isopropanol was added. Solution was vortexed and centrifuged as before. The remaining pellet was washed with 70 % ethanol, air-dried at room temperature and dissolved in 100 µL of water.

2.5.1.2. Plasmid DNA isolation from *E. coli* (miniprep).

Single *E. coli* colony 5 mL LB cultures supplemented with the appropriate antibiotics were pelleted by 1 min centrifugation at 16,000 *g*. Plasmid DNA was extracted using the NucleoSpin Plasmid Miniprep Kit (Macherey-Nagel) according to the manufacturer's instructions. Isolated DNA was dissolved in 30-50 μ L of water.

2.5.1.3. Plasmid DNA isolation from *E. coli* (maxiprep).

Single *E. coli* colony 200 mL LB cultures supplemented with the appropriate antibiotics were pelleted 10 min centrifugation at 5,000 *g* at 4 °C. Plasmid DNA was extracted using the HiSpeed Plasmid Maxi Kit (Qiagen) according to the manufacturer's instructions. DNA was eluted in 1 mL water.

2.5.1.4. Nucleic acid separation on agarose gels.

DNA fragments or total RNA were separated by electrophoresis on 1-2% agarose gels, prepared in 1 x TAE buffer (40 mM Tris-HCl, 20 mM NaOAc, 1 mM EDTA, pH 7.9) containing 1 μ g/mL ethidium bromide (Sigma). 10 x loading buffer [50 % (m/v) glycerol, 50 mM EDTA, 10 x TAE, 0.25 % (m/v) Orange G (Sigma-Aldrich)] was added to the samples and gels ran at 80-100 V. Gels were visualized using a UV transilluminator (GelDoc 1000, Bio-Rad).

2.5.1.5. DNA extraction from Agarose gels.

DNA fragments were excised from gel under UV light. DNA was extracted using the NucleoSpin Gel and PCR Clean-up (Macherey-Nagel) following the manufacturer's instructions.

2.5.1.6. DNA sequencing

Each reaction consisted of 2.5 µL DNA, 2.5 µL primer (10 µM stock) and 5 µL water. Sequencing was performed by GATC Biotech AG (Cologne, Germany) and results analysed using the CLC Workbench (QIAGEN) software.

2.5.2. PCR methods

2.5.2.1. General PCR conditions

All primers used in this study were purchased from Sigma-Aldrich and used in 0.5 µM final concentration. dNTPs were purchased from Invitrogen and used in 200 µM final concentration. Cloning and genotyping PCRs were performed using the proof-reading Phusion High-Fidelity DNA Polymerase (NEB) or the Taq DNA Polymerase (NEB), respectively, with the supplied reaction buffers. Reactions were incubated in a G-Storm Thermocycler (Life Science Research) programmed as described in Tables 2.3. All primers used in this study are listed in Table 2.4.

Table 2.3. Program for cloning and genotyping PCRs.

Step	Temperature	Duration	Number of cycles
Initial denaturation	98 °C	5 min	1
Denaturation	98 °C	30 sec	30-35
Annealing	50-60 °C*	30 sec	
Extension	72 °C	0.5-3 min**	
Final extension	72 °C	5 min	1

* The annealing temperature was set according to the melting temperature of the primer pair.

** The elongation time was set according to the length of the PCR fragment (30 sec per 1 Kb for Phusion Polymerase; 1 min per 1 Kb for NEB Taq Polymerase).

Table 2.4: Primers used in this study.

Primer name	Primer sequence (5'-3')
Genotyping <i>pp2c38-1</i> and <i>pp2c48-1</i> mutant lines	
SALK_036920L	CCTCTTCGACAACATCAGGAG
SALK_036920R	TTGCTGCCTCTCTTAGAGCTG
SALKseq_061058L	GGTATTGGAGAAGATTCTAGTCCTG
SALKseq_061058R	GACAGAGATCGGAGTTTCGAGTAGC
Quantitative RT-PCR	
<i>PP2C38</i> F1	TGTTGGAGCTTGTTGTCTGG
<i>PP2C38</i> R1	ACGATAACTGAACGGCCTTG
<i>PP2C48</i> F1	AGGCTGCTCGGTTTGTAAC
<i>PP2C48</i> R1	TCCTCCTCTGTTGCTACAAACC
<i>UBQ10</i> F1	TGCGCTGCCAGATAATACACTATT
<i>UBQ10</i> R1	TGCTGCCCAACATCAGGTT
Molecular cloning and site-directed mutagenesis	
<i>EFR_CD</i> F1	ACAACAATGCCAGTGAT GGT
<i>EFR_CD</i> R1	GCTACATAGTATGCATGTC
<i>PP2C38_Bam</i> HI F1	TCAg gatccGTATCATCGGCAACTATATTGCG
<i>PP2C38_Xho</i> I R1	CCTctc gagTCAAGTAGAAGGTCCAGC
<i>PP2C38</i> GTW F1	CACCGCCA ACTTGTTTATTTA
<i>PP2C38</i> GTW R1	CACCATGGTATCATCGGCAAC
<i>PP2C38_S77A</i> F1	CTGTTAGTATGTTTGATgCTGGTCCTCAAGCTAC
<i>PP2C38_S77A</i> R1	GTAGCTTGAGGACCAGcATCAAACATACTAACAG
<i>PP2C38_D87N</i> F1	CTTTTGTTGGTGTTTATaaTGGTCATGGTGGTCC
<i>PP2C38_D87N</i> R1	GGACCACCATGACCAttATAAACACCAACAAAAG
<i>PP2C38_D289N</i> F1	GTTTCTTATATTTGCATCAaaCGGCTTGTGGGAGCAC
<i>PP2C38_D289N</i> R1	GTGCTCCCACAAGCCGttTGATGCAAATATAAGAAAC
<i>PP2C58</i> GTW F1	CACCCATCCACAGAAGACAGTAAAAGC
<i>PP2C58</i> GTW R1	CACCATGGCAGGCAGTAATATTCTCC

2.5.2.2. Colony PCR

A small fraction of a single *E. coli* or *A. tumefaciens* colony was resuspended in 10 μ L water and mixed with 10 μ L of PCR reaction mixture. Colony PCRs were performed using Taq DNA Polymerase (NEB). Reactions were run in a G-Storm Thermocycler (Life Science Research) programmed as described in Table 2.5.

Table 2.5. Program for colony PCR.

Step	Temperature	Duration	Number of cycles
Initial denaturation	98 °C	10 min	1
Denaturation	98 °C	30 sec	30-35
Annealing	50-60 °C*	30 sec	
Extension	72 °C	0.5-2 min**	
Final extension	72 °C	5 min	1

*The annealing temperature was set according to the melting temperature of the primer pair.

** The elongation time was set according to the length of the PCR fragment (1 min per 1 Kb for NEB Taq Polymerase).

2.5.2.3. Site-directed mutagenesis

Site-directed mutagenesis was performed by PCR amplification of DNA fragment with complementary forward and reverse primers harbouring the desired mutation; a small plasmid vector (typically pENTR) containing the desired DNA fragment was used as template. PCR mixture was prepared with 0.75 μ M Phusion High-Fidelity DNA Polymerase (NEB), GC buffer, 1.5 μ L DMSO, 25-50 μ g DNA template plasmid, 0.5 μ M of each primer in a total volume of 50 μ L. A reaction without primers and polymerase was used as a control. Reactions were incubated in a G-Storm Thermocycler (Life Science Research) programmed as described in Table 2.6. In order to eliminate template DNA after the PCR, 10 μ L PCR product were digested with the restriction enzyme 2 μ L DpnI in 15 μ L 1 x Buffer 3.1 (NEB) for 3 hours at 37 °C. Five microliters of the reaction were then transformed in chemically competent cells and plated in LB plates with appropriate antibiotics.

Table 2.6. PCR program for site-directed mutagenesis.

Step	Temperature	Duration	Number of cycles
Initial denaturation	98 °C	1 min	1
Denaturation	98 °C	10 sec	18
Annealing	58 °C	60 sec	
Extension	72 °C	2-4 min*	
Final extension	72 °C	5 min	1

* The elongation time was set according to the length of the PCR fragment (30 sec per 1 Kb).

2.5.3. RNA methods

2.5.3.1. Isolation of total RNA from plants

RNA was isolated from soil-grown *Arabidopsis* plants or 2-week-old seedlings grown in liquid MS medium. Total RNA was extracted as described in (Couto *et al.*, 2015). Briefly, tissue was ground in liquid nitrogen and cells lysed by adding Lysis buffer, vortexing and incubating at room temperature for 5 min. Then, Protein-DNA precipitation solution was added and samples were incubated for 10 min on ice. Samples were centrifuged for 15 min at 16,000 *g* and supernatant collected. The same volume of isopropanol was added and samples mixed, and centrifuged for 5 min at 16,000 *g*. Resultant pellet was then washed with 70 % ethanol, air-dried and resuspended in RNase-free water. Remaining gDNA was removed by addition of DNase I (RQ1 RNase-free DNase, Promega). RNA was the precipitated with isopropanol and sodium citrate to remove DNase. Finally, the pellet was dissolved in RNase-free water. The quality and concentration of the isolated RNA was assessed by checking the absorbance ratios with a Nanodrop device (ThermoFisher), and by running it on an agarose gel. A PCR using the isolated RNA as template was performed to check for gDNA contamination; in case this was found, addition DNase digestion was performed.

Lysis buffer:

2 % SDS; 68 mM sodium citrate; 132 mM citric acid; 1 mM EDTA

Protein-DNA precipitation solution:

4 M NaCl; 16 mM sodium citrate; 32 mM citric acid

2.5.3.2. Reverse transcription PCR

First-strand cDNA synthesis was performed using 2-5 µg total RNA with SuperScript III RNA transcriptase (Invitrogen) and oligo(dT₁₈)-primers, according to the manufacturer's instructions.

2.5.3.3. Quantitative real-time PCR

The qRT-PCR was performed using SYBR Green JumpStart Taq ReadyMix (Sigma-Aldrich) in a CFX96 real-time system (Bio-Rad), programmed as indicated in Table 2.7. The relative expression values were determined by using U-box gene (*At5g15400*) as reference and the comparative Ct method ($2^{-\Delta\Delta Ct}$). Primers used for quantitative PCR are listed in Table 2.4.

Table 2.7. Program used for qRT-PCR.

Step	Temperature	Duration	Number of cycles
Initial denaturation	95 °C	4 min	1x
Denaturation	94 °C	10 sec	39 x
Annealing	60 °C	15 sec	
Extension	72 °C	10 sec	
read plate			
Melting curve	65 to 95 °C	5 sec	
read plate			

2.5.4. Molecular cloning

Both classical “cut and paste” and GATEWAY (Invitrogen) methods were used for cloning in this study. PCR fragments were separated on agarose gel and extracted. After cloning into primary/entry vector, the insert sequence was confirmed by performing a colony PCR or restriction digest, followed by DNA sequencing. A list of the vector backbones and constructs used in this study can be consulted in Tables 2.8 and 2.9.

Table 2.8. Vector backbones used in this study.

Vector	Use	Method	Source/ reference	Resistance
pGEM-Teasy	Subcloning	Classical	Promega	Carbenicillin
pENTR-D-TOPO	Subcloning	GATEWAY	Invitrogen	Kanamycin
pGWB411 (C-term. FLAG)	Plant expression	GATEWAY	Nakagawa <i>et al.</i> (2007)	Spectinomycin
pUC19-35S-FLAG- RBS (N/C-term. FLAG)	Plant expression	Classical	Li <i>et al.</i> (2005)	Carbenicillin
pK7FWG2,0 (C- term. GFP)	Plant expression	GATEWAY	Karimi <i>et al.</i> (2005)	Carbenicillin/ Hygromycin (plant)
pGEX-4T1 (N-term. GST)	<i>E. coli</i> expression	Classical	GE Healthcare	Carbenicillin
pMALc4e (N-term. MBP)	<i>E. coli</i> expression	Classical	NEB	Carbenicillin

Table 2.9. Constructs used in this study.

Construct	Backbone	Use	Source/ reference
35S:EFR-GFP-His	pEarleyGate103	<i>N. benthamiana</i> expression	Cloned by Yasuhiro Kadota
35S:FLS2-GFP-His	pEarleyGate103	<i>N. benthamiana</i> expression	Cloned by Benjamin Schwessinger
35S:BIK1-eGFP	pK7FWG2,0	<i>N. benthamiana</i> expression	Cloned by Cecile Segonzac
35S:PP2C38-FLAG	pGWB411	<i>N. benthamiana</i> expression	-
35S:PP2C38 ^{S77A} -FLAG	pGWB411	<i>N. benthamiana</i> expression	-
35S:PP2C38 ^{D87N D289N} -FLAG	pGWB411	<i>N. benthamiana</i> expression	-
35S:PP2C38-FLAG	pUC19-35S-FLAG-RBS	Protoplast expression	Cloned by Xiangxiu Liang
35S:PP2C38 ^{S77A} -FLAG	pUC19-35S-FLAG-RBS	Protoplast expression	-
35S:PP2C38 ^{D87N D289N} -FLAG	pUC19-35S-FLAG-RBS	Protoplast expression	-
35S:BIK1-HA	pUC19-35S-FLAG-RBS	Protoplast expression	Zhang <i>et al.</i> (2010)
35S:BIK1 ^{K105E} -HA	pUC19-35S-FLAG-RBS	Protoplast expression	Zhang <i>et al.</i> (2010)
35S:FLAG-RBOHD	pUC19-35S-FLAG-RBS	Protoplast expression	Li <i>et al.</i> (2014b)
35S:PP2C38-eGFP	pK7FWG2.0	<i>Arabidopsis</i> and <i>N. benthamiana</i> expression	Cloned by Roda Niebergall
35S:PP2C58-eGFP	pK7FWG2.0	<i>N. benthamiana</i> expression	Cloned by Roda Niebergall
GST-BIK1	pGEX-4T1	<i>E. coli</i> expression	Kadota <i>et al.</i> (2014)
GST-BIK1 ^{K105E}	pGEX-4T1	<i>E. coli</i> expression	Kadota <i>et al.</i> (2014)
MBP-PP2C38	pMALc4e	<i>E. coli</i> expression	-
MBP-PP2C38 ^{S77A}	pMALc4e	<i>E. coli</i> expression	-
MBP-PP2C38 ^{D87N D289N}	pMALc4e	<i>E. coli</i> expression	-

2.5.4.1. Restriction digests

For test digestions, 0.5 µg DNA were incubated with 1 µL restriction buffer, 1 µL restriction enzyme and water up to 10 µL. For subcloning, 1-2 µL DNA were incubated with 1.5 µL restriction buffer, 1.5 µL restriction enzyme and water up to 15

µl. Reactions were incubated at 37 °C for 1 to 3 hours. Restriction fragments were separated by agarose gel-electrophoresis. Restriction enzymes used in this study were purchased from NEB, Roche or Invitrogen and used according to the manufacturer's instructions.

2.5.4.2. Subcloning into pGEM-T easy

Per reaction 1.5 µL of adenylated PCR product were mixed with 2.5 µL 2 x Ligation buffer (Promega), 0.5 µL pGEM-T Easy (Promega) and 0.5 µL T4 Ligase (Promega). Reactions were incubated for 1 hour at 16 °C, and transformed into chemical competent cells.

2.5.4.3. Cloning into destination vector

Inserts were cut from subcloning vectors by restriction digest. Resulting insert fragments and digested destination vector were ligated following a 3:1 molar ratio (using 100-200 ng plasmid DNA), with 1 µL ligation buffer (NEB) and 1 µL T4-ligase (NEB) in a final volume of 10 µL. Reactions were incubated 1-3 hours at 16 °C, and transformed into chemical competent cells.

2.5.4.4. GATEWAY cloning into pENTR vectors

For GATEWAY cloning, all forward cloning primers contained a CACC extension at the 5'-end. First, PCR fragments were cloned into pENTR-D-TOPO (Invitrogen) by combining 0.5 µL plasmid DNA, 0.5 µL salt solution (Invitrogen), 2.5 µL insert DNA and 1.5 µL water. The reaction was incubated for 30 min at room temperature and transformed into chemically competent cells

2.5.4.5. GATEWAY cloning into pDEST vectors (LR reaction)

To clone inserts from pENTR D-TOPO into a destination vector (Table 2.8), the GATEWAY LR reaction was performed. Reactions contained 1 μ L pENTR clone, 2 μ L pDEST vector, 1 μ L Tris-EDTA (pH 8.0) and 1 μ L LR clonase II mix (Invitrogen), and were incubated for 1-2 hours at room temperature. Reactions were transformed into chemically competent cells.

2.5.4.6. Transformation of plasmids into *E. coli* by heat shock

Chemically competent cells were thawed on ice. For each transformation, 2.5-5 μ L DNA were gently mixed with 50-100 μ L chemically competent cells, followed by heat shock was performed at 42 °C for 45 sec, and incubation on ice for 90 sec. After addition of 1 mL LB, cells were incubated with shaking at 37 °C for 1 hour, plated on selection plates (LB with appropriate antibiotic) and grown ON at 37 °C.

2.5.4.7. Transformation of plasmids into *A. tumefaciens* by electroporation

Electro-competent cells were thawed on ice. For each transformation, 2.5-5 μ L DNA were gently mixed with 20 μ L electro-competent cells and 40 μ L 10 % glycerol in a 1 mm electroporation cuvette. Electroporator (Bio-Rad) set as follows: 1800 V with a capacity of 25 μ F over 200 Ω resistance. After adding 500 μ L LB, cells were incubated with shaking at 28 °C for 1 hour and plated on selection plates (LB with appropriate antibiotics), and grown for 2-3 days at 28 °C.

2.6. Protein work

2.6.1. Protein separation by polyacrylamide gel electrophoresis

The Mini-PROTEAN Tetra Electrophoresis System (Bio-Rad) was used for all polyacrylamide gel electrophoresis (PAGE), except if otherwise stated. Stacking and resolving bisacrylamide gels were prepared as described by (Laemmli, 1970). Gels were run in Mini-PROTEAN III gel tanks (Bio-Rad) filled with SDS-running buffer (25 mM Tris, 250 mM glycine, pH 8.3, 0.1 % SDS). The gel electrophoresis was performed in a continuous buffer system at 90 V until samples reached the separating gel and then with 100-130 V until the desired separation was reached. At least one lane of each gel was loaded with 5 μ L of PageRuler Prestained Protein Ladder, 10 to 180 kDa (ThermoFisher).

2.6.2. Wet blotting

After PAGE, proteins were transferred to a PVDF membrane (ThermoFisher). For this, gels were equilibrated for at least 5 min in pre-chilled transfer buffer [25 mM Tris-HCl, 192 mM glycine, 20 % (v/v) methanol, pH 8.3]. PVDF membranes were activated by brief incubation in methanol and washed in transfer buffer. Transfer cassettes were assembled as follows: the cathode panel of the gel holder cassette (black side) was placed in a tray containing transfer buffer, then a sponge was placed on top, followed by one square of Whatman paper and the gel. The activated membrane was placed on top of the gel; care was taken to keep both the gel and membrane wet and to avoid air bubbles. A second square of Whatman paper and a sponge pad were placed on top of the membrane, the cassette closed and placed on the transfer system. Proteins were transferred for 90 min at 100 V or O/N at 30 V and 4 °C.

2.6.3. Immunodetection

PVDF transfer membranes containing immobilised proteins were blocked for at least one hour at RT in blocking solution [5 % (m/v) dried skimmed milk powder in TBS buffer [50 mM Tris-HCl, pH=7.5; 150 mM NaCl, supplemented with 0.1 % (v/v)

Tween-20 (TBST)] with gentle shaking. Membranes were then incubated with desired antibody (Table 2.10) in TBST containing 5 % dried skimmed milk powder (m/v). The membranes were washed three times for 5 min with TBST before incubation with a secondary antibody. Before detection, membranes were washed three times in TBST and once in TBS to rinse the excess detergent. Peroxidase signal of the antibody-HRP conjugate was detected with ECL (ThermoFisher) or ECL femto (ThermoFisher), following the manufacturer's instructions. The membranes were exposed for variable times onto Fuji Medical X-Ray Film (Fuji).

Table 2.10. Antibodies used in this study.

Antibody	Company	Origin	Final dilution	Incubation time
α -HA-HRP	Santa Cruz	Rabbit	1:5,000	2 hours
α -GFP-HRP	Santa Cruz	Rabbit	1:5,000	2 hours
α -FLAG-HRP	Sigma-Aldrich	Mouse	1:5,000	2 hours
α -FLS2	Eurogentec	Rabbit	1:5,000	4 hours
α -BAK1	Eurogentec	Rabbit	1:5,000	4 hours
α -RBOHD-pS39	Abmart	Rabbit	1:2,000	4 hours
α -Rabbit-HRP (A0545)	Sigma-Aldrich	Goat	1:10,000	1 hour

2.6.4. Coomassie brilliant blue (CBB) staining

Membrane bound proteins were stained for 30 sec with CBB staining solution [0.5 % (m/v) Coomassie brilliant blue R-250 (Sigma-Aldrich), 50 % (v/v) methanol, and 7.5 % (v/v) glacial acetic acid] and de-stained for 30-60 min with de-stain solution [20 % (v/v) methanol, 5 % (v/v) acetic acid].

2.6.5. Expression of recombinant proteins in *N. benthamiana*

A. tumefaciens cells containing the desired plasmid were grown at 28 °C for 2 days LB agar plates supplemented with the appropriate antibiotics. Cells were collected with a plastic tip and resuspended in 10 mM MgCl₂ and 150 μ M Acetosyringone,

pelleted by centrifugation at 5,000 *g*, and washed twice in the same buffer. Cell suspensions were adjusted to OD_{600nm} = 0.3 before infiltration of four-week-old *N. benthamiana* leaves using a 1 mL needleless syringe. All samples were collected two days post inoculation, subjected to PAMP treatment if required, frozen in liquid nitrogen and stored at -80 °C.

2.6.6. Isolation and transfection of *Arabidopsis* protoplasts

Arabidopsis plants were soil-grown in short-light (10/14 hour) photoperiod for 4-5 weeks. Leaves were cut into 0.5-1 mm strips with a razor blade, transferred to enzyme solution, vacuum infiltrated for 3 min and incubated at room temperature with gentle shaking (30 rpm/min) for 1.5-2 hours. Protoplasts were then released by increasing shaking to 80 rpm/min for 2 min. Protoplasts were filtered through a 35-75 mm nylon mesh, pelleted by 3 min centrifugation at 100 *g*, resuspended in W5 buffer and left to rest on ice for 30 min. Protoplasts were again pelleted by centrifugation and resuspended in MMg buffer at a concentration of 2-5 10⁵ cells/mL. For transfection, 200 µL–2 mL protoplast solution (depending on amount required) and 5-100 µg plasmid DNA were gently mixed together. PEG solution was then added to protoplast solution (1:1 ratio) and gently mixed for 2 min, and then incubated for 10 min. Transfection was stop by addition of W5 (1:1.5 to initial protoplast solution). Protoplasts were pelleted by centrifugation, resuspended in 0.5-2 mL W5 buffer and incubated O/N in the dark in a controlled environment chamber at 23 °C. If required, protoplasts were then treated with PAMP solution, pelleted by centrifugation and frozen in liquid nitrogen.

Enzyme solution:

1.5 % cellulase R10 (Duchefa Biochemie); 0.4 % macerozyme R10 (Yakult Honsha, Tokyo, Japan); 0.4 M mannitol; 20 mM KCl; 20 mM MES, pH 5.7; 10 mM CaCl₂; 0.1 % BSA (Sigma-Aldrich, A-6793). Solution was heated for 10 min at 55 °C before

addition of CaCl₂ and BSA to help enzyme solubilisation. Finally, solution was filtered with a 0.45 mm filter.

W5 buffer:

154 mM NaCl; 125 mM CaCl₂; 5 mM KCl; 2 mM MES (pH 5.7)

MMg buffer:

0.4 M mannitol; 15 mM MgCl₂; 4 mM MES (pH 5.7)

PEG solution:

40 % (m/v) PEG4000 (Sigma-Aldrich); 0.2 M mannitol; 100 mM CaCl₂

2.6.7. Protein extraction from *N. benthamiana* and *Arabidopsis*

Plant material was grinded in liquid nitrogen with pre-chilled pestle and mortar and transferred to pre-chilled tubes. *N. benthamiana* samples for immunoprecipitation were added 20 mg PVPP per g of frozen tissue. Extraction buffer was added to ground tissue (2:1 v/m) and incubate for 60 min with gentle mixing at 4 °C. Extracts were centrifuged for 20 min at 16,000 g and 4 °C (Sorvall RC-5B centrifuge with SM-24/ 34 rotor). For large samples, extracts were filtered through Bio-Spin exclusion columns (Bio-Rad) into 50 mL falcon tubes.

In all protein extractions performed in this study, protein concentrations were determined using the Bio-Rad Protein Assay Kit (Bio-Rad) and samples were normalised to the same protein concentration in Falcon tubes or 1.5 mL micro-centrifuge tubes. For total extract preparation, 100 µL of samples was separated and mixed with 20 µL 6 x SDS sample buffer and 10 mM DTT.

Extraction buffer:

150 mM Tris pH 7.5; 150 mM NaCl; 10 % Glycerol; 10 mM EDTA; 5-10 mM DTT; 1 % protease inhibitor (Sigma); 0.5-2 % IGEPAL CA-630 (Sigma-Aldrich) (v/v).

For analysis of phosphorylation status, 1 mM Sodium Molybdate and 1 mM NaF was added. In case samples for mass spectrometry (MS) analysis, 1 % Phosphatase Inhibitors 3 and 4 (Sigma-Aldrich) were added.

SDS sample buffer (6x):

300 mM Tris-HCl (pH 6.8); 60 % glycerol; 6 % SDS; 0.05 % Bromophenol blue; 50 mM DTT (added fresh)

2.6.8. Protein immunoprecipitation

Protein extracts were extracted as described above and incubated with the desired beads (as described below) for 1-3 hours at 4 °C with gentle mixing. Beads were collected by centrifugation for 30 sec at 500 g. Beads were washed 3-5 times with extraction buffer. After the last washing, the remaining supernatant was carefully removed with a needle fitted on a syringe. Unless otherwise stated, proteins were eluted from the beads by adding 50 µL 2 x SDS sample buffer + 10 mM DTT. Samples for MS analysis were eluted in 50 µL 2 x LDS-buffer (Invitrogen) + 10 mM DTT. Proteins were denatured by incubating for 5-15 min at 70-90 °C, centrifuged for 5 min at 16,000 g and separated by PAGE.

2.6.9. α-GFP and α-HA immunoprecipitation

Per sample, 20-100 µL GFP-Trap (Chromotek) or anti-HA Affinity Matrix (Roche) beads were washed twice in extraction buffer and added to protein extracts.

2.6.10. α-FLAG immunoprecipitation

Per sample 20-100 µl ANTI-FLAG M2 Affinity Gel (Sigma) were washed twice in extraction buffer. For MS analysis samples, immunoprecipitated proteins were eluted three times with 50 µL 0.2 M FLAG peptide (Sigma-Aldrich) in extraction buffer with vigorous shaking for 10 min at room temperature. Eluted sample collected after centrifugation for 1 min at 500 g. Samples were passed through a Micro Bio-Spin exclusion column (Bio-Rad) to remove remaining beads. Samples were then mixed with 4 x NuPAGE LDS Sample Buffer (ThermoFisher).

2.6.11. Submission of immunoprecipitated protein samples for mass spectrometry analysis

Immunoprecipitated protein samples for MS analysis were run in pre-cast gels using the NuPAGE SDS-PAGE Gel System (ThermoFisher), in 1x MOPS buffer (ThermoFisher) supplemented with Antioxidant solution (ThermoFisher) for 90 min at 150 V. Gels were then washed three times with boiling water, stained with Simply Blue Safe Stain (ThermoFisher) for 2 hours or ON, and destained with water. Desired protein fractions were excised with a razor blade, cut into small pieces and further destained by washing with 50 % ethanol at 55 °C and strong shaking.

2.6.12. Identification of phosphosites by mass spectrometry

Immunoprecipitated proteins were digested in-gel by Trypsin and AspN. LC-MS/MS analysis was performed using an LTQ-Orbitrap mass-spectrometer (Thermo Scientific) and a nanoflow-HPLC system (nanoAcquity; Waters) as described previously (Kadota *et al.*, 2014). The *Arabidopsis* database (TAIR10) was searched using Mascot (v 2.4.1 Matrix Science). Parameters were set for 10 ppm peptide mass tolerance and allowing for Met oxidation and three missed cleavages. Carbamidomethylation of Cys residues was specified as a fixed modification, and oxidized Met and phosphorylation of Ser, Tyr or Thr residues were allowed as variable modifications. Scaffold (v4; Proteome Software) was used to validate MS/MS-based peptide and protein identifications and annotate spectra. The position and quality of spectra for phosphopeptides were also manually examined before acceptance. Mass spectrometry analysis was performed by the TSL Proteomics Support Group.

2.6.13. Expression of GST- and MBP-tagged recombinant of proteins in *E. coli*

For each purification, chemically competent *E. coli* BL21 cells were freshly transformed with the desired plasmid, and a single colony inoculated in 5 ml LB

medium supplied with appropriate antibiotic and grown ON with shaking at 37 °C. On the next day, 2 mL of culture were transferred to a 100 mL LB culture with antibiotic (2g/L glucose was added for MBP protein samples) and cells were grown with shaking at 37 °C until $OD_{600nm} = 0.6-0.9$. Recombinant protein expression was induced by adding 0.1 mM IPTG. Cultures were incubated with shaking at 20-28 °C for 2-4 hours. Cells were pelleted by centrifugation for 10 min at 5,000 g, frozen in liquid nitrogen and stored at -20 °C.

2.6.14. Purification of GST-tagged proteins

Harvested frozen cells were resuspended in 6 mL BugBuster Protein Extraction Reagent (Milipore), 1 mM DTT, 1 mM phenylmethylsulfonyl fluoride (PMSF), 1 mM EDTA and 2 μ L Benzonase Nuclease (Sigma-Aldrich), and incubated for 20 min at room temperature. Samples were diluted to 10 mL with column buffer and centrifuged for 20 min at 12,000 g at 4 °C. Supernatant was filtered through a Bio-Spin exclusion column (Bio-Rad). GST-tagged proteins were batch-purified by adding 50 μ L Glutathione Sepharose High Performance (GE Healthcare) affinity matrix and incubating 30-60 min with gentle mixing at 4 °C. Beads were pelleted by centrifuging 1 min at 1,000 g and washed three times with column buffer. GST proteins were eluted three times with 50 μ L elution buffer (50 mM Tris-HCl, pH 8.0 and 10 mM reduced glutathione). If required, GST proteins were concentrated in Amicon Ultra-4 Centrifugal Filter columns (Milipore). Proteins were mixed with DTT (final concentration of 0.5 mM) and glycerol [final concentration of 10 % (v/v)], frozen in liquid nitrogen and stored at -80 °C.

Column buffer:

50 mM Tris-HCl pH= 7.5; 150 mM NaCl; 1 mM EDTA; 1 mM DTT

2.6.15. Purification of MBP-tagged proteins

Harvested frozen cells were resuspended in 6 mL BugBuster Protein Extraction Reagent (Milipore), 1 mM DTT, 1 mM phenylmethylsulfonyl fluoride (PMSF), 1 mM EDTA and 2 μ L Benzonase Nuclease (Sigma-Aldrich), and incubated for 20 min at room temperature. Samples were diluted to 10 mL with binding buffer and centrifuged for 20 min at 12,000 *g* at 4 °C. Supernatant was filtered through a Bio-Spin exclusion column (Bio-Rad). MBP-tagged proteins were batch-purified by adding 50 μ L Amylose Resin (NEB) affinity matrix and incubating 30-60 min with gentle mixing at 4 °C. Beads were pelleted by centrifuging 1 min at 1,000 *g* and washed three times with column buffer. MBP proteins were eluted three times with 50 μ L binding buffer + 10 mM maltose. If required, MBP proteins were concentrated in Amicon Ultra-4 Centrifugal Filter columns (Milipore). Proteins were mixed with DTT (final concentration of 0.5 mM) and glycerol [final concentration of 10 % (v/v)], frozen in liquid nitrogen and stored at -80 °C.

Binding buffer:

20 mM Tris-HCl (pH= 7.4); 200 mM NaCl; 1 mM EDTA

2.7. Enzymatic assays

2.7.1. Phosphatase treatment

To dephosphorylate PP2C38, FLAG-tagged PP2C38 was co-expressed with EFR-GFP in *N. benthamia*, and samples treated with 100 nM elf18 for 20 min. PP2C38-FLAG was immunoprecipitated, beads were washed (without phosphatase inhibitors) and 270 μ L water and 30 μ L Buffer 3 (NEB) were added. Solutions were mixed thoroughly and equally divided in three tubes. The first tube was used as a control and no phosphatase was added; the second and third tubes were added 4 μ L calf intestinal phosphatase (CIP, NEB). To the third tube, in addition, different phosphatase inhibitors [50 mM NaF, 50 mM EDTA, 10 mM NaVO₃] were added. Reactions were incubated for 1 hour at 37 °C. Then 30 μ L 4 x LDS buffer

(Invitrogen) were added. Proteins were denaturated by incubation for 10 min at 90 °C, centrifuged for 2 min at 16,000 *g* and separated on 12 % bisacrylamide gels.

2.7.2. PP2C activity assays

PP2C phosphatase activity was measured using a Serine/Threonine Phosphatase Assay kit (Promega, 2009) according to the manufacturer's instructions. Briefly, immunoprecipitated or purified recombinant phosphatase proteins were incubated in 1 x PP2C buffer with the synthetic phosphopeptide in a final volume of 80 µL for 15 min at 30 °C with shaking. Reaction was stopped by addition of provided Molybdate dye solution. Samples were separated in three as technical replicate, and absorbance measured at 600 nm in a plate reader (Varioscan).

PP2C buffer (5x): 250 mM imidazole (pH 7.2); 1 mM EGTA; 25 mM MgCl₂; 1mM DTT; 0.5 mg/ml BSA.

2.7.3. Trans-phosphorylation assays

Recombinant kinase proteins were incubated in kinase buffer supplemented with 1 µM unlabeled ATP and 183 kBq of [³²P]γ-ATP for 30-60 min at 30 °C with vigorous shaking. Phosphorylated kinases were then incubated with substrate protein for 30 min. Reactions were stopped by adding SDS sample buffer and heating at 70 °C for 15 min. Proteins were separated by SDS-PAGE and transferred onto PVDF membranes (Biorad), followed by staining with CBB. Phosphorylation was analyzed by autoradiography using a FUJI Film FLA5000 PhosphorImager (Fuji, Tokyo, Japan).

Kinase buffer:

50 mM Tris-HCl (pH 7.5); 5 mM MnCl₂; 1 mM DTT

2.7.4. IP-kinase assays

After the last wash of the protein immunoprecipitation procedure, the beads were washed with kinase buffer (to remove EDTA) and then were incubated in kinase buffer supplemented with 1 μ M unlabeled ATP and 183 kBq of [32 P] γ -ATP for 30-60 min at 30 °C with vigorous shaking. Reactions were stopped by adding SDS sample buffer and heating at 70 °C for 15 min. Proteins were separated by SDS-PAGE and transferred onto PVDF membranes (Biorad), followed by staining with CBB. Phosphorylation was analyzed by autoradiography using a FUJI Film FLA5000 PhosphorImager (Fuji, Tokyo, Japan).

Kinase buffer:

50 mM Tris-HCl (pH 7.5); 5 mM MnCl₂; 1 mM DTT

2.8. Cell biological assays

For subcellular visualization of fluorescent-tagged proteins, *N. benthamiana* leaves transiently overexpressing the desired proteins, or transgenic *Arabidopsis* cotyledons, were analysed with a Leica SP5 Confocal Microscope (Leica Microsystems, Germany).

2.9. Yeast two-hybrid screen

The EFR cytoplasmic domain (EFR-CD) was amplified from cDNA, cloned into the pAs-attR yeast two-hybrid screening bait plasmid and transformed into yeast strain AH109 (MATa). A cDNA libraries was generated from two-weeks-old *Arabidopsis* seedlings treated for 30 min with 10 μ M flg22, and cloned into pACT-attR yeast two-hybrid screening prey plasmids. Together with a cDNA library derived from *Arabidopsis* cell suspension culture (Nemeth *et al.*, 1998), as well as a commercially available cDNA library derived from *Arabidopsis* plants (Clontech), these three libraries were screened against EFR-CD by interaction mating as described

previously (Soellick & Uhrig, 2001). A total of eight million zygotes were screened, and 47 candidate interaction partners were obtained, facilitating yeast growth on triple-dropout media (lacking leucine, tryptophan and histidine, supplemented with 5 mM 3-Amino triazole). Three clones were identified as PP2C38, and five clones matched PP2C58. All yeast two-hybrid experiments were performed by Denise Altenbach and Joachim Uhrig at the University of Cologne (Germany).

2.10. Statistical analysis

All statistical analysis was performed using the Graph Pad Prism software. Here, the student t-test was used to analyse the values of two sample groups while the one-way ANOVA Tukey or Dunnet tests were used to analyse the values of three or more sample groups.

Chapter 3: The *Arabidopsis* protein phosphatase PP2C38 controls the phosphorylation status of the central immune kinase BIK1

3.1. Prologue

Plants recognize PAMPs/DAMPs by means of PRRs that associate in dynamic RK complexes at the PM. Ligand perception leads to recruitment of regulatory RKs, initiating a series of trans-phosphorylation events that spread from within the PRR complex to downstream signalling cascades and eventually lead to the establishment of PAMP-triggered immunity (Bohm *et al.*, 2014; Macho & Zipfel, 2014). It is becoming increasingly clear that the first immediate downstream substrates of activated RK complexes at the PM are RLCKs (Macho & Zipfel, 2014). This is particularly evident in PTI signalling, where BIK1 and related PBL proteins have emerged as central immune regulators, after proving to be crucial for signal transduction in a variety of PRR-dependent pathways (Lu *et al.*, 2010; Zhang *et al.*, 2010; Liu *et al.*, 2013).

At the time when the present study was initiated, the mechanisms negatively regulating PRR complexes were poorly understood. The protein phosphatases KAPP and XB15 had already been proposed to negatively regulate FLS2 and XA21, but particularly for KAPP, biochemical and mechanistic data were sparse. Conversely, the project led by Cecile Segonzac in our laboratory that would culminate with the characterization of PP2A as a key negative regulator of BAK1 had just been started (Segonzac *et al.*, 2014). Moreover, despite the importance of RLCKs for RK-mediated signalling, hardly anything was known about the negative regulation of RLCKs. The identification and characterization of mutant suppressors of the PTI-impaired allele of *bak1-5* was also being carried out by Jacqueline Monaghan in parallel to this study in our laboratory. This project led to the identification of CPK28 as a negative regulator of BIK1, through control of protein turnover via the 26S proteasome (Monaghan *et al.*, 2014). Crucially, it became clear that CPK28 did not affect PAMP-induced

BIK1 hyper-phosphorylation, suggesting that additional regulatory mechanisms could still exist.

Within this scientific context, and with the knowledge that activation of PTI signalling is intimately associated with protein phosphorylation (Park *et al.*, 2012; Macho *et al.*, 2015), we decided to follow up on the characterization of the protein phosphatase PP2C38 as a potential regulator of PRR complexes. This was part of an on-going project in our laboratory initiated by the former PhD student Roda Niebergall. PP2C38 had initially been picked up in a yeast two-hybrid screen as an interactor of the EFR cytoplasmic domain. Before the end of her PhD, Roda successfully identified PP2C38 as a member of PRR complexes, associating *in planta* with EFR, FLS2 and BIK1. We decided to capitalise on these findings and extend on the molecular and mechanistic characterization of PP2C38 as a potential novel regulator of PRR complexes. We were particularly interested in identifying whether PP2C38 could dephosphorylate any or all of its newly identified interaction partners, and what would be the resulting consequences for the activation of the PRR complex.

3.2. Results

3.2.1. PP2C38 associates dynamically with the EFR-BIK1 and FLS2-BIK1 complexes

To identify novel regulators of PRR complexes in *Arabidopsis*, we performed a yeast two-hybrid (Y2H) screen using the cytoplasmic domain of EFR as bait against a prey library generated from *Arabidopsis* cDNA. This was done in collaboration with Joachim Uhrig at the University of Cologne (Germany). Given the crucial role of protein phosphorylation for activation of the PRR complex following PAMP perception and initiation of PTI signaling (Macho & Zipfel, 2014), we were particularly interested in two PP2C-type protein phosphatases, PP2C38 (At3g12620: (Xue *et al.*, 2008); also named PP2C-D3 (Spartz *et al.*, 2014) or APD1 (Tovar-Mendez *et al.*, 2014)) and PP2C58 (At4g28400), retrieved from this initial screen (Table 3.1).

Table 3.1. List of proteins interacting with EFR-CD in Y2H screen.

Y2H experiments were performed by Denise Altenbach and Joachim Uhrig at the University of Cologne (Germany).

AGI code	Name	Predicted function
At4G28400	PP2C58	Predicted PP2C phosphatase
At3G12620	PP2C38	Predicted PP2C phosphatase
At1G22410	-	3-deoxy-7-phosphoheptulonate synthase
At3G11773	-	Electron carrier/ protein disulfide oxidoreductase
At5G63930	-	LRR-RLK (subfamily XI)
At2G20890	THYLAKOID FORMATION1 (THF1)	Involved in vesicle-mediated formation of thylakoid membranes
At1G51760	IAA-ALANINE RESISTANT 3 (IAR3)	IAA-Ala (indole-3-acetic acid alanine)-conjugate hydrolase
At2G17560	HIGH MOBILITY GROUP B4 (HMGB4)	Assembly of nucleoprotein complexes
At4G34990	MYB DOMAIN PROTEIN 32 (MYB32)	Transcription factor

To test if PP2C38 and PP2C58 also associate with EFR *in planta*, we transiently co-expressed full-length EFR-GFP with PP2C38-FLAG or PP2C58-FLAG in *N. benthamiana*. After immunoprecipitation using GFP-Trap beads we detected a specific association between EFR-GFP and PP2C38-FLAG (Fig. 3.1A). However, the association between EFR-GFP and PP2C58-FLAG appeared nonspecific as PP2C58-FLAG also co-immunoprecipitated with free GFP (Fig 3.2A). Similarly, no association could be detected between PP2C58-HA and EFR-GFP (Fig 3.2B). Hence, we decided to focus our studies on the biochemical and functional characterization of PP2C38 only.

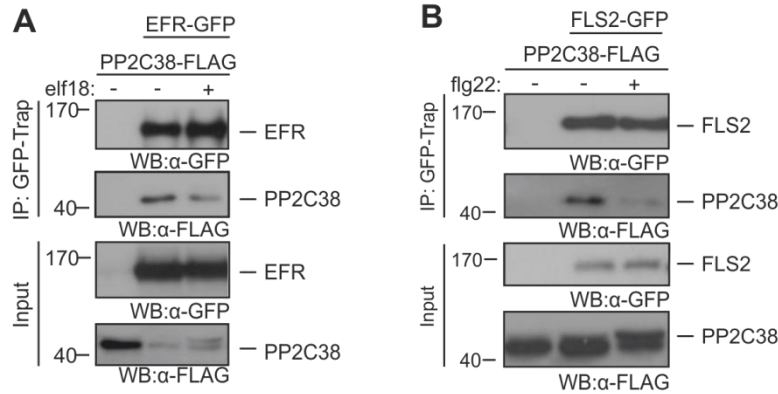


Figure 3.1. PP2C38 associates dynamically with EFR and FLS2 *in planta*.

(A-B) Co-immunoprecipitation of PP2C38 and EFR (A) or FLS2 (B) transiently expressed in *N. benthamiana* leaves treated (+) or not (-) with 100 nM elf18 (A) or flg22 (B) for 20 min. Experiments performed by Roda Niebergall.

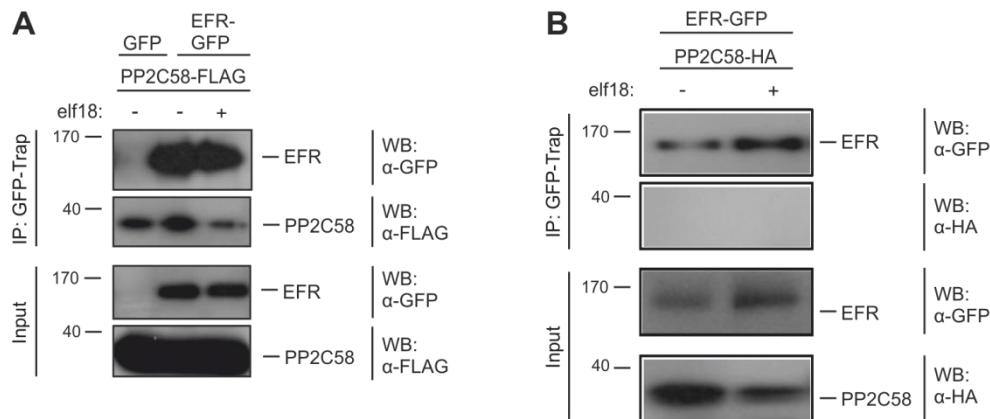


Figure 3.2. PP2C58 does not associate with EFR *in planta*.

(A-B) Co-immunoprecipitation of FLAG-tagged (A) or HA-tagged (B) PP2C58 and EFR proteins transiently expressed in *N. benthamiana* leaves treated (+) or not (-) with 100 nM elf18. Experiments performed by Roda Niebergall.

Remarkably, we consistently observed reduced levels of co-immunoprecipitated PP2C38-FLAG (but not of total protein) after elf18 treatment (Fig. 3.1A), indicating that PP2C38 dissociates from EFR after elf18 perception. Given the commonality of signalling components between the FLS2 and EFR pathways (Macho & Zipfel, 2014), we tested whether PP2C38 also associates *in planta* with FLS2. As observed with EFR, PP2C38-FLAG also formed a complex with FLS2-GFP, which was disrupted after flg22 treatment (Fig. 3.1B). Intriguingly, we noted that both elf18 and flg22 treatment induced a band shift of

PP2C38-FLAG protein on the immunoblot (Figs. 3.1A,B). To confirm the observed associations in *Arabidopsis*, we generated homozygous transgenic lines expressing *PP2C38-GFP* both in Col-0 and *pp2c38-1* background under the control of 35S promoter (Fig. 3.3). The line *pp2c38-1/ PP2C38-GFP 7.4* exhibited the highest expression levels (Fig 3.3B) and was thus selected for Co-IP experiments. We detected endogenous FLS2 in the PP2C38-GFP pull-down in mock-treated but not in flg22-treated seedlings (Fig. 3.4). Together, we concluded that PP2C38 forms a complex with FLS2 and EFR, and that this association is destabilized upon ligand perception.

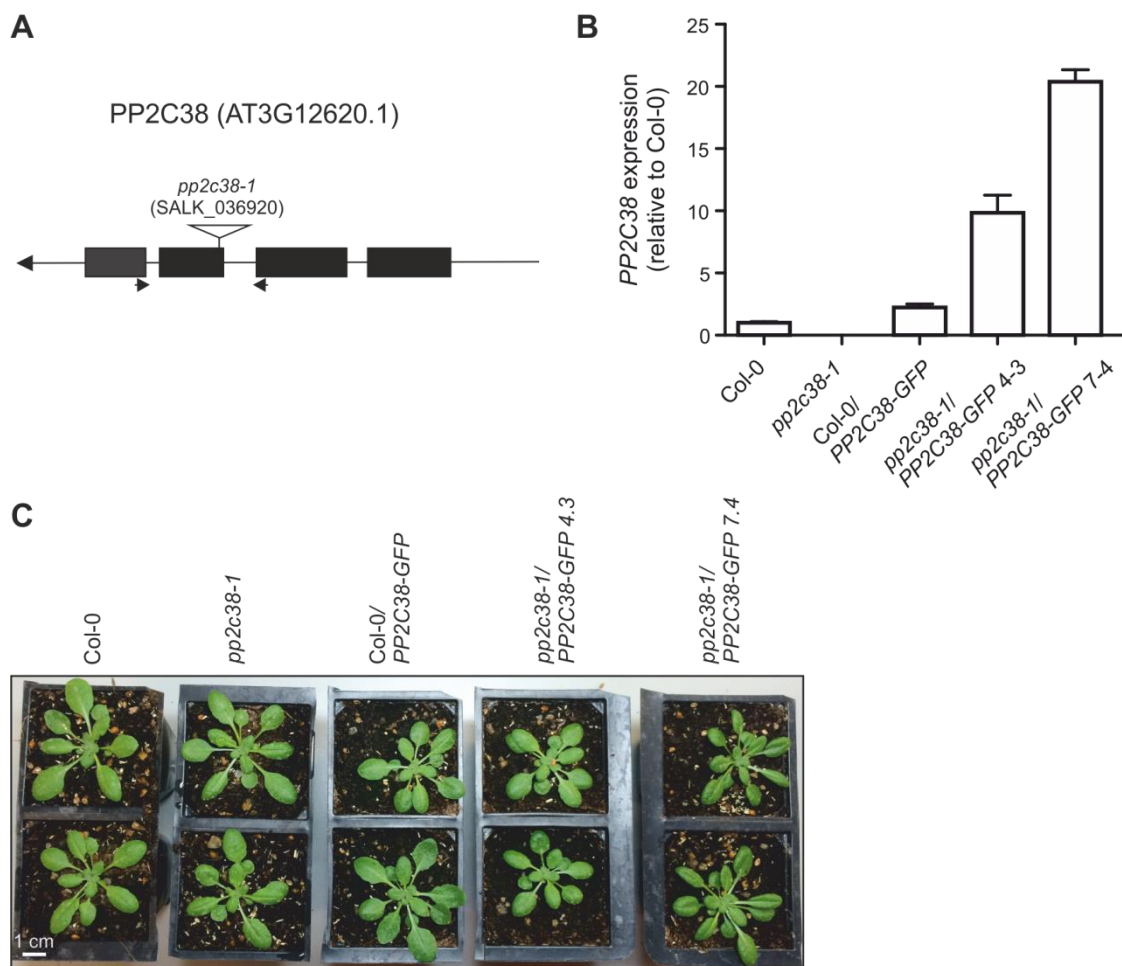


Figure 3.3. Characterization of *PP2C38* over-expression and mutant lines.

(A) Gene structure of *PP2C38* showing position of exons (boxes), introns (lines) and T-DNA insertion sites (triangle); arrows indicate position of primers used for genotyping.

(B) *PP2C38* expression analysis by quantitative RT-PCR. Expression was normalized to *UBQ10* and Col-0.

(C) Four-week-old *PP2C38* mutant and over-expression plants grown under short-days.

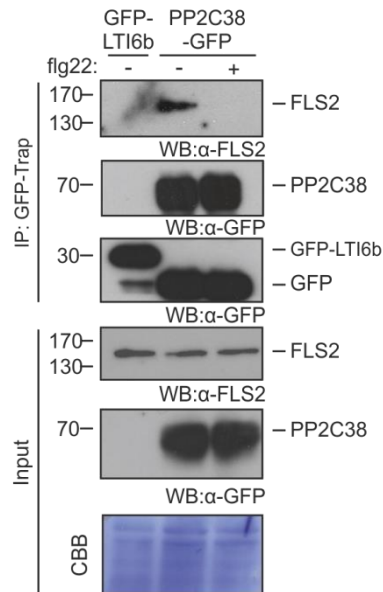


Figure 3.4. PP2C38 dynamically associates with FLS2 in *Arabidopsis* plants.

Co-immunoprecipitation of PP2C38 and FLS2 in stable transgenic *Arabidopsis* pp2c38-1/PP2C38-GFP 7.4 seedlings (T3). Seedlings were treated (+) or not (-) with 1 μ M flg22 for 20 min. Native FLS2 protein visualized in immunoblot using α -FLS2 antibody. The PM marker GFP-LTI6b (Cutler *et al.*, 2000) was used as a negative control. CBB staining used included for loading control.

EFR and FLS2 form dynamic complexes with different kinases, such as BAK1 and BIK1 (Chinchilla *et al.*, 2007; Heese *et al.*, 2007; Lu *et al.*, 2010; Zhang *et al.*, 2010; Roux *et al.*, 2011). Therefore, we tested whether PP2C38 also associates with these kinases. Co-immunoprecipitation of transiently expressed epitope-tagged proteins in *N. benthamiana* showed that PP2C38-FLAG also associates with BIK1-GFP (Fig. 3.5A). Similar to our previous observations with EFR and FLS2, PP2C38-FLAG dissociated from BIK1-GFP after flg22 treatment in *N. benthamiana* (Fig. 3.5A). A similar observation was made after elf18 treatment in *Arabidopsis* protoplasts co-expressing PP2C38-FLAG and BIK1-HA (Fig. 3.5B). In contrast, no association was detected between PP2C38-FLAG and BAK1-GFP in *N. benthamiana* (Fig. 3.5A). A band with a lower molecular size can be observed in Fig 3.5A in BAK1-containing samples that most likely corresponds to a BAK1-GFP cleavage product; such cleavage is frequently observed in our lab for different RKs (eg. EFR and FLS2), especially under over-expression conditions. Since C-terminally tagged BAK1 proteins are impaired in PTI signalling but not in their ligand-induced association with FLS2 (Ntoukakis *et*

al., 2011), we tested if PP2C38-FLAG could associate with endogenous BAK1 in *Arabidopsis* protoplasts. In line with previous experiments, we did not find evidence for their association (Fig. 3.5C). Interestingly, we noted that PP2C38-FLAG exhibits a constitutive band shift when co-expressed with BIK1-GFP (Fig. 3.5A). Taken together, our results indicate that PP2C38 associates dynamically with BIK1, in addition to forming a dynamic complex with EFR and FLS2.

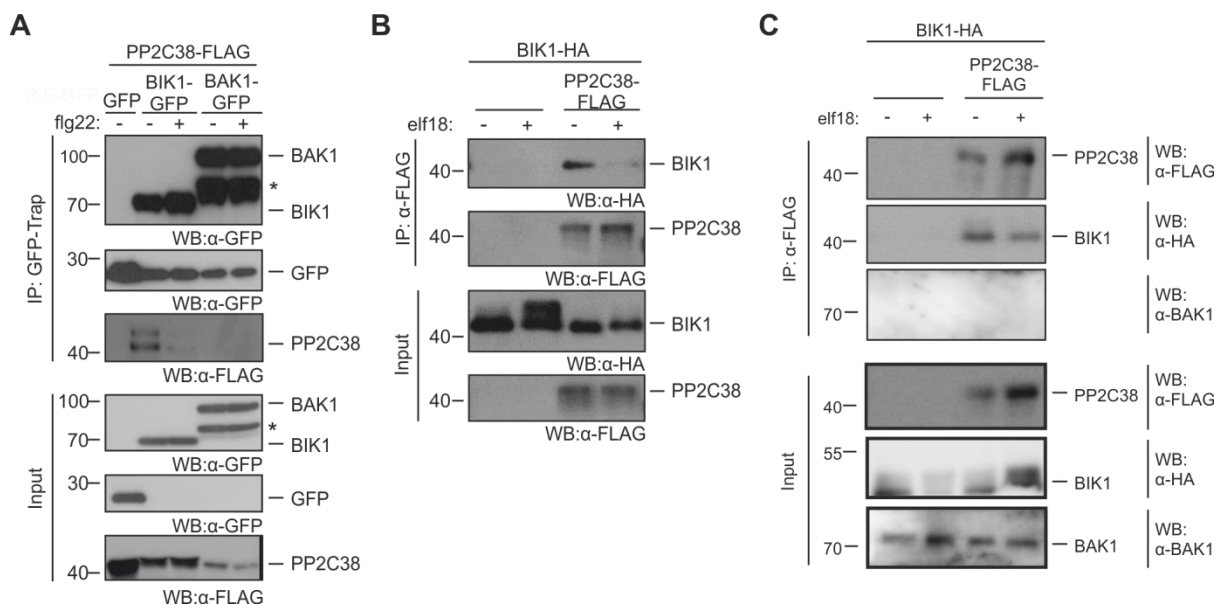


Figure 3.5. PP2C38 associates dynamically with BIK1 but not BAK1.

(A) Co-immunoprecipitation of PP2C38 and BIK1 or BAK1 transiently expressed in *N. benthamiana* leaves treated (+) or not (-) with 100 nM flg22 for 20 min. * indicates BAK1 cleavage product. Experiment performed by Roda Niebergall.

(B-C) Co-immunoprecipitation of PP2C38 and BIK1 transiently expressed in *Arabidopsis* Col-0 protoplasts. Protoplasts were treated (+) or not (-) with 1 μM elf18 for 30 min. Endogenous BAK1 was detected using α-BAK1 antibody (C).

All experiments were performed at least three times with similar results.

3.2.2. PP2C38 is an active PM-localized phosphatase

PP2C38 belongs to the clade D of *Arabidopsis* PP2Cs together with eight other members (Fig. 3.6A) (Fuchs *et al.*, 2013). PP2C38 clustered with PP2C48, with which it shares 75 % of amino acid identity and 92% of similarity. A BLAST analysis on the available genomes of several plant species retrieved several potential PP2C38 orthologs, including in monocots (Fig. 3.6B).

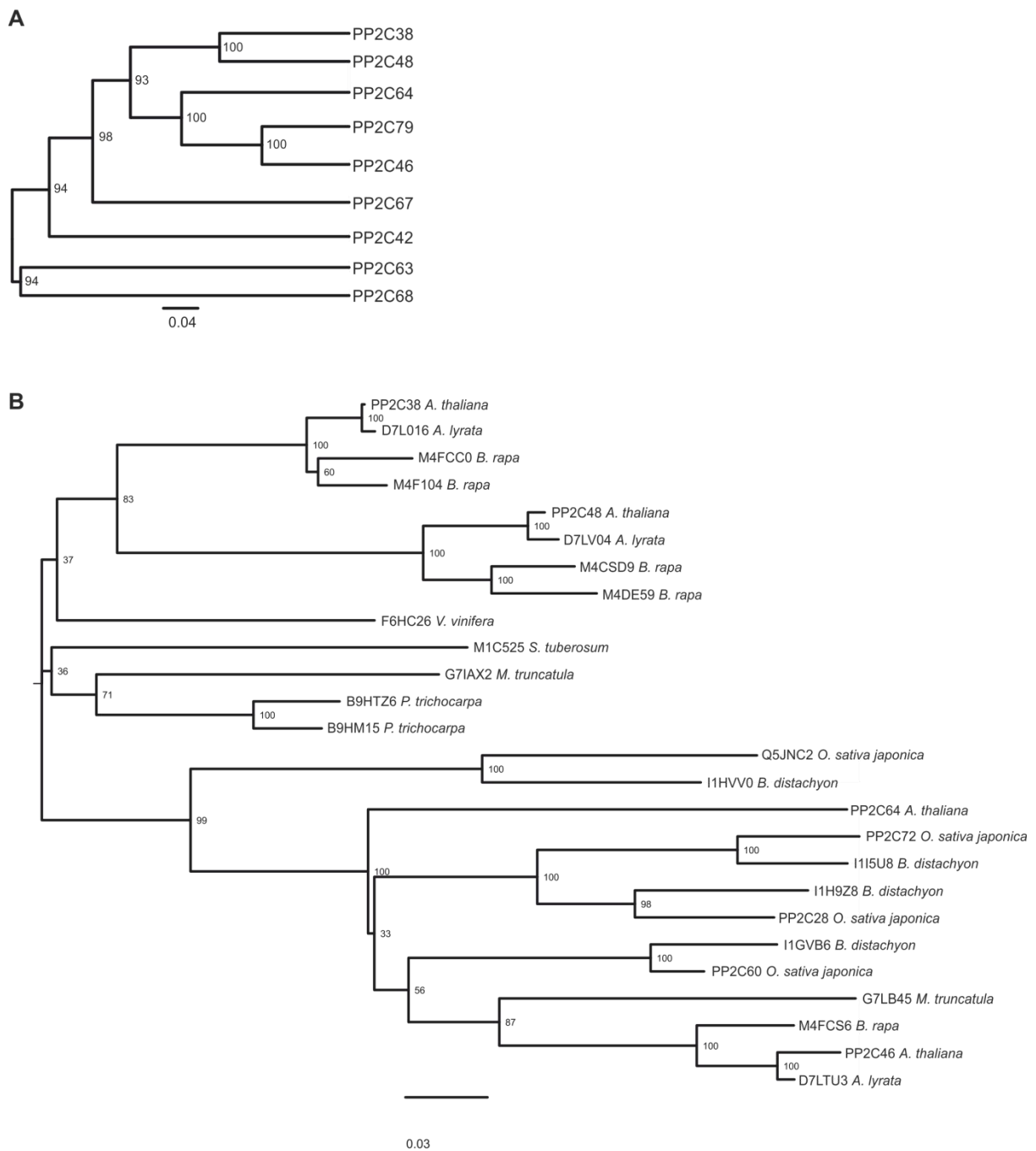


Figure 3.6. Phylogenetic analysis of *Arabidopsis* PP2C clade D and PP2C38 orthologs. (A) Protein sequences were aligned using clustalW and the tree generated using UPGMA. Numbers indicate bootstrap values from 100 replicates. (B) Distance trees are based on protein sequences aligned with MUSCLE (produced with SEAVIEW, using neighbour joining). Protein sequences retrieved from pBLAST search using PP2C38 as query. Nomenclature of *Arabidopsis* and *O. sativa japonica* proteins according to Xue *et al.* (2008); nomenclature of proteins from other plant species according to UniProt identifiers.

Alignment of PP2C38 with previously characterized plant PP2Cs, revealed its catalytic site is conserved (Fig 3.7A), including the Asp residues required for coordination of Mg²⁺ ions during catalysis (Conner *et al.*, 2006). To test if PP2C38 is a catalytically active protein phosphatase, we incubated recombinant MBP-PP2C38 with a generic synthetic phosphopeptide and assessed the release of inorganic phosphate in a colorimetric assay. PP2C38 exhibited typical Mg²⁺-dependent PP2C activity (Fig. 3.7B). As a control, we generated a phosphatase-inactive PP2C38* variant by converting the two Mg²⁺-coordinating aspartic acids D87 and D289. As expected, this variant was completely devoid of catalytic activity (Fig. 3.7B). Similarly, we detected phosphatase activity from transiently expressed PP2C38-FLAG protein purified from *N. benthamiana* leaves (Fig. 3.7C).

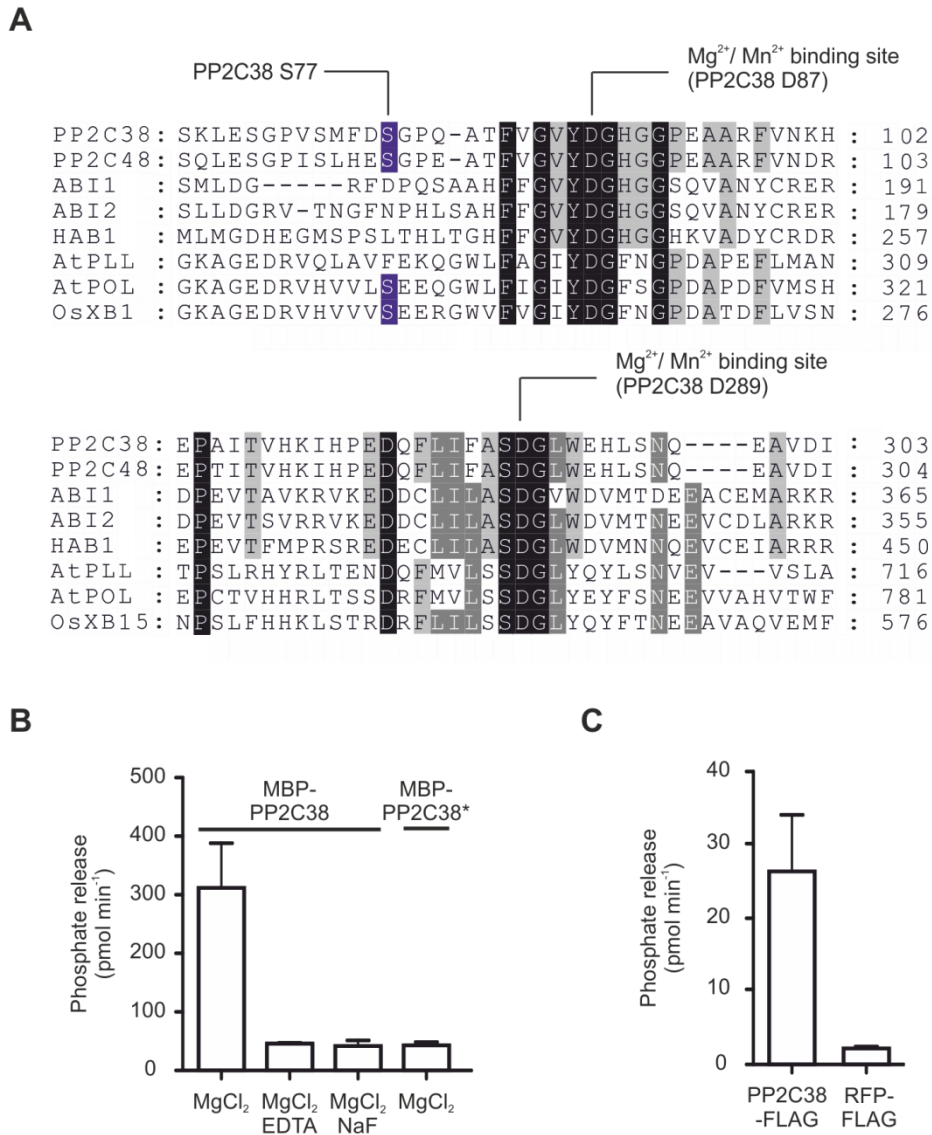


Figure 3.7. PP2C38 is an active PP2C.

(A) Alignment of PP2C38 and PP2C48 protein sequences with previously characterized plant PP2Cs. Conserved catalytic domain and Mg²⁺/Mn²⁺-binding aspartate residues are shown. Sequences were aligned using clustalW, and alignment was edited using GenDoc software.

(B) PP2C38 is an active phosphatase *in vitro*. Recombinant MBP-PP2C38 or MBP-PP2C38* proteins (where PP2C38* is a catalytically-inactive variant) were incubated with a synthetic phosphopeptide in the presence or absence of Mg²⁺ ions, cation chelator EDTA or phosphatase inhibitor NaF. Release of inorganic phosphate was quantified using a colorimetric assay. Values are averages ± SD (n = 3).

(C) PP2C38 is an active phosphatase *in vivo*. Immunoprecipitated PP2C38-FLAG or control RFP-FLAG proteins from *N. benthamiana* leaves were incubated with a synthetic phosphopeptide, and release of inorganic phosphate was quantified using a colorimetric assay.

To gain insight into PP2C38 function, we determined its subcellular localization by confocal microscopy analysis of cotyledons of *Arabidopsis* seedlings stably expressing *PP2C38-GFP*. We detected a strong GFP signal at the PM and in intracellular puncta (Fig. 3.8). The PM localization was further confirmed by induction of plasmolysis with a hyperosmotic sucrose solution (Fig. 3.8). PP2C38 has a putative palmitoylation site at position C154, which may explain its PM localization. Thus, the subcellular localization of PP2C38 is consistent with its interaction with EFR, FLS2 and the PM-associated cytoplasmic kinase BIK1 (Fig. 3.1), and suggests a potential role of PP2C38 in the regulation of PRR complexes.

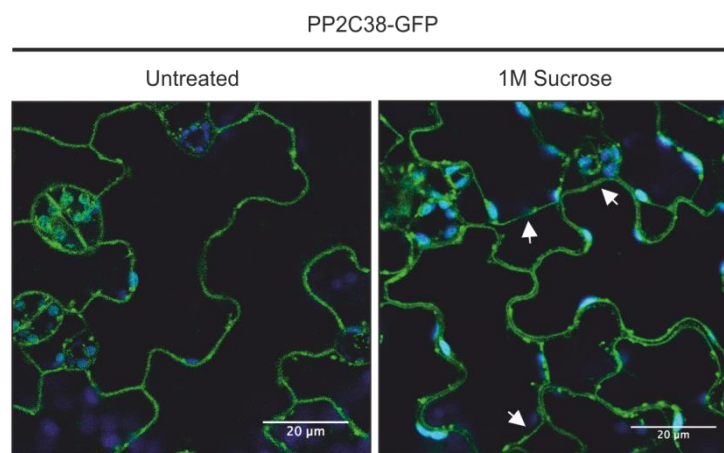


Figure. 3.8. PP2C38 localizes to the plasma membrane.

Confocal microscopy of *Arabidopsis* cotyledons stably expressing *PP2C38-GFP*. Plasmolysis (arrows) after 1 M sucrose treatment indicates plasma membrane localization. Images obtained with the help of Christoph A. Bücherl.

3.2.3. PP2C38 regulates BIK1 phosphostatus and activity

EFR and FLS2 phosphorylation is greatly enhanced after ligand perception, a step that is crucial for the activation of EFR kinase (Albrecht *et al.*, 2012; Sun *et al.*, 2013b; Macho *et al.*, 2014). Given the interaction between PP2C38 and EFR (Fig. 3.1), we first tested whether PP2C38 over-expression affects elf18-induced EFR kinase activation. We transfected PP2C38-FLAG or PP2C38*-FLAG into protoplasts obtained from *Arabidopsis* plants stably expressing EFR-GFP, and subsequently performed an *in vitro* kinase assay using ³²P-radiolabelled ATP on immunoprecipitated EFR (IP-kinase assay). Phosphorylation of EFR

was specifically detected after elf18 treatment (Fig. 3.9). Interestingly, this phosphorylation pattern was not affected by PP2C38 or PP2C38* over-expression (Fig. 3.9). We observed that PP2C38 and PP2C38* proteins exhibit a different migration pattern in the input. A possible explanation for this is discussed in Chapters 5 and 6. Although PP2C38 associates with EFR (Table 3.1; Fig. 3.1A), we concluded that PP2C38 is most likely not involved in the regulation of EFR phosphorylation status. Also, consistent with the lack of evidence for PP2C38-BAK1 association (Figs. 3.5), PP2C38 or PP2C38* over-expression did not affect the phosphorylation status of EFR-associated BAK1 upon elf18 treatment (Fig. 3.9).

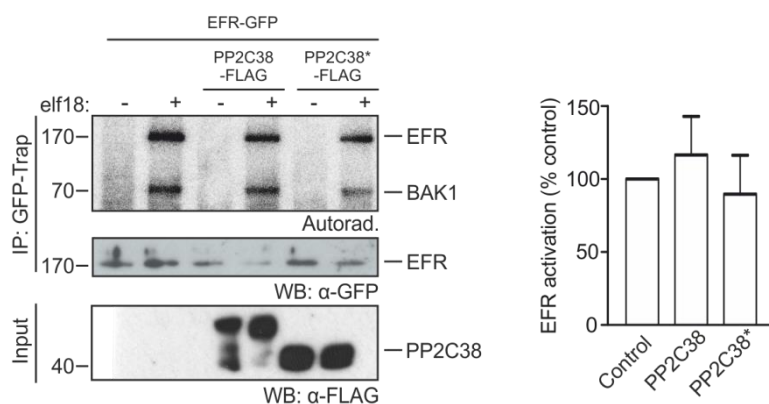


Figure 3.9. PP2C38 does not regulate EFR activation.

PP2C38 does not affect EFR activation. Protoplasts from *efr/pEFR:EFR-GFP* transgenic *Arabidopsis* plants transfected with PP2C38/PP2C38*-FLAG were treated with water (-) or 1 μ M elf18 (+). Immunoprecipitated EFR-GFP was incubated with [32 P] γ -ATP. *In vitro* phosphorylation is revealed by autoradiography. Graph (right panel) represents the densitometry measurements from three independent experiments; no significant differences were found based on one-way ANOVA analysis.

Besides EFR and FLS2 (Figs. 3.1 and 3.4), PP2C38 also associates with BIK1 (Fig. 3.5). To test if PP2C38 regulates BIK1 phosphorylation, we assessed the band shift of BIK1 induced by PAMP treatment due to hyper-phosphorylation (Lu *et al.*, 2010; Zhang *et al.*, 2010; Laluk *et al.*, 2011). Elf18 treatment enhanced BIK1 phosphorylation (pBIK1) in *Arabidopsis* protoplasts expressing BIK1-HA (Fig. 3.10A). Remarkably, BIK1 phosphorylation was markedly reduced when PP2C38-FLAG was co-transfected (Fig. 3.10A). Importantly, the reduction of BIK1 phosphorylation specifically required PP2C38 phosphatase activity, as co-expression of PP2C38*-FLAG restored elf18-induced BIK1 phosphorylation to normal levels

(Fig. 3.10A). Considering that PP2C38 over-expression did not affect EFR or BAK1 phosphorylation (Fig. 3.10A), these results are consistent with the hypothesis that PP2C38 directly dephosphorylates BIK1.

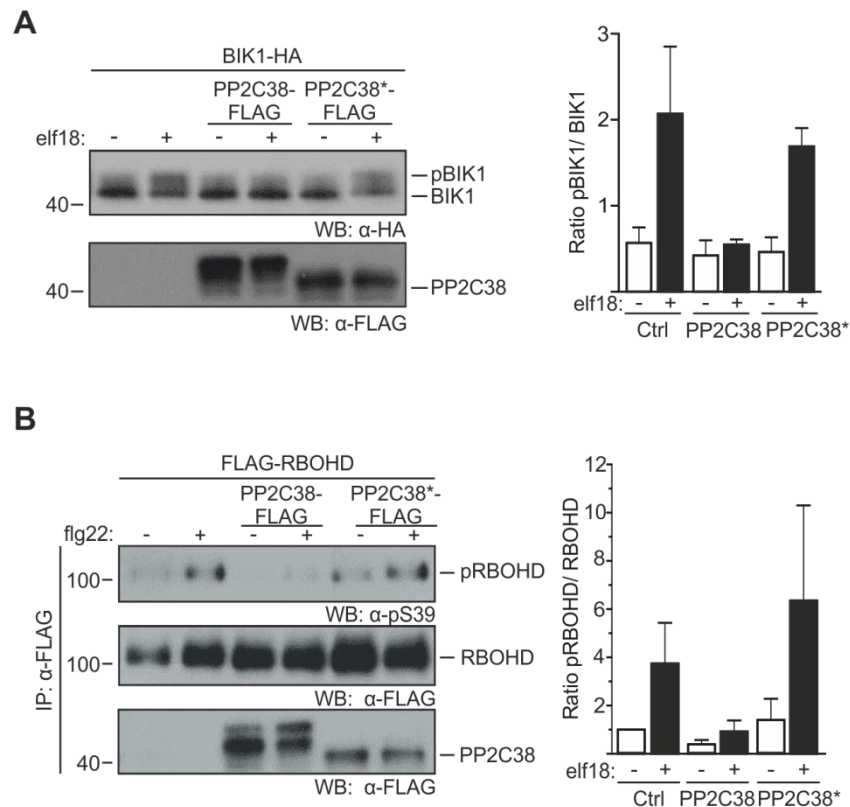


Figure 3.10. PP2C38 regulates BIK1 activation.

(A) PP2C38 negatively regulates elf18-induced BIK1 hyper-phosphorylation. *Arabidopsis* Col-0 protoplasts co-transfected with BIK1-HA and PP2C38/PP2C38*-FLAG were treated with water (-) or 1 μM elf18 (+). BIK1 phosphorylation ratio (right panel) calculated using densitometry measurements from three independent experiments. Experiments performed by Xiangxiu Liang in the lab of Jian-Min Zhou (Chinese Academy of Sciences, Beijing).

(B) PP2C38 inhibits elf18-triggered BIK1-dependent RBOHD phosphorylation. *Arabidopsis* Col-0 protoplasts co-transfected with FLAG-RBOHD and PP2C38/PP2C38*-FLAG were treated with water (-) or 1 μM flg22 (+). FLAG-RBOHD proteins were immunoprecipitated and S39 phosphorylation analysed using α-pS39 antibodies. Phosphorylation ratio (right panel) calculated using densitometry measurements from pRBOHD and immunoprecipitated RBOHD immunoblots, normalized to control (untreated) samples; average of three independent experiments. Experiments performed by Xiangxiu Liang in the laboratory of Jian-Min Zhou (Chinese Academy of Sciences, Beijing).

Next, we investigated whether PP2C38-mediated inhibition of BIK1 hyper-phosphorylation affects its ability to phosphorylate downstream targets. The NADPH oxidase RBOHD is, so far, the only known downstream substrate of BIK1 (Kadota *et al.*, 2014; Li *et al.*, 2014b).

Work previously carried out in our lab, as well as in the laboratory of Jian-Min Zhou (Chinese Academy of Sciences, Beijing, China), identified a number of BIK1-dependent RBOHD phosphosites (Kadota *et al.*, 2014; Li *et al.*, 2014b). These can be monitored using phosphosite-specific antibodies, and therefore be used as an effective proxy for BIK1 activation *in vivo*. We co-transfected FLAG-RBOHD with or without PP2C38/PP2C38*-FLAG in *Arabidopsis* protoplasts. FLAG-RBOHD was enriched by immunoprecipitation and phosphorylation of the BIK1-specific phosphosite S39 was assessed using anti-phospho S39 (α -pS39) antibodies (Li *et al.*, 2014b). After elf18 treatment, we detected a significant increase in RBOHD-S39 phosphorylation, which was reduced when PP2C38-FLAG, but not PP2C38*, was co-expressed (Fig. 3.10B). Interestingly, basal RBOHD-S39 phosphorylation was observed in the absence of PAMP treatment, but this was almost undetectable when PP2C38 was over-expressed (Fig. 3.10B). These results clearly demonstrate the requirement of PP2C38 phosphatase activity for repressing BIK1-mediated RBOHD phosphorylation. Taken together, our results indicate that PP2C38 is a negative regulator of BIK1 phosphorylation status and activity.

Chapter 4: PP2C38 is a negative regulator of PRR-triggered immunity

4.1. Prologue

In Chapter 3 we have shown that PP2C38 dynamically associates with EFR, FLS2 and BIK1 *in planta*. Consistent with these findings, we observed that PP2C38 mostly localizes to the PM. Moreover, we demonstrated that PP2C38 exhibits typical Mg²⁺-dependent phosphatase activity both when purified from bacterial or from plant. Notably, we further demonstrated that over-expression of PP2C38 did not affect the phosphorylation status of EFR or BAK1, but had a significant negative impact on PAMP-induced BIK1 hyper-phosphorylation, most likely through direct dephosphorylation. We then showed that PP2C38-mediated dephosphorylation inactivated BIK1, which could not fully phosphorylate RBOHD following PAMP treatment when co-expressed with PP2C38.

BIK1-mediated RBOHD phosphorylation activates ROS production, which is crucial for triggering PAMP-induced stomatal closure, an early PTI response thought to restrict pathogen entry into leaf tissues (Kadota *et al.*, 2014; Li *et al.*, 2014b). Accordingly, loss of BIK1 or BIK1-mediated phosphorylation of RBOHD results in deficient stomatal immunity against hypovirulent *P. syringae* strains (Kadota *et al.*, 2014; Li *et al.*, 2014b). The biological importance of BIK1 and related PBL kinases is further demonstrated by the fact that bacteria, such as *Pseudomonas syringae* and *Xanthomonas campestris*, secrete type-III secreted effectors into plant cells to cleave or inhibit these kinases, and thus block their action (Zhang *et al.*, 2010; Feng *et al.*, 2012).

In the present Chapter, we examine the consequences of tampering with BIK1 phosphorylation status, while attempting to determine the biological role PP2C38 within the context of PTI signalling.

4.2. Results

We sought to investigate the biological role of PP2C38-mediated BIK1 dephosphorylation. Having shown that PP2C38 inhibits PAMP-induced BIK1 hyper-phosphorylation and subsequent trans-phosphorylation of the NADPH oxidase RBOHD (Fig. 3.3), we tested whether this translates into an inhibition of BIK1-mediated immune outputs. We measured the flg22-induced ROS burst in *N. benthamiana* after transient over-expression of PP2C38. We observed that leaves expressing PP2C38-FLAG exhibited significantly reduced flg22-induced ROS burst (Fig. 4.1A). Similarly, stable homozygous *Arabidopsis* transgenic plants over-expressing *PP2C38-GFP* exhibited a significantly reduced flg22- and elf18-triggered ROS burst (Fig. 4.1B).

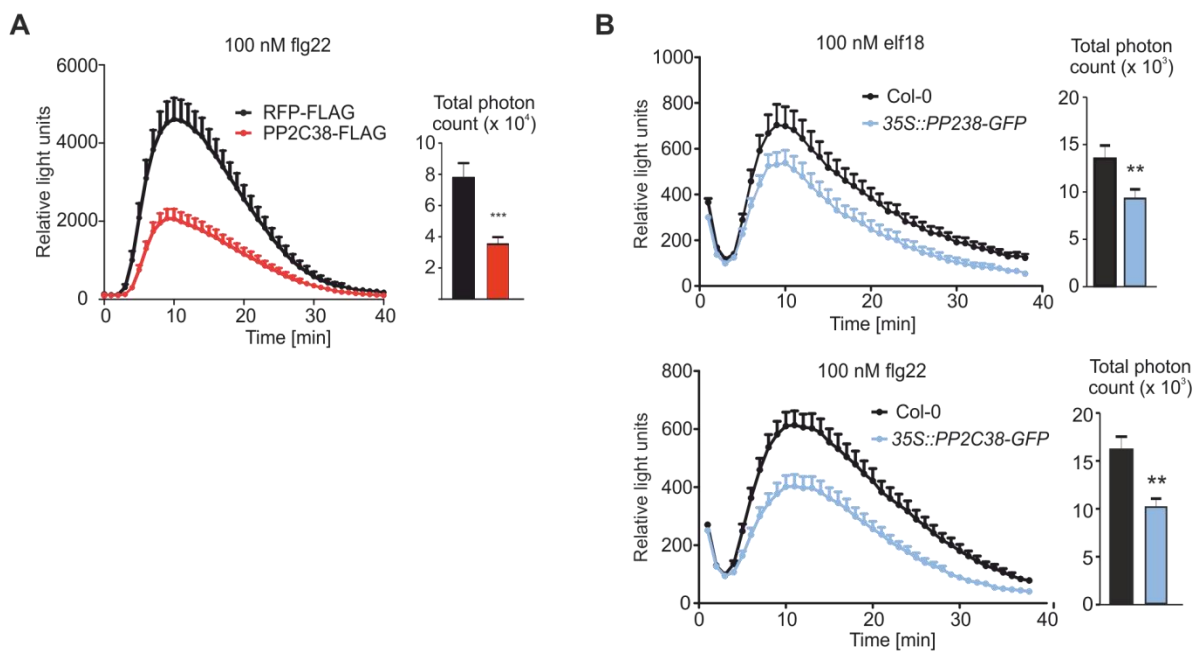


Figure 4.1 Overexpression of *PP2C38* impairs the PAMP-induced ROS burst.

(A-B) Overexpression of *PP2C38* impairs the ROS burst induced by 100 nM flg22 in *N. benthamiana* (A), and by 100 nM flg22 or elf18 in *Arabidopsis* (B). Values are mean \pm SE ($n = 12$) and are expressed in relative light units (RLU). Significant differences are designated by asterisks (***) $p < 0.001$; ** $p < 0.01$) based on unpaired Student's *t* test. Experiment replicated three times with similar results.

When characterizing transgenic lines, it is important to test more than one independent line.

After transformation of Col-0 plants with the *35S::PP2C38-GFP* construct, and despite

screening several positive transformants, we could only find one line effectively over-expressing *PP2C38* (Figs. 3.3 and 4.1). When we re-transformed the *35S:PP2C38-GFP* construct in the *pp2c38-1* mutant background, we were successful in obtaining two additional lines over-expressing *PP2C38* (Fig. 3.3). The negative impact of *PP2C38* on PAMP-induced ROS burst was further confirmed using these independent homozygous lines over-expressing *PP2C38-GFP* (Fig. 4.2).

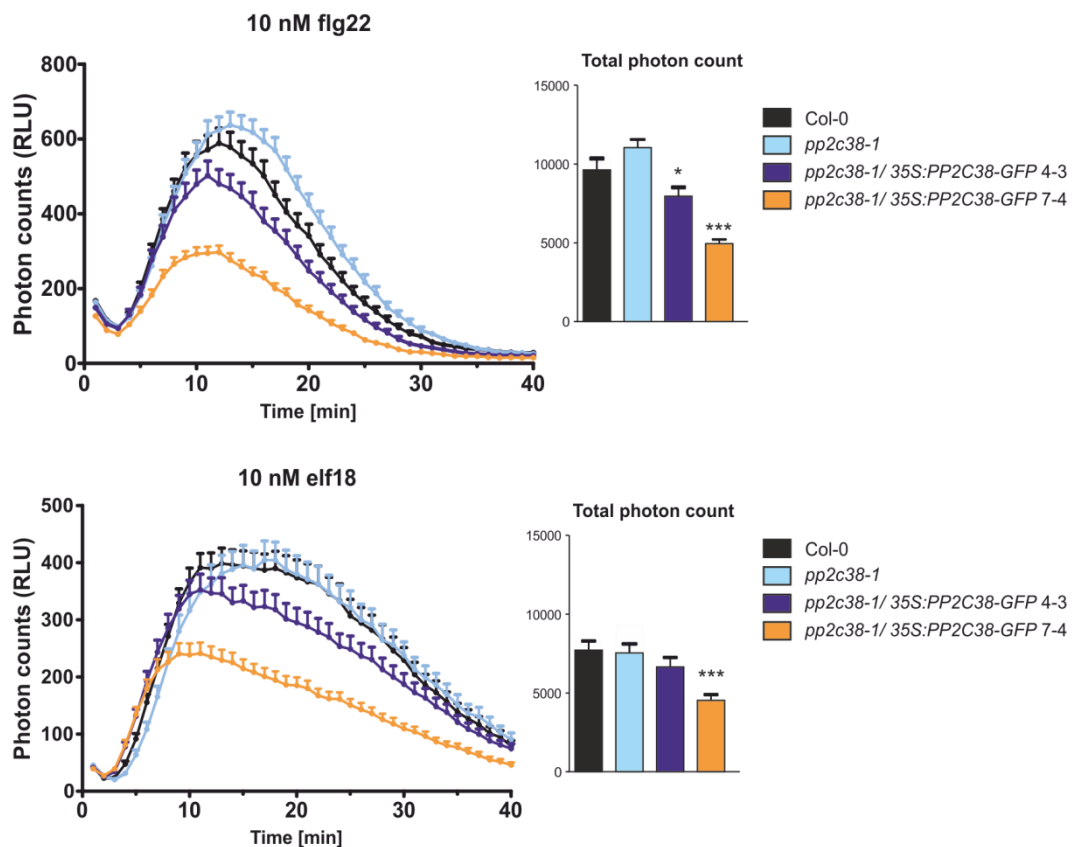


Figure 4.2. PAMP-induced ROS burst on *PP2C38* over-expression and mutant lines.

Two independent Arabidopsis transgenic lines expressing *35S:PP2C38-GFP* in the *pp2c38-1* background show reduced ROS burst induced by 10 nM flg22 (upper panel) and 10 nM elf18 (lower panel). Values are mean \pm SE ($n = 12$) and are expressed in relative light units (RLU). Asterisks indicate significant differences compared to Col-0 (one-way ANOVA, Dunnett post hoc test, *** $p < 0.001$; * $p < 0.05$). Experiment replicated three times with similar results.

PAMP-induced stomatal closure helps preventing pathogens from entering leaf tissues (Melotto *et al.*, 2008). This immune response is dependent on RBOHD and its activation by BIK1-mediated phosphorylation (Mersmann *et al.*, 2010; Zhang *et al.*, 2010; Macho *et al.*,

2012; Kadota *et al.*, 2014; Li *et al.*, 2014b). Loss of BIK1 activation or BIK1-mediated RBOHD phosphorylation leads to increased susceptibility to bacteria (Laluk *et al.*, 2011; Kadota *et al.*, 2014; Li *et al.*, 2014b). Consistent with the suggested role of PP2C38 in BIK1 dephosphorylation, we observed that elf18-induced stomatal closure was abolished in *PP2C38-GFP* over-expressing plants to the same extent as in the elf18-insensitive mutant line *fls2 efr cerk1* (Fig. 4.3A). Similar results were obtained after treatment with flg22 (Fig. 4.3B). Importantly, plants over-expressing *PP2C38-GFP* showed normal stomatal closure in response to abscisic acid (ABA) treatment (Fig. 4.3A), demonstrating that the general stomatal closure machinery is not affected by *PP2C38* over-expression. In accordance with these results, *PP2C38-GFP* over-expressing plants exhibited enhanced susceptibility to the hypovirulent bacterial strain *Pto* DC3000 *hrcC* when compared to the wild type (Fig. 4.3C).

We did not observe statistically significant differences in PAMP-induced ROS burst when analysing the *pp2c38-1* knock-out mutant (Fig 4.2). We reasoned this could be due to functional redundancy with closely related phosphatases. As mentioned in the previous Chapter, PP2C38 has a closely related paralog, PP2C48, which shows over 90% similarity (Fig. 3.6). We generated a homozygous loss-of-function line for both *PP2C38* and *PP2C48*, by crossing *pp2c38-1* and *pp2c48-1* single mutants (Fig. 4.4). Genetic disruption of both phosphatases led to increased elf18-induced ROS production in comparison to Col-0 (Fig. 4.5), which was comparable in terms of difference to the decrease observed upon *PP2C38* over-expression (Figs. 4.1 and 4.2). However, for flg22, this effect was variable and not always statistically significant (Fig. 4.5).

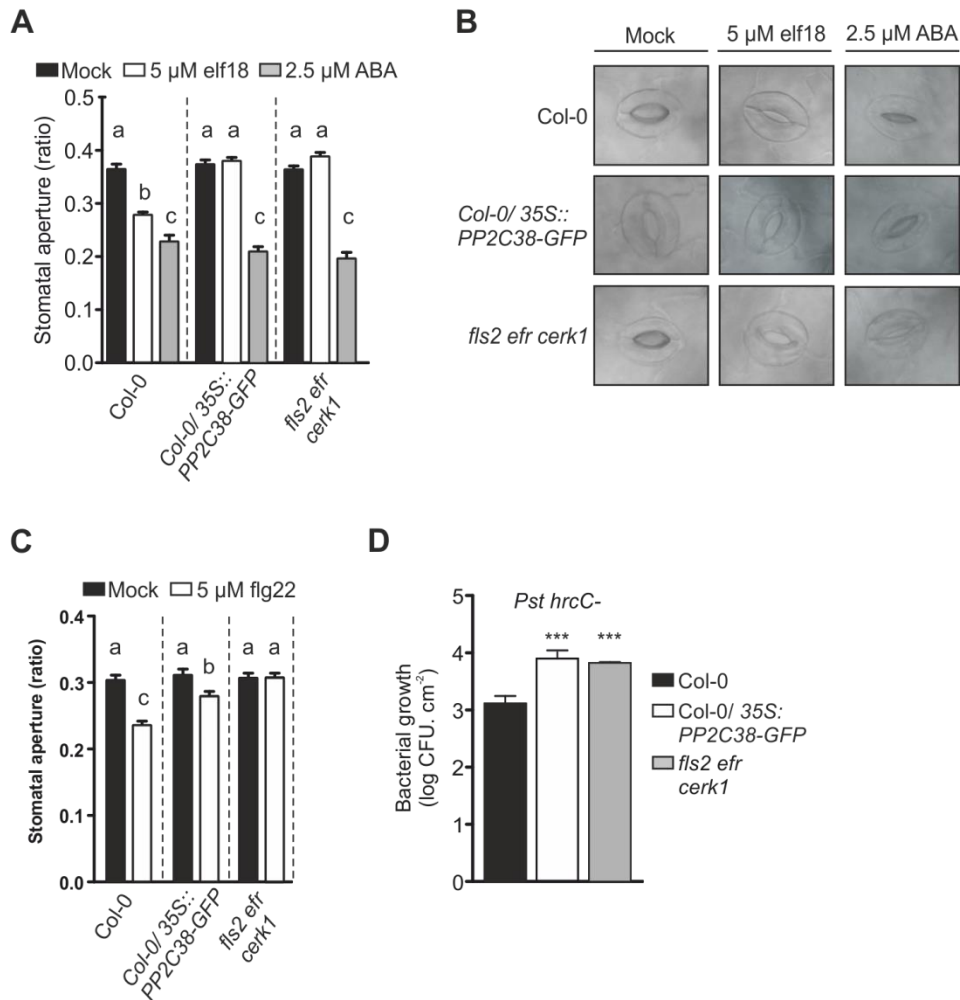


Figure 4.3. PP2C38 negatively regulates stomatal immunity.

(A) PP2C38 regulates elf18- but not ABA-induced stomatal closure. Stomatal aperture was measured 2 h after 5 μ M elf18 or 5 μ M ABA treatment. Values are mean \pm SE (n>50; one-way ANOVA, Tukey post hoc test). Different letters indicate significantly different values at $p < 0.001$. Experiment replicated three times with similar results.

(B) Representative pictures of stomata used for measurements in (A).

(C) PP2C38 regulates flg22-induced stomatal closure. Stomatal aperture was measured 2 h after 5 μ M flg22. Values are mean \pm SE (n>50; one-way ANOVA, Tukey post hoc test). Different letters indicate significantly different values at $p < 0.001$. Experiment replicated three times with similar results.

(D) PP2C38 is a negative regulator of anti-bacterial immunity. *Pto* DC3000 *hrcC*⁻ was sprayed onto leaf surface. Bacterial growth was determined 4 days post-inoculation. Values are mean \pm SE (n = 4). Asterisks indicate significant differences compared with Col-0 (one-way ANOVA, Dunnett post hoc test, *** $p < 0.001$). Cfu indicates colony-forming units. Experiments performed three times with similar results.

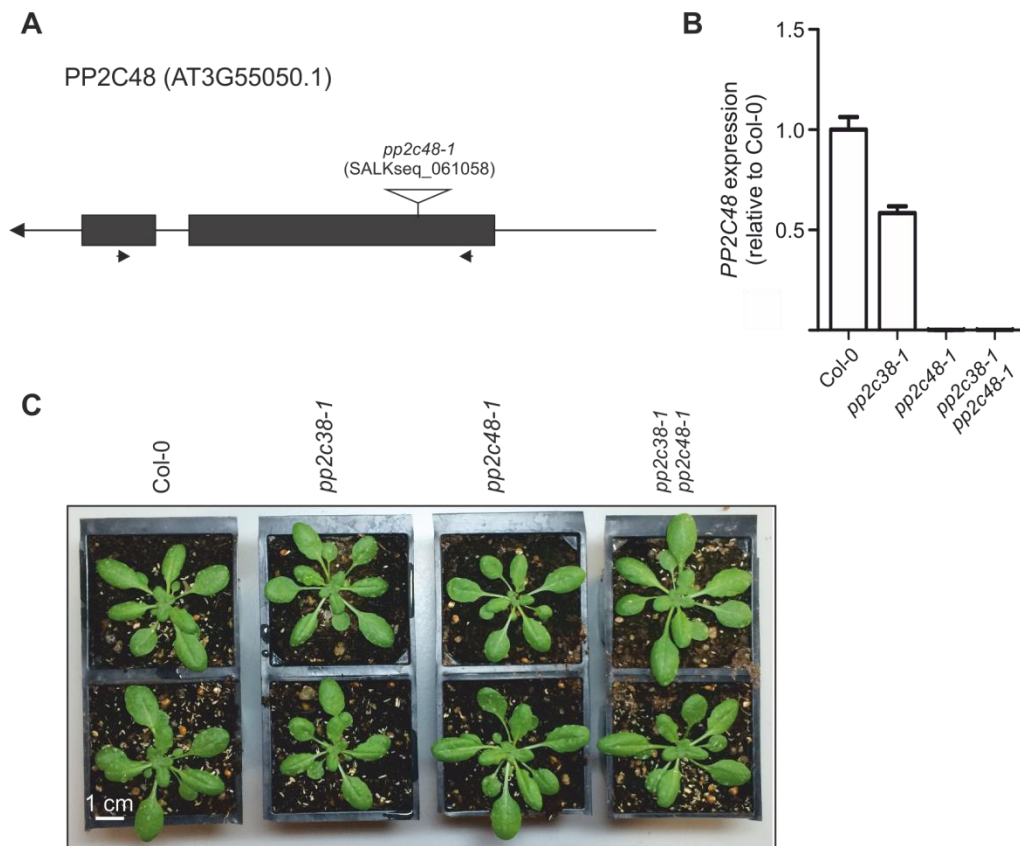


Figure 4.4. Characterization of PP2C48 mutant lines.

(A) Gene structure of *PP2C48* showing position of exons (boxes), introns (lines) and T-DNA insertion sites (triangle); arrows indicate position of primers used for genotyping.

(B) *PP2C48* expression analysis by quantitative RT-PCR. Expression was normalized to *UBQ10* and Col-0.

(C) Four-week-old *pp2c38-1* and *pp2c48-1* single and double mutant plants grown under short days.

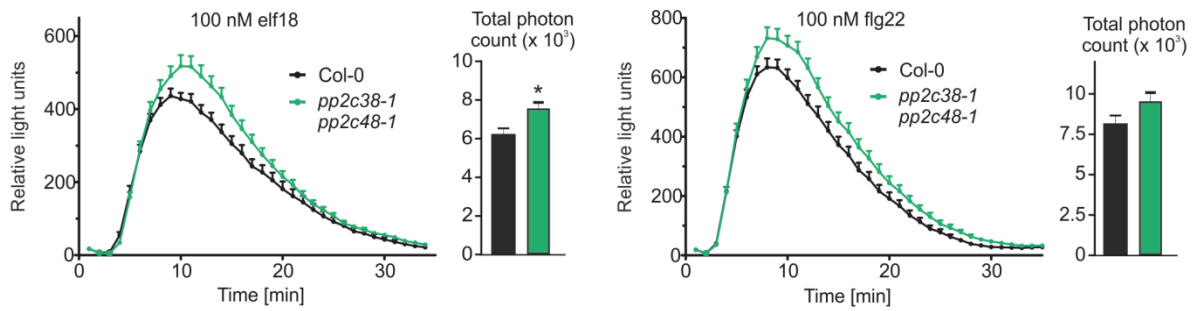


Figure 4.5. Loss of *PP2C38* and *PP2C48* enhances PAMP-induced ROS production.

ROS production induced by 100 nM elf18 or flg22. Values are mean \pm SE ($n \geq 20$) and are expressed in relative light units (RLU). Significant differences are designated by asterisks ($*p < 0.05$) based on unpaired Student's t test. Experiment replicated three times with similar results.

In addition, preliminary data suggest that *PP2C38* similarly negatively regulates the ROS burst triggered upon chitin perception (Fig 4.6). The *pp2c38-1 pp2c48-1* double mutant exhibited an enhanced response, whereas a *PP2C38* over-expressing line showed significantly compromised chitin-triggered ROS burst.

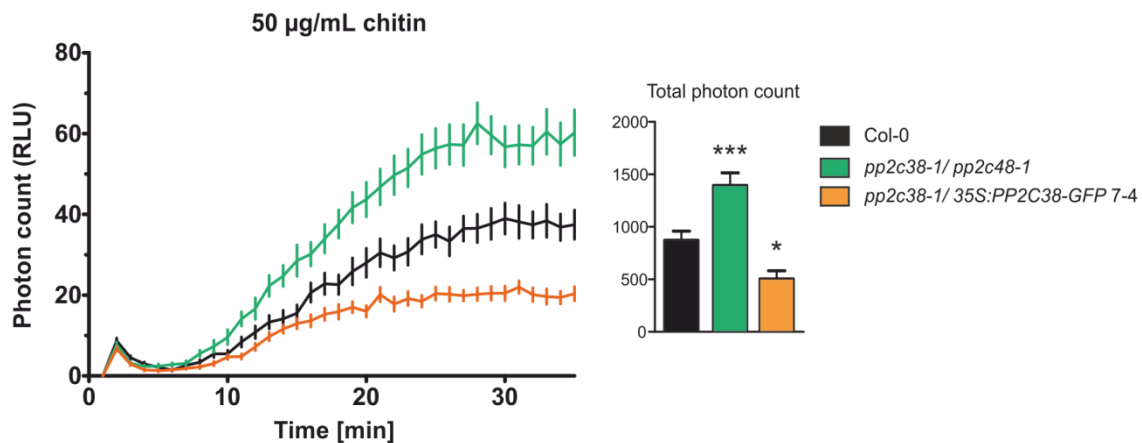


Figure 4.6. *PP2C38* negatively regulates chitin-triggered ROS burst.

ROS production triggered by 50 $\mu\text{g/mL}$ chitin. ROS burst was reduced in an *Arabidopsis* transgenic line expressing *35S:PP2C38-GFP* in the *pp2c38-1* background, and enhanced in the *pp2c38-1 pp2c48-1* double mutant. Values are mean \pm SE ($n \geq 20$) and are expressed in relative light units (RLU). Asterisks indicate significant differences compared to Col-0 (one-way ANOVA, Tukey post hoc test, $***p < 0.001$; $*p < 0.05$). Preliminary results; experiment performed only once.

Taken together, our results support a model, in which PP2C38 controls BIK1 phosphorylation status to modulate BIK1-induced immune responses, including ROS production and stomatal immunity. This role is also played, in a redundant manner, by PP2C38 closest homolog PP2C48. Furthermore, PP2C38-imposed inhibition on BIK1 does not appear to be restricted to BAK1-dependent immune responses, as we could observe in preliminary data a similar negative regulatory effect of PP2C38 on chitin-triggered ROS burst, consistent with the demonstrated role of BIK1 for chitin-mediated responses (Zhang *et al.*, 2010; Monaghan *et al.*, 2015)

Chapter 5: Phosphorylation of PP2C38 on serine 77 leads to its dissociation from BIK1

5.1. Prologue

In the previous Chapters, we have shown that PP2C38 associates with EFR, FLS2 and BIK1. Importantly, we demonstrated that the enzymatic activity of PP2C38 negatively affected BIK1 phosphorylation and activation states. As a consequence, *PP2C38* over-expression impaired BIK1-mediated phosphorylation of RBOHD and reduced the PAMP-induced ROS burst. Such perturbations on PTI signalling extended to the control of PAMP-induced stomatal closure, known to depend on BIK1 and RBOHD activities, and to resistance against hypovirulent bacterial strains. Moreover, regulation of ROS production is a role played redundantly by PP2C38 and its paralog PP2C48, most likely through dephosphorylation of BIK1.

Interestingly, we have also observed that PP2C38 dissociated from PRR complexes after PAMP treatment. This was accompanied by a PP2C38 band shift in SDS-PAGE (Fig. 3.1). Protein band shifts are typically caused by post-translation modifications, such as phosphorylation, that may alter the isoelectric point (pI) and/or the protein mass, resulting in slower migration patterns during electrophoresis. BIK1 is a great example for such phenomena: hyper-phosphorylation of BIK1 in response to PAMP perception leads to a double-band pattern that corresponds to unphosphorylated and phosphorylated forms, lower and upper bands respectively (Fig 3.10) (Lu *et al.*, 2010; Zhang *et al.*, 2010).

Phosphorylation can have dramatic effects on the modified proteins, by altering its activity, subcellular localization, or its ability to interact with other proteins. Because PP2C38 band shift and dissociation from PRR complexes both happened specifically in response to PAMPs, we hypothesized PP2C38 phosphorylation could be responsible for its dissociation from the PRR complex. This could provide a mechanism by which the inhibitory regulation imposed by PP2C38 on BIK1 is relieved to allow complete phosphorylation and activation of

the PRR complex. This prompted us to expand on the characterization of potential PP2C38 phosphorylation and on its possible roles during PTI signalling. In this Chapter, we were able to confirm that PP2C38 band shift was indeed caused by phosphorylation, and succeeded in identifying a major phosphorylation site by mass spectrometry analysis. Moreover, we suggest that BIK1 is most likely responsible for PP2C38 phosphorylation and show that phosphorylation is crucial for its dissociation from the PRR complex.

5.2. Results

Our previous results indicate that PP2C38 negatively regulates BIK1 activation and subsequent BIK1-mediated immune outputs, including anti-bacterial immunity. We have also observed that PP2C38 dissociates from the BIK1 complex upon PAMP perception (Fig. 3.5), suggesting an active PAMP-induced mechanism to relieve PP2C38-mediated negative regulation. In addition, PP2C38-FLAG exhibited a band shift on SDS-PAGE after PAMP treatment (Figs. 3.1A and 3.1B). In a more detailed time-course analysis, we detected a double band for PP2C38-FLAG already 5 min after elf18 or flg22 treatment in *N. benthamiana* leaves co-expressing PP2C38-FLAG and EFR-GFP (Fig. 5.1).

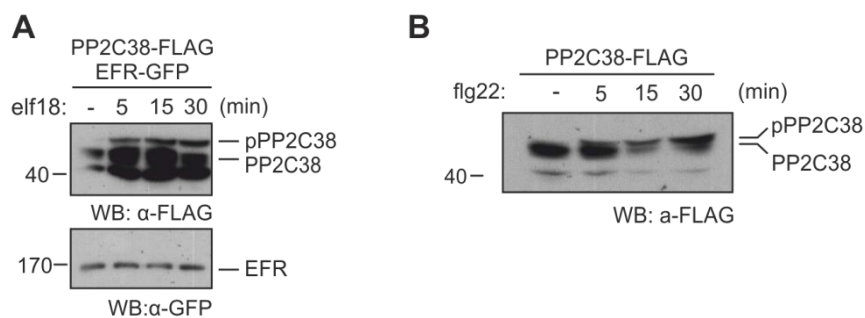


Figure 5.1. PAMP perception induces PP2C38 band shift.

(A-B) PPC2C38-FLAG protein expressed in *N. benthamiana* leaves and treated (+) or not (-) with 100 nM elf18 (A) or flg22 (B) for the indicated times. Upper band corresponds to phosphorylated PP2C38 form (pPP2C38). Twelve percent bisacrylamide gels were used for better protein separation. Experiment repeated two times with similar results.

Addition of phosphate groups to a protein has only a marginal impact on the overall mass of the modified protein (80 Da per phosphate), and is unlikely to affect the protein migration on SDS-PAGE. However, protein phosphorylation does often alter migration on SDS-PAGE and can in some case produce band shifts. This is thought to be dependent on the capacity of a given phosphate to change the local charge of the surrounding residues and alter the SDS coating, resulting in slower migration on gel (Peck, 2006). To test if PP2C38 band shift was due to phosphorylation, we incubated immunoprecipitated PP2C38-FLAG protein from elf18-treated *N. benthamiana* leaves with calf intestine alkaline phosphatase (CIP). This dissipated elf18-induced PP2C38-FLAG band shift (Fig. 5.2), confirming that the higher molecular weight band corresponds to a phosphorylated form of PP2C38.

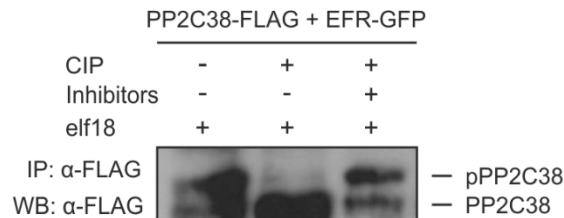


Figure 5.2. PP2C38 band shift is caused by phosphorylation.

Immunoprecipitated PP2C38-FLAG proteins from *N. benthamiana* leaves co-expressing EFR-GFP treated with 100 nM elf18 were incubated with calf intestine phosphatase (CIP) in the presence or absence of the phosphatase inhibitor NaF. Experiment performed by Roda Niebergall.

To identify PP2C38 phosphorylated residues *in vivo*, we transiently expressed PP2C38-FLAG in *N. benthamiana* and analysed immunoprecipitated protein phosphorylation using liquid chromatography-tandem mass spectrometry (LC-MS/MS) after separation on SDS-PAGE and cutting the band migrating at the predicted size for PP2C38. The serine residue 77 (S77) was identified as being phosphorylated (Fig. 5.3).

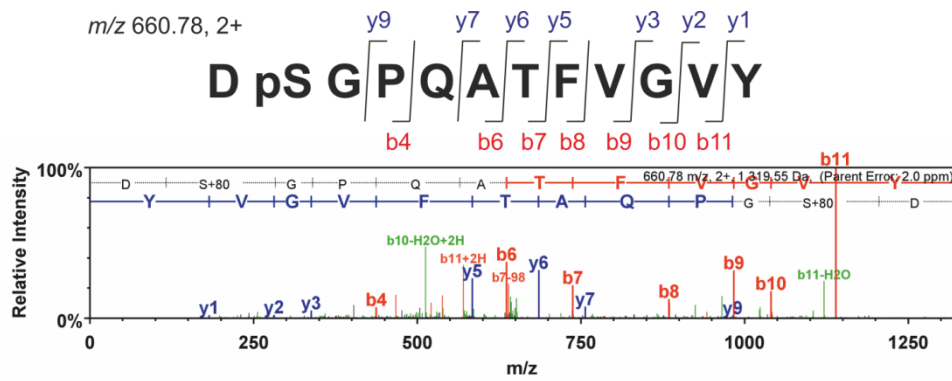


Figure 5.3. PP2C38 is phosphorylated on S77 *in vivo*.

Immunoprecipitated PP2C38-FLAG proteins from *N. benthamiana* were submitted for LTQ-Orbitrap MS/MS analysis. The DpSGPQATFVG VY phosphopeptide was identified as a doubly charged precursor (m/z 660.78) with fragmentation pattern consisting of singly and doubly charged b- and y- ions. Modified peptide sequence and fragmentation pattern shown above spectrum. MS analysis was performed by the TSL proteomics team.

Intriguingly, during Co-IP experiments of PP2C38 and BIK1 in *N. benthamiana*, we noted that PP2C38-FLAG showed a constitutive band shift when BIK1 was over-expressed (Fig. 3.1). We confirmed this observation on additional experiments where PP2C38 and BIK1 were co-expressed under control of the 35S promoter in *N. benthamiana* (Fig. 5.4). This suggested that PP2C38 phosphorylation was dependent on BIK1. Presumably, over-expressing BIK1 enhances its basal activity, or enhances *N. benthamiana* responsiveness to the presence of *A. tumefaciens*. In either case, activated BIK1 may directly phosphorylate PP2C38 or promote the activation of another kinase that phosphorylates PP2C38.



Figure 5.4. BIK1 over-expression results in constitutive PP2C38 phosphorylation.

BIK1-HA and PPC2C38-FLAG proteins were co-expressed in *N. benthamiana* leaves and treated (+) or not (-) with 100 nM flg22. Upper band corresponds to phosphorylated PP2C38 form (pPP2C38). Twelve percent bisacrylamide gels were used for better protein separation. Experiment repeated two times with similar results.

To test whether BIK1 could directly phosphorylate PP2C38 we performed an *in vitro* trans-phosphorylation assay. Remarkably, GST-BIK1 could trans-phosphorylate MBP-PP2C38, and this phosphorylation was S77-dependent, as it was strongly reduced when this serine was substituted to the non-phosphorylatable residue alanine (S77A) (Fig. 5.5A). This proved to be a critical control since GST-BIK1 was also capable of phosphorylating MBP on its own (Fig. 5.5A). Notably, a reduction of BIK1 auto-phosphorylation status can be observed both as a reduction in the autoradiogram signal, and on the CBB staining as a band shift towards a lower molecular weight (unphosphorylated form) (Fig. 5.5A). This was dependent on PP2C38 catalytic activity, as BIK1 was found mostly on its phosphorylated state in the presence of MBP-PP2C38* (higher molecular weight band; Fig. 5.5A). Intriguingly, BIK1 appeared to be in an intermediate phosphorylation state in the presence of MBP-PP2C38^{S77A}, suggesting that the S77A mutation partially compromises PP2C38 activity. We later confirmed that although MBP-PP2C38^{S77A} still exhibits catalytic activity towards a synthetic substrate, it was reduced in comparison to the wild-type protein (data not shown). In addition, the *in vitro* PP2C38 phosphorylation by BIK1 indicates these proteins can directly interact.

Next we tested whether the PAMP-induced PP2C38 band shift was dependent on S77. Strikingly, expression of the PP2C38^{S77A}-FLAG variant abolished the band shift of PP2C38-FLAG normally observed upon PAMP treatment in *N. benthamiana* (Fig. 5.5B). Together, our *in vitro* and *in vivo* data indicate that S77 is a major PP2C38 residue phosphorylated after PAMP perception, most likely by BIK1.

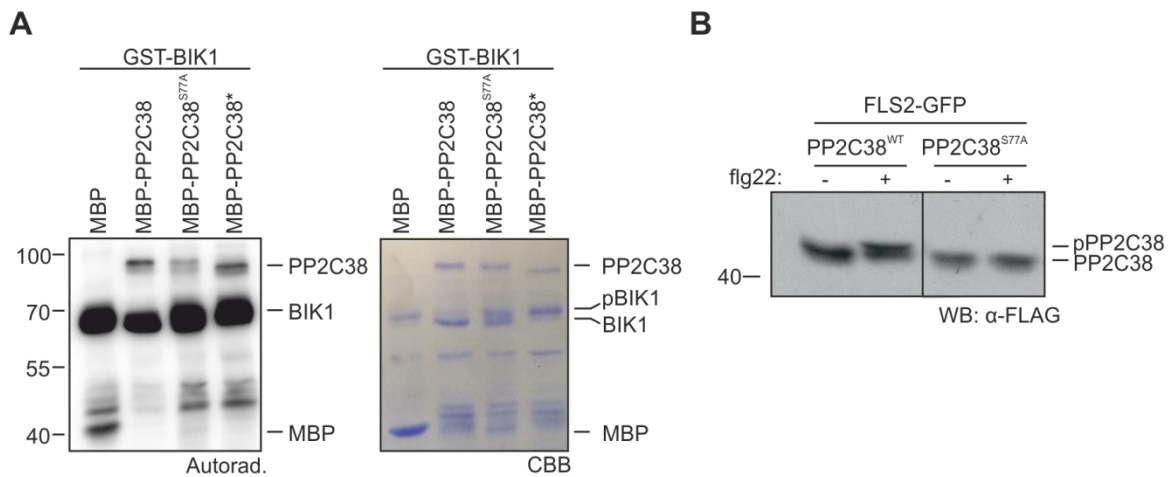


Figure 5.5. BIK1 phosphorylates PP2C38 on S77.

(A) Recombinant GST-BIK1 was incubated with [³²P]γ-ATP to promote auto-phosphorylation, followed by addition of recombinant MBP-PP2C38. *In vitro* PP2C38 trans-phosphorylation is revealed by autoradiography. CBB staining shown as loading control. Experiment repeated two times with similar results.

(B) Phospho-dead PP2C38^{S77A}-FLAG variant transiently expressed in *N. benthamiana* does not exhibit a band shift after 20 min 100 nM flg22 treatment. Twelve percent bisacrylamide gels were used for better protein separation.

Experiment repeated three times with similar results.

We had initially hypothesised that PP2C38 phosphorylation following PAMP perception could trigger its dissociation from the PRR complex. The identification of S77A as a phosphorylation-deficient mutant enabled us to test if S77 phosphorylation was required for the dissociation of PP2C38 from the BIK1 complex. We co-expressed PP2C38-FLAG or PP2C38^{S77A}-FLAG with BIK1-HA or BIK1*-HA [BIK1* being the kinase-dead variant BIK1^{K105E}; (Li *et al.*, 2014b)] in *Arabidopsis* protoplasts. After immunoprecipitation, we detected a clear association of PP2C38-FLAG with BIK1 that was disrupted after elf18 treatment (Fig. 5.6), as previously observed (Fig. 3.5). In contrast, the PP2C38^{S77A} variant remained stably associated with BIK1, even after elf18 treatment (Fig. 5.6). Intriguingly, in most of our experiments using *Arabidopsis* protoplasts, we could not observe a clear PAMP-induced PP2C38 band shift. Instead, PP2C38 was mostly observed in its phosphorylated form (Fig. 5.6). This could be due to BIK1 co-expression, which causes constitutive PP2C38 phosphorylation (Fig. 5.4), or due to enhanced basal activation of BIK1 and PBL proteins in the protoplast system. It is important to note that the S77A mutant exhibited a lower

molecular weight band, corresponding to the unphosphorylated form of the wild type (Fig. 5.6). From this experiment, it is difficult to conclude if the phosphorylated PP2C38 form still associates with BIK1 or if phosphorylation immediately triggers PP2C38 phosphorylation. Nevertheless, it clearly demonstrates the importance of PP2C38 phosphorylation, especially on S77, during its dissociation from BIK1 in response to PAMP perception.

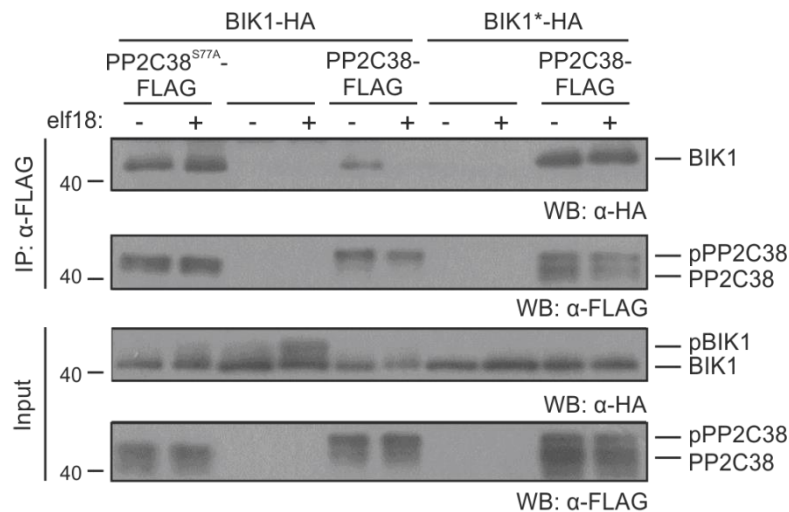


Figure 5.6. S77 phosphorylation is required for PAMP-induced PP2C38-BIK1 complex dissociation.

Arabidopsis Col-0 protoplasts were co-transfected with PP2C38/PP2C38^{S77A}-FLAG and BIK1/BIK1*-HA, and treated (+) or not (-) with 1 μM elf18 for 30 min. PP2C38-BIK1 complexes were analysed by immunoblotting following α-FLAG immunoprecipitation. Experiment repeated three times with similar results. Experiment performed by Xiangxiu Liang in the laboratory of Jian-Min Zhou (Chinese Academy of Science, Beijing).

Interestingly, PP2C38 failed to dissociate from BIK1* following elf18 treatment (Fig. 5.6). PP2C38 was also in a less phosphorylated state, as indicated by the presence of two bands (increased unphosphorylated to phosphorylated ratio) (Fig. 5.6). This clearly implicated BIK1 kinase activity in PP2C38 phosphorylation and dissociation. Furthermore, EFR and FLS2 kinases do not seem to play an important role in this, as PP2C38 normally dissociated from EFR* and FLS2* kinase-dead variants following treatment with the respectively ligand (Fig. 5.7)

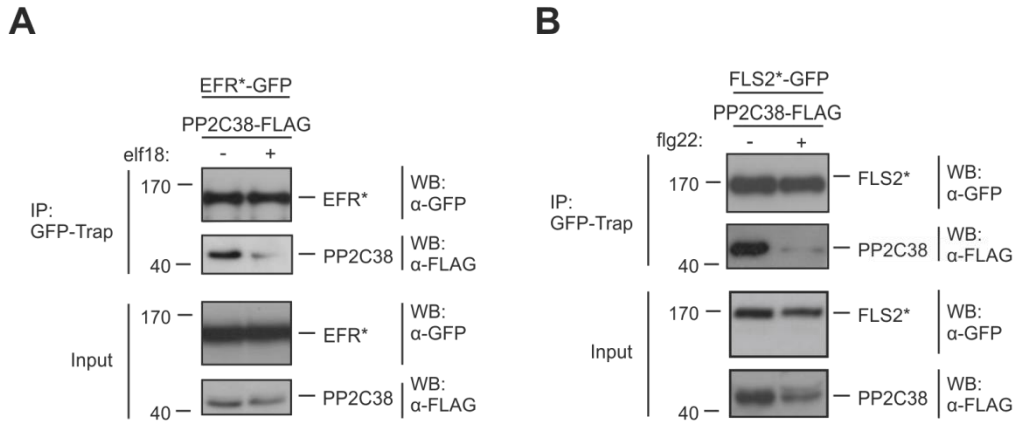


Figure 5.7. EFR and FLS2 kinase activities are not required for PAMP-induced dissociation of PP2C38.

(A-B) PP2C38 and kinase-dead versions of EFR* (A) or FLS2* (B) proteins were co-immunoprecipitated from *N. benthamiana* leaves treated (+) or not (-) with 100 nM elf18 (A) or flg22 (B) for 20 min. Experiments performed by Roda Niebergall.

Altogether, our results point towards an important role of PP2C38 phosphorylation for its dissociation from BIK1. The dynamic, PAMP-dependent BIK1-PP2C38 association suggests that PP2C38-mediated negative regulation of BIK1 is relieved upon PAMP-induced phosphorylation of PP2C38 to enable full BIK1 activation and optimal downstream immune signalling.

Chapter 6: Discussion

6.1. PP2C38 is a novel regulator of BIK1 activity

Appropriate immune signalling initiation, timing and amplitude must be carefully regulated to avoid excessive or nonspecific activation of immune responses, which can lead to autoimmune and inflammatory diseases (Coll & O'Neill, 2010; Kondo *et al.*, 2012). The mechanisms and pathways that negatively regulate PRR-triggered immunity (PTI) in mammals have been extensively characterized (Kondo *et al.*, 2012; Anwar *et al.*, 2013; Moynagh, 2014). However, much less is known in plants, where a fine balance between immunity and growth is important for their optimal growth (Belkhadir *et al.*, 2014; Lozano-Duran & Zipfel, 2015).

BIK1 is a central positive regulator of immune signalling acting downstream of both LRR- and LysM-containing PRRs (Lu *et al.*, 2010; Zhang *et al.*, 2010; Liu *et al.*, 2013). Yet, despite the importance of BIK1 for plant immunity, knowledge surrounding its action, substrates or regulation is still sparse. The first example of a downstream BIK1 substrate was the NADPH oxidase RBOHD, which generates PAMP-induced ROS burst (Kadota *et al.*, 2014; Li *et al.*, 2014b). Notably, PAMP-activated BIK1 directly phosphorylates RBOHD, which is required for ROS production and subsequent stomatal immunity (Kadota *et al.*, 2014; Li *et al.*, 2014b). Furthermore, BIK1 turnover was recently shown to be controlled by the calcium-dependent protein kinase CPK28 in a proteasome-dependent manner (Monaghan *et al.*, 2014; Monaghan *et al.*, 2015), which provides one mechanism by which plant cells control this key regulator and the amplitude of immune signalling. Yet, the regulation imposed by CPK28 appears to be constitutive, as no effect of PAMP treatment could be noted on CPK28 activity or association with BIK1 (Monaghan *et al.*, 2014). Importantly, neither *CPK28* deletion nor over-expression affected PAMP-induced BIK1 hyper-phosphorylation. Thus it seems that CPK28 represents a mechanism used by plant cells to constantly buffer immune signalling by constitutively regulating BIK1 protein levels, but not necessarily its activation state.

In this study, we revealed a protein phosphatase of type 2C, PP2C38, as a dynamic regulator of BIK1, which controls its phosphorylation status, most likely to maintain basal immune signalling levels to a minimum in the absence of elicitation, and/or to fine-tune the immune responses upon pathogen attack.

PP2C38 was initially identified in a Y2H screen as an interactor of EFR (Table 3.1). While we confirmed that PP2C38 associates with EFR (as well as with FLS2; Figs 3.1 and 3.4), we also found that PP2C38 associates with BIK1 *in planta* (Fig. 3.5). Notably, no association could be observed between PP2C38 and BAK1 (Fig. 3.5). It thus appears that PP2C38 is part of the PRR-BIK1 complex, most likely through direct interaction with both EFR/FLS2 and BIK1. Accordingly, BIK1 phosphorylates PP2C38 *in vitro* (Fig. 5.5), which could be seen as proof for direct interaction. Direct PP2C38 pull-down experiments *in vitro* by EFR, FLS2, BIK1, as well as by BAK1, have already been planned for the future to confirm these direct interactions.

PP2C38 is an active PM-localized phosphatase (Figs. 3.7 and 3.8). Interestingly, PP2C38 over-expression affected elf18-induced BIK1 hyper-phosphorylation (Fig 3.10A), but had no impact on EFR or BAK1 phosphorylation (Fig. 3.9). Since EFR and BAK1 are directly upstream and phosphorylate BIK1, these results suggest that PP2C38 directly dephosphorylates BIK1, and thus BIK1 is a biologically relevant substrate of PP2C38. Given that hyper-phosphorylation is key for BIK1 activation (Lu *et al.*, 2010; Zhang *et al.*, 2010; Laluk *et al.*, 2011), it also suggests that PP2C38 negatively regulates BIK1 activity. This is further substantiated by our findings that PP2C38 over-expression leads to reduced PAMP-induced phosphorylation of RBOHD on the BIK1-specific phosphosite S39 (Fig. 3.10B). Interestingly, we noted that basal RBOHD-S39 phosphorylation was almost undetectable when PP2C38 was over-expressed (Fig. 3.10B). Basal RBOHD-S39 phosphorylation in the absence of PAMP treatment was previously shown to be dependent on BIK1/ PBL1 (Li *et al.*, 2014b). This suggests that BIK1 can be partially activated during the protoplasting procedure, possibly by the release of DAMPs during cell wall digestion. Together, these

results support a role of PP2C38 in preventing basal BIK1 activation in the absence of a strong eliciting stimulus.

The next step towards understanding how PP2C38 deactivates BIK1 would be to identify which phosphosites are being targeted by PP2C38. A number of BIK1 *in vitro* auto- and/or trans-phosphorylated Ser and Thr residues, such as S236, T237 or T242, have been identified by MS analysis, and were shown through mutagenic approaches to play important roles in kinase activation and PTI signalling transduction (Lu *et al.*, 2010; Zhang *et al.*, 2010; Laluk *et al.*, 2011; Xu *et al.*, 2013; Lin *et al.*, 2014). Whether these phosphosites are PP2C38 targets could be tested by performing quantitative MS analysis after an *in vitro* BIK1 dephosphorylation assay. However, it would be difficult to conclude on the biological relevance and specificity of such data, mainly because phosphatases often show poor substrate discrimination in *in vitro* conditions. The ideal approach would be to take advantage of the protoplast system developed during this study and quantitatively analyse PAMP-induced BIK1 phosphorylation, comparing it in the presence or absence of PP2C38 over-expression. Unfortunately, identification of *in vivo* BIK1 phosphosites by MS analysis has not yet been reported. Together with the TSL Proteomics support team, our laboratory is currently developing MS spectrometry methods to detect BIK1 phosphorylation, which in the future could allow the identification of *in vivo* phosphosites targeted by PP2C38.

6.2. Multi-level regulation of PRR complexes

Ectopic *PP2C38* expression led to a significant reduction of PAMP-triggered ROS burst in *N. benthamiana* and *Arabidopsis* plants (Figs. 4.1 and 4.2), and compromised PAMP-induced stomatal closure, resulting in enhanced susceptibility to a hypovirulent *Pto* strain (Figs. 4.3). In addition, loss of *PP2C38* and its paralog *PP2C48* led to enhanced ROS productions in response to elf18, and to a certain extent flg22 (Fig. 4.5). Together, these results implicate PP2C38 as a negative regulator of BIK1-mediated immune signalling and stomatal anti-

bacterial immunity, while revealing the importance of keeping the phosphorylation status of PRR complexes under tight control.

This is further demonstrated by the increasing number of protein phosphatases that have been previously shown to act at the PRR level. The unclustered PP2C KAPP interacts with FLS2 cytoplasmic domain in yeast two-hybrid assays and *KAPP* over-expression results in flg22 insensitivity (Gomez-Gomez *et al.*, 2001); however, KAPP is known to interact with several unrelated RKs (Ding *et al.*, 2007), which questions the specificity of this action. In rice, the PP2C XB15 associates with the PRR XA21 and negatively regulates XA21-mediated resistance to *Xoo* (Park *et al.*, 2008). Interestingly, the *Arabidopsis* XB15 orthologs PLL4 and PLL5 associate with EFR (which is phylogenetically closely related to XA21) and negatively regulate EFR-mediated responses, demonstrating the conservation of regulatory mechanisms between evolutionary-distant plants (Holton *et al.*, 2015). Recently, a specific protein phosphatase 2A (PP2A) holoenzyme (composed of the subunits A1, C4 and B' η / ζ) was shown to negatively regulate PTI by directly targeting the co-receptor BAK1 (Segonzac *et al.*, 2014). While BAK1-associated PP2A activity was reduced after PAMP treatment, it is still unclear whether this is due to the dissociation of PP2A from BAK1, or to the inhibition of PP2A activity. The identification of PP2C38 and PP2C48 as regulators of BIK1 further illustrates the negative regulation of plant immune signalling that occurs at multiple levels within PRR complexes.

Similar mechanisms seem to be employed by pathogens, which are able to secrete effectors that target PRR complex components and disrupt their phosphorylation status (Section 1.5). Remarkably, the *Pseudomonas* effector AvrAC uridylylates key phosphosites on BIK1 activation loop (i.e. S236 and T237). This modification renders these phosphosites permanently unphosphorylatable, and thus we could think of AvrAc as a phosphatase that inflicts 'irreversible dephosphorylation' on its substrates. At the moment, the BIK1 phosphosites targeted by PP2C38 are currently unknown. Given that AvrAC efficiently suppresses immune signalling by having evolved to target BIK1 S236 and T237, these

residues are thus prime candidates to be tested in the future for PP2C38-mediated dephosphorylation.

6.3. PP2C38 and BIK1: a 'phospho-standoff'

Notably, we observed that PP2C38 becomes phosphorylated and dissociates from the PRR complex upon PAMP treatment (Figs. 3.1, 3.2, 3.5 and 5.6). Furthermore, the non-phosphorylatable PP2C38^{S77A} variant could not dissociate anymore from BIK1 after elf18 perception (Fig. 5.6), indicating that phosphorylation is critical for PP2C38 dissociation from the PRR complex. Phosphorylation on S77 residue most likely triggers the dissociation of PP2C38 from BIK1, as the non-phosphorylatable PP2C38^{S77A} variant could not dissociate anymore from BIK1 after elf18 perception (Fig. 5.6).

Over-expression of BIK1 produced a constitutive PP2C38 band shift in *N. benthamiana* leaves and in *Arabidopsis* protoplasts (Figs. 3.5, 5.4 and 5.6). Moreover, PP2C38 failed to dissociate from a kinase-dead BIK1 variant (carrying the K105E mutation), which is known to be dominant-negative (Li *et al.*, 2014b), and exhibited reduced phosphorylation levels (Fig. 5.6). In addition, EFR or FLS2 kinase activity is not required for PP2C38 dissociation (Fig. 5.7), and BAK1 does not associate with PP2C38 *in planta* (Fig. 3.5). Furthermore, BIK1 can trans-phosphorylate PP2C38 *in vitro* in a manner that mostly depends on S77 (Fig. 5.4). Altogether, these data suggest that BIK1 is responsible for PP2C38 phosphorylation.

In most of our experiments with *Arabidopsis* protoplasts, PP2C38 was found mostly in its phosphorylated form and the PAMP-inducible band shift was difficult to detect. Similarly to the enhanced basal RBOHD-S39 phosphorylation, this could be caused by BIK1 and other PBL proteins that become activated during protoplasting. Strangely, we also noted that the PP2C38* variant migrated as a single low molecular weight band (Figs. 3.9 and 3.10), in a similar manner to PP2C38^{S77A}. It is possible that mutation of the two negatively charged Asp residues (D87 and D289) could interfere with the migration in SDS-PAGE and impede the observation of a band shift, even after phosphorylation. Alternatively, and since D87 and

D289 are highly conserved residues within the PP2C catalytic pocket, the mutation to Asn might somehow alter the normal PP2C38 fold in a way that prevents its phosphorylation on S77. We could still detect an association between BIK1 and PP2C38* by co-immunoprecipitation (preliminary data not shown), suggesting that, at least to a certain degree, it must retain its normal fold. Our preliminary data showed that PP2C38* could not dissociate from BIK1 after PAMP treatment, suggesting that PP2C38* might not actually be phosphorylatable (data not shown). We are currently working to confirm these results.

We propose a model in which PP2C38, and likely PP2C48, associate with BIK1 in the resting state, keeping its phosphorylation state under control. Upon PAMP perception, BAK1 forms a stable complex with EFR/FLS2, resulting in trans-phosphorylation between these proteins and BIK1, leading to BIK1 activation. Although not depicted in our model for reasons of simplicity, BIK1 is also phosphorylated and activated by CERK1 during CERK1-dependent responses, for example to chitin. Subsequent to BIK1 activation, PP2C38 is phosphorylated and released from BIK1 allowing its full activation (Fig. 6.1). This model is somewhat reminiscent of the negative regulation imposed by the PM-anchored protein BKI1 on the brassinosteroid (BR) receptor BRI1. BKI1 interacts with BRI1 kinase domain preventing its phosphorylation (Wang & Chory, 2006; Jaillais *et al.*, 2011; Wang *et al.*, 2014). BR perception by BRI1 results in BKI1 phosphorylation, which triggers BKI1 dissociation and relocalization to the cytoplasm (Jaillais *et al.*, 2011). Notably, BIK1 also integrates signalling from BRI1, acting as a negative regulator of BR-dependent responses (Lin *et al.*, 2013). Whether PP2C38 also negatively regulates BIK1 to control BR responses (in this case, to potentially activate them) remains to be determined. In the process of our work however, we have not observed a growth phenotype indicating a potential role of PP2C38 in BR signalling.

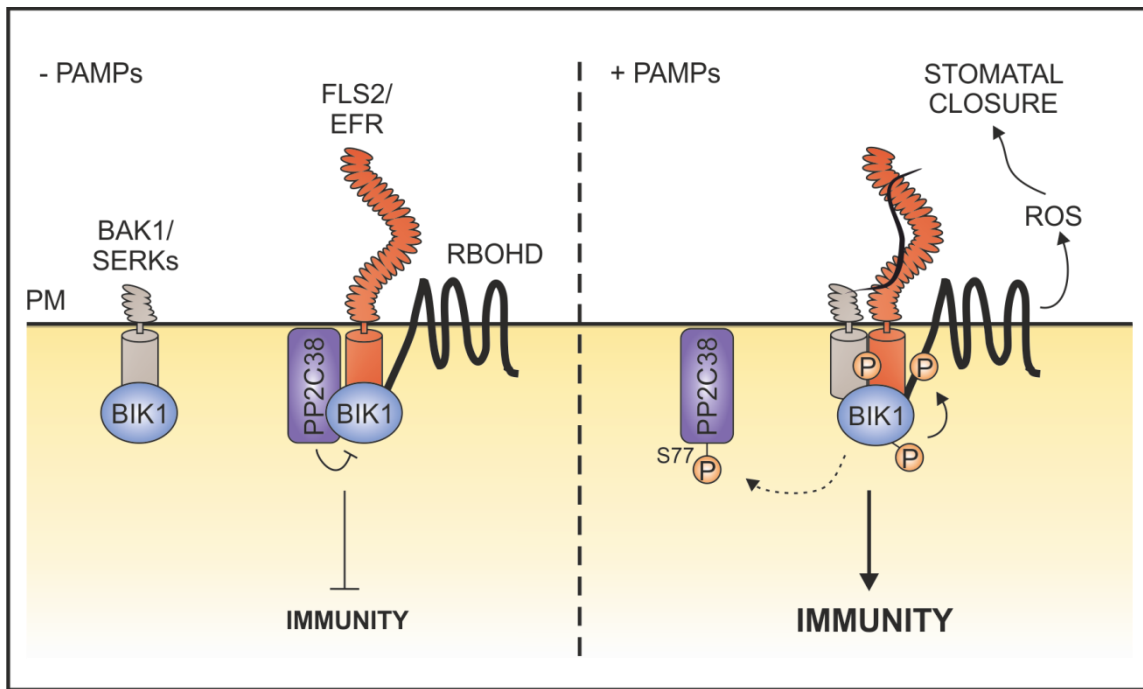


Figure 6.1. Model: PP2C38 dephosphorylates BIK1 to attenuate innate immune signalling.

In the absence of pathogen elicitation, PP2C38 associates with PRR-BIK1 complexes to dephosphorylate BIK1 and prevent its activation. Upon PAMP perception, BAK1 is recruited and trans-phosphorylation of the PRR complex triggers BIK1 hyper-phosphorylation. In turn, activated BIK1 presumably phosphorylates PP2C38 on S77 to enable its dissociation from the PRR complex. The release of PP2C38 relieves the negative regulation imposed on BIK1, allowing efficient subsequent activation of downstream targets.

Chapter 7: Conclusions and outlook

In this study we identified a novel mechanism controlling the activation state of the central immune regulator BIK1. This consisted of a previously uncharacterised protein phosphatase, PP2C38, which is present on PRR-BIK1 complexes at the PM under resting state conditions. PP2C38 controls BIK1 phosphostatus, presumably through direct dephosphorylation, to prevent unintended immune signalling initiation and/or fine-tune immune responses. In addition, we revealed a curious double-sided mechanism in which PP2C38 is phosphorylated after PAMP perception, most likely by BIK1, resulting in its dissociation from the PRR complex. This is in compliance with a model where, upon PAMP perception, PP2C38 dissociation relieves the negative regulation imposed on BIK1, allowing efficient PRR complex activation, and subsequent activation of appropriate immune responses.

The fate of PP2C38 after dissociation from the PRR complex remains a mystery. We have previously observed that PAMP treatment before immunoprecipitation of transiently expressed PP2C38 leads to a small, but significant increase of its catalytic activity (data not shown). The biological relevance of this observation is yet to be investigated; but raises the possibility that phosphorylated PP2C38 may act on other PTI signalling components, either repressing or activating immune responses. A similar mechanism has been described in BR signalling: BKI1 prevents phosphorylation of BRI1, but BR perception leads to BKI1 relocalization to the cytoplasm, where it plays a positive role in BR signalling by interacting with 14-3-3 proteins (Jaillais *et al.* 2011, Wang *et al.* 2011).

To our knowledge, this study represents the first example of a plant RLCK being directly targeted by a protein phosphatase. While unravelling new mechanisms by which RLCKs are negatively regulated, our findings provide further evidence for a multi-layered system that regulates the phosphostatus of PRR complexes. Phosphatases are now known to control PRRs, regulatory RKs, and RLCKs, emerging as a critical part of the plant immune system. Together with other immune negative regulatory mechanisms, which also feedback onto growth and development pathways, they are likely to play an important role in maintaining

cellular homeostasis, and ensuring the overall plant fitness. Whether the differential action of these inhibitory mechanisms can favour specific immune pathways in detriment of others, and hence modulate immune responses against different pathogens is something that remains to be addressed.

References

- Abramovitch R.B., Janjusevic R., Stebbins C.E., Martin G.B.** (2006) Type III effector AvrPtoB requires intrinsic E3 ubiquitin ligase activity to suppress plant cell death and immunity. *Proc Natl Acad Sci USA* 103: 2851-2856
- Akamatsu A., Wong H.L., Fujiwara M., Okuda J., Nishide K., Uno K., Imai K., Umemura K., Kawasaki T., Kawano Y., Shimamoto K.** (2013) An OsCEBiP/OsCERK1-OsRacGEF1-OsRac1 module is an essential early component of chitin-induced rice immunity. *Cell Host Microbe* 13: 465-476
- Albert I., Böhm H., Albert M., Feiler C.E., Imkamp J., Wallmeroth N., Brancato C., Raaymakers T.M., Oome S., Zhang H., Krol E., Grefen C., Gust A.A., Chai J., Hedrich R., Van den Ackerveken G., Nürnberger T.** (2015) An RLP23–SOBIR1–BAK1 complex mediates NLP-triggered immunity. *Nature Plants* 1: 15140
- Albrecht C., Boutrot F., Segonzac C., Schwessinger B., Gimenez-Ibanez S., Chinchilla D., Rathjen J.P., de Vries S.C., Zipfel C.** (2012) Brassinosteroids inhibit pathogen-associated molecular pattern-triggered immune signaling independent of the receptor kinase BAK1. *Proc Natl Acad Sci USA* 109: 303-308
- Anderson J.C., Bartels S., Gonzalez Besteiro M.A., Shahollari B., Ulm R., Peck S.C.** (2011) *Arabidopsis* MAP Kinase Phosphatase 1 (AtMKP1) negatively regulates MPK6-mediated PAMP responses and resistance against bacteria. *Plant J* 67: 258-268
- Anwar M.A., Basith S., Choi S.** (2013) Negative regulatory approaches to the attenuation of Toll-like receptor signaling. *Exp Mol Med* 45: e11
- Ao Y., Li Z., Feng D., Xiong F., Liu J., Li J.F., Wang M., Wang J., Liu B., Wang H.B.** (2014) OsCERK1 and OsRLCK176 play important roles in peptidoglycan and chitin signaling in rice innate immunity. *Plant J* 80: 1072-1084
- Arthur J.S., Ley S.C.** (2013) Mitogen-activated protein kinases in innate immunity. *Nat Rev Immunol* 13: 679-692
- Asai T., Tena G., Plotnikova J., Willmann M.R., Chiu W.L., Gomez-Gomez L., Boller T., Ausubel F.M., Sheen J.** (2002) MAP kinase signalling cascade in *Arabidopsis* innate immunity. *Nature* 415: 977-983
- Ausubel F.M.** (2005) Are innate immune signaling pathways in plants and animals conserved? *Nat Immunol* 6: 973-979
- Axtell M.J., Staskawicz B.J.** (2003) Initiation of RPS2-specified disease resistance in *Arabidopsis* is coupled to the AvrRpt2-directed elimination of RIN4. *Cell* 112: 369-377
- Bartels S., Anderson J.C., Gonzalez Besteiro M.A., Carreri A., Hirt H., Buchala A., Mettraux J.P., Peck S.C., Ulm R.** (2009) MAP kinase phosphatase1 and protein tyrosine phosphatase1 are repressors of salicylic acid synthesis and SNC1-mediated responses in *Arabidopsis*. *Plant Cell* 21: 2884-2897
- Belkhadir Y., Jaillais Y., Epple P., Balsemao-Pires E., Dangl J.L., Chory J.** (2012) Brassinosteroids modulate the efficiency of plant immune responses to microbe-associated molecular patterns. *Proc Natl Acad Sci USA* 109: 297-302
- Belkhadir Y., Yang L., Hetzel J., Dangl J.L., Chory J.** (2014) The growth-defense pivot: crisis management in plants mediated by LRR-RK surface receptors. *Trends Biochem Sci* 39: 447-456
- Ben Khaled S., Postma J., Robatzek S.** (2015) A moving view: subcellular trafficking processes in pattern recognition receptor-triggered plant immunity. *Ann Rev Phytopathol* 53: 379-402
- Berriri S., Garcia A.V., Frei dit Frey N., Rozhon W., Pateyron S., Leonhardt N., Montillet J.L., Leung J., Hirt H., Colcombet J.** (2012) Constitutively active mitogen-activated protein kinase

- versions reveal functions of *Arabidopsis* MPK4 in pathogen defense signaling. *Plant Cell* 24: 4281-4293
- Bethke G., Pecher P., Eschen-Lippold L., Tsuda K., Katagiri F., Glazebrook J., Scheel D., Lee J.** (2012) Activation of the *Arabidopsis thaliana* mitogen-activated protein kinase MPK11 by the flagellin-derived elicitor peptide, flg22. *Mol Plant Microbe Interact* 25: 471-480
- Blaum B.S., Mazzotta S., Noldeke E.R., Halter T., Madlung J., Kemmerling B., Stehle T.** (2014) Structure of the pseudokinase domain of BIR2, a regulator of BAK1-mediated immune signaling in *Arabidopsis*. *J Struct Biol* 186: 112-121
- Bohm H., Albert I., Fan L., Reinhard A., Nurnberger T.** (2014) Immune receptor complexes at the plant cell surface. *Curr Opin Plant Biol* 20: 47-54
- Boller T., Felix G.** (2009) A renaissance of elicitors: perception of microbe-associated molecular patterns and danger signals by pattern-recognition receptors. *Ann Rev Plant Biol* 60: 379-406
- Boudeau J., Miranda-Saavedra D., Barton G.J., Alessi D.R.** (2006) Emerging roles of pseudokinases. *Trends Cell Biol* 16: 443-452
- Boudsocq M., Willmann M.R., McCormack M., Lee H., Shan L., He P., Bush J., Cheng S.H., Sheen J.** (2010) Differential innate immune signalling via Ca²⁺ sensor protein kinases. *Nature* 464: 418-422
- Boutrot F., Segonzac C., Chang K.N., Qiao H., Ecker J.R., Zipfel C., Rathjen J.P.** (2010) Direct transcriptional control of the *Arabidopsis* immune receptor FLS2 by the ethylene-dependent transcription factors EIN3 and EIL1. *Proc Natl Acad Sci USA* 107: 14502-14507
- Brock A.K., Willmann R., Kolb D., Grefen L., Lajunen H.M., Bethke G., Lee J., Nurnberger T., Gust A.A.** (2010) The *Arabidopsis* mitogen-activated protein kinase phosphatase PP2C5 affects seed germination, stomatal aperture, and abscisic acid-inducible gene expression. *Plant Physiol* 153: 1098-1111
- Brutus A., Sicilia F., Macone A., Cervone F., De Lorenzo G.** (2010) A domain swap approach reveals a role of the plant wall-associated kinase 1 (WAK1) as a receptor of oligogalacturonides. *Proc Natl Acad Sci USA* 107: 9452-9457
- Cao Y., Liang Y., Tanaka K., Nguyen C.T., Jedrzejczak R.P., Joachimiak A., Stacey G.** (2014) The kinase LYK5 is a major chitin receptor in *Arabidopsis* and forms a chitin-induced complex with related kinase CERK1. *eLife* 3
- Castells E., Casacuberta J.M.** (2007) Signalling through kinase-defective domains: the prevalence of atypical receptor-like kinases in plants. *J Exp Bot* 58: 3503-3511
- Caunt C.J., Keyse S.M.** (2013) Dual-specificity MAP kinase phosphatases (MKPs): shaping the outcome of MAP kinase signalling. *FEBS J* 280: 489-504
- Cesari S., Bernoux M., Moncuquet P., Kroj T., Dodds P.N.** (2014) A novel conserved mechanism for plant NLR protein pairs: the "integrated decoy" hypothesis. *Front Plant Sci* 5: 606
- Chandra S., Low P.S.** (1995) Role of phosphorylation in elicitation of the oxidative burst in cultured soybean cells. *Proc Natl Acad Sci USA* 92: 4120-4123
- Chen X., Chern M., Canlas P.E., Ruan D., Jiang C., Ronald P.C.** (2010) An ATPase promotes autophosphorylation of the pattern recognition receptor XA21 and inhibits XA21-mediated immunity. *Proc Natl Acad Sci USA* 107: 8029-8034
- Chen X., Zuo S., Schwessinger B., Chern M., Canlas P.E., Ruan D., Zhou X., Wang J., Daudi A., Petzold C.J., Heazlewood J.L., Ronald P.C.** (2014) An XA21-associated kinase (OsSERK2) regulates immunity mediated by the XA21 and XA3 immune receptors. *Mol Plant* 7: 874-892
- Cheng Y., Zhou Y., Yang Y., Chi Y.J., Zhou J., Chen J.Y., Wang F., Fan B., Shi K., Zhou Y.H., Yu J.Q., Chen Z.** (2012) Structural and functional analysis of VQ motif-containing proteins in *Arabidopsis* as interacting proteins of WRKY transcription factors. *Plant Physiol* 159: 810-825

- Cheng Z.Y., Li J.F., Niu Y.J., Zhang X.C., Woody O.Z., Xiong Y., Djonovic S., Millet Y., Bush J., McConkey B.J., Sheen J., Ausubel F.M.** (2015) Pathogen-secreted proteases activate a novel plant immune pathway. *Nature* 521: 213+
- Chinchilla D., Bauer Z., Regenass M., Boller T., Felix G.** (2006) The *Arabidopsis* receptor kinase FLS2 binds flg22 and determines the specificity of flagellin perception. *Plant Cell* 18: 465-476
- Chinchilla D., Zipfel C., Robatzek S., Kemmerling B., Nurnberger T., Jones J.D., Felix G., Boller T.** (2007) A flagellin-induced complex of the receptor FLS2 and BAK1 initiates plant defence. *Nature* 448: 497-500
- Choi J., Huh S.U., Kojima M., Sakakibara H., Paek K.H., Hwang I.** (2010) The cytokinin-activated transcription factor ARR2 promotes plant immunity via TGA3/NPR1-dependent salicylic acid signaling in *Arabidopsis*. *Dev Cell* 19: 284-295
- Choi J., Tanaka K., Cao Y., Qi Y., Qiu J., Liang Y., Lee S.Y., Stacey G.** (2014) Identification of a plant receptor for extracellular ATP. *Science* 343: 290-294
- Chung E.H., da Cunha L., Wu A.J., Gao Z.Y., Cherkis K., Afzal A.J., Mackey D., Dangl J.L.** (2011) Specific Threonine Phosphorylation of a Host Target by Two Unrelated Type III Effectors Activates a Host Innate Immune Receptor in Plants. *Cell Host Microbe* 9: 125-136
- Coll R.C., O'Neill L.A.J.** (2010) New Insights into the Regulation of Signalling by Toll-Like Receptors and Nod-Like Receptors. *J Innate Immun* 2: 406-421
- Conner S.H., Kular G., Peggie M., Shepherd S., Schuttelkopf A.W., Cohen P., Van Aalten D.M.F.** (2006) TAK1-binding protein 1 is a pseudophosphatase. *Biochem J* 399: 427-434
- Couto D., Stransfeld L., Arruabarrena A., Zipfel C., Lozano-Duran R.** (2015) Broad application of a simple and affordable protocol for isolating plant RNA. *BMC Res Notes* 8: 154
- Cutler S.R., Ehrhardt D.W., Griffiths J.S., Somerville C.R.** (2000) Random GFP::cDNA fusions enable visualization of subcellular structures in cells of *Arabidopsis* at a high frequency. *Proc Natl Acad Sci USA* 97: 3718-3723
- Ding S.W.** (2010) RNA-based antiviral immunity. *Nature reviews Immunology* 10: 632-644
- Ding Z., Wang H., Liang X., Morris E.R., Gallazzi F., Pandit S., Skolnick J., Walker J.C., Van Doren S.R.** (2007) Phosphoprotein and phosphopeptide interactions with the FHA domain from *Arabidopsis* kinase-associated protein phosphatase. *Biochemistry* 46: 2684-2696
- Dodds P.N., Rathjen J.P.** (2010) Plant immunity: towards an integrated view of plant-pathogen interactions. *Nat Rev Gen* 11: 539-548
- Dubiella U., Seybold H., Durian G., Komander E., Lassig R., Witte C.P., Schulze W.X., Romeis T.** (2013) Calcium-dependent protein kinase/NADPH oxidase activation circuit is required for rapid defense signal propagation. *Proc Natl Acad Sci USA* 110: 8744-8749
- Edwards K., Johnstone C., Thompson C.** (1991) A simple and rapid method for the preparation of plant genomic DNA for PCR analysis. *Nucleic Acids Res* 19: 1349
- Fan M., Bai M.Y., Kim J.G., Wang T., Oh E., Chen L., Park C.H., Son S.H., Kim S.K., Mudgett M.B., Wang Z.Y.** (2014) The bHLH transcription factor HBI1 mediates the trade-off between growth and pathogen-associated molecular pattern-triggered immunity in *Arabidopsis*. *Plant Cell* 26: 828-841
- Felix G., Duran J.D., Volko S., Boller T.** (1999) Plants have a sensitive perception system for the most conserved domain of bacterial flagellin. *Plant J* 18: 265-276
- Felix G., Regenass M., Spanu P., Boller T.** (1994) The protein phosphatase inhibitor calyculin A mimics elicitor action in plant cells and induces rapid hyperphosphorylation of specific proteins as revealed by pulse labeling with [33P]phosphate. *Proc Natl Acad Sci USA* 91: 952-956
- Feng B., Liu C., de Oliveira M.V., Intorne A.C., Li B., Babilonia K., de Souza Filho G.A., Shan L., He P.** (2015) Protein poly(ADP-ribosyl)ation regulates *Arabidopsis* immune gene expression and defense responses. *PLoS Gen* 11: e1004936
- Feng F., Yang F., Rong W., Wu X., Zhang J., Chen S., He C., Zhou J.M.** (2012) A *Xanthomonas* uridine 5'-monophosphate transferase inhibits plant immune kinases. *Nature* 485: 114-118

- Ferrao R., Zhou H., Shan Y.B., Liu Q., Li Q.B., Shaw D.E., Li X.X., Wu H.** (2014) IRAK4 Dimerization and trans-Autophosphorylation Are Induced by Myddosome Assembly. *Mol Cell* 55: 891-903
- Flury P., Klauser D., Schulze B., Boller T., Bartels S.** (2013) The anticipation of danger: microbe-associated molecular pattern perception enhances AtPep-triggered oxidative burst. *Plant Physiol* 161: 2023-2035
- Frei dit Frey N., Garcia A.V., Bigeard J., Zaag R., Bueso E., Garmier M., Pateyron S., de Tauzia-Moreau M.L., Brunaud V., Balzergue S., Colcombet J., Aubourg S., Martin-Magniette M.L., Hirt H.** (2014) Functional analysis of *Arabidopsis* immune-related MAPKs uncovers a role for MPK3 as negative regulator of inducible defences. *Genome Biol* 15: R87
- Fuchs S., Grill E., Meskiene I., Schweighofer A.** (2013) Type 2C protein phosphatases in plants. *FEBS J* 280: 681-693
- Galletti R., Ferrari S., De Lorenzo G.** (2011) *Arabidopsis* MPK3 and MPK6 play different roles in basal and oligogalacturonide- or flagellin-induced resistance against *Botrytis cinerea*. *Plant Physiol* 157: 804-814
- Gao M., Liu J., Bi D., Zhang Z., Cheng F., Chen S., Zhang Y.** (2008) MEKK1, MKK1/MKK2 and MPK4 function together in a mitogen-activated protein kinase cascade to regulate innate immunity in plants. *Cell Res* 18: 1190-1198
- Gao M., Wang X., Wang D., Xu F., Ding X., Zhang Z., Bi D., Cheng Y.T., Chen S., Li X., Zhang Y.** (2009) Regulation of cell death and innate immunity by two receptor-like kinases in *Arabidopsis*. *Cell Host Microbe* 6: 34-44
- Gao X., Chen X., Lin W., Chen S., Lu D., Niu Y., Li L., Cheng C., McCormack M., Sheen J., Shan L., He P.** (2013) Bifurcation of *Arabidopsis* NLR immune signaling via Ca²⁺-dependent protein kinases. *PLoS Pathog* 9: e1003127
- Gay N.J., Symmons M.F., Gangloff M., Bryant C.E.** (2014) Assembly and localization of Toll-like receptor signalling complexes. *Nat Rev Immunol* 14: 546-558
- Geng X., Jin L., Shimada M., Kim M.G., Mackey D.** (2014) The phytotoxin coronatine is a multifunctional component of the virulence armament of *Pseudomonas syringae*. *Planta* 240: 1149-1165
- Gibson B.A., Kraus W.L.** (2012) New insights into the molecular and cellular functions of poly(ADP-ribose) and PARPs. *Nat Rev Mol Cell Biol* 13: 411-424
- Gimenez-Ibanez S., Boter M., Fernandez-Barbero G., Chini A., Rathjen J.P., Solano R.** (2014) The bacterial effector HopX1 targets JAZ transcriptional repressors to activate jasmonate signaling and promote infection in *Arabidopsis*. *PLoS Biol* 12: e1001792
- Gimenez-Ibanez S., Hann D.R., Ntoukakis V., Petutschnig E., Lipka V., Rathjen J.P.** (2009a) AvrPtoB targets the LysM receptor kinase CERK1 to promote bacterial virulence on plants. *Curr Biol* 19: 423-429
- Gimenez-Ibanez S., Ntoukakis V., Rathjen J.P.** (2009b) The LysM receptor kinase CERK1 mediates bacterial perception in *Arabidopsis*. *Plant Sign Behav* 4: 539-541
- Gohlke J., Deeken R.** (2014) Plant responses to *Agrobacterium tumefaciens* and crown gall development. *Front Plant Sci* 5: 155
- Gohre V., Spallek T., Haweker H., Mersmann S., Mentzel T., Boller T., de Torres M., Mansfield J.W., Robatzek S.** (2008) Plant pattern-recognition receptor FLS2 is directed for degradation by the bacterial ubiquitin ligase AvrPtoB. *Curr Biol* 18: 1824-1832
- Goldszmid R.S., Trinchieri G.** (2012) The price of immunity. *Nat Immunol* 13: 932-938
- Gomez-Gomez L., Bauer Z., Boller T.** (2001) Both the extracellular leucine-rich repeat domain and the kinase activity of FLS2 are required for flagellin binding and signaling in *Arabidopsis*. *Plant Cell* 13: 1155-1163
- Gravino M., Savatin D.V., Macone A., De Lorenzo G.** (2015) Ethylene production in *Botrytis cinerea*- and oligogalacturonide-induced immunity requires calcium-dependent protein kinases. *Plant J* doi:10.1111/tpj.13057

- Gust A.A., Felix G.** (2014) Receptor like proteins associate with SOBIR1-type of adaptors to form bimolecular receptor kinases. *Curr Opin Plant Biol* 21: 104-111
- Halter T., Imkampe J., Mazzotta S., Wierzba M., Postel S., Bucherl C., Kiefer C., Stahl M., Chinchilla D., Wang X., Nurnberger T., Zipfel C., Clouse S., Borst J.W., Boeren S., de Vries S.C., Tax F., Kemmerling B.** (2014) The leucine-rich repeat receptor kinase BIR2 is a negative regulator of BAK1 in plant immunity. *Curr Biol* 24: 134-143
- Hann D.R., Dominguez-Ferreras A., Motyka V., Dobrev P.I., Schornack S., Jehle A., Felix G., Chinchilla D., Rathjen J.P., Boller T.** (2014) The *Pseudomonas* type III effector HopQ1 activates cytokinin signaling and interferes with plant innate immunity. *New Phytol* 201: 585-598
- Hayafune M., Berisio R., Marchetti R., Silipo A., Kayama M., Desaki Y., Arima S., Squeglia F., Ruggiero A., Tokuyasu K., Molinaro A., Kaku H., Shibuya N.** (2014) Chitin-induced activation of immune signaling by the rice receptor CEBiP relies on a unique sandwich-type dimerization. *Proc Natl Acad Sci USA* 111: E404-413
- Heese A., Hann D.R., Gimenez-Ibanez S., Jones A.M.E., He K., Li J., Schroeder J.I., Peck S.C., Rathjen J.P.** (2007) The receptor-like kinase SERK3/BAK1 is a central regulator of innate immunity in plants. *Proc Natl Acad Sci USA* 104: 12217-12222
- Holton N., Nekrasov V., Ronald P.C., Zipfel C.** (2015) The phylogenetically-related pattern recognition receptors EFR and XA21 recruit similar immune signaling components in monocots and dicots. *PLoS Pathog* 11: e1004602
- Hubbard L.L., Moore B.B.** (2010) IRAK-M regulation and function in host defense and immune homeostasis. *Infect Dis Rep* 2
- Igarashi D., Tsuda K., Katagiri F.** (2012) The peptide growth factor, phytosulfokine, attenuates pattern-triggered immunity. *Plant J* 71: 194-204
- Iizasa E., Mitsutomi M., Nagano Y.** (2010) Direct binding of a plant LysM receptor-like kinase, LysM RLK1/CERK1, to chitin in vitro. *J Biol Chem* 285: 2996-3004
- Jaillais Y., Hothorn M., Belkhadir Y., Dabi T., Nimchuk Z.L., Meyerowitz E.M., Chory J.** (2011) Tyrosine phosphorylation controls brassinosteroid receptor activation by triggering membrane release of its kinase inhibitor. *Genes Dev* 25: 232-237
- Jiang S., Yao J., Ma K.W., Zhou H., Song J., He S.Y., Ma W.** (2013) Bacterial effector activates jasmonate signaling by directly targeting JAZ transcriptional repressors. *PLoS Pathog* 9: e1003715
- Jiménez-Góngora T., Kim S.-K., Lozano-Durán R., Zipfel C.** (2015) Flg22-triggered immunity negatively regulates key BR biosynthetic genes. *Front Plant Sci* 6
- Jones J.D., Dangl J.L.** (2006) The plant immune system. *Nature* 444: 323-329
- Kadota Y., Shirasu K., Zipfel C.** (2015) Regulation of the NADPH Oxidase RBOHD During Plant Immunity. *Plant Cell Physiol* 56: 1472-1480
- Kadota Y., Sklenar J., Derbyshire P., Stransfeld L., Asai S., Ntoukakis V., Jones J.D., Shirasu K., Menke F., Jones A., Zipfel C.** (2014) Direct regulation of the NADPH oxidase RBOHD by the PRR-associated kinase BIK1 during plant immunity. *Mol cell* 54: 43-55
- Kaku H., Nishizawa Y., Ishii-Minami N., Akimoto-Tomiyama C., Dohmae N., Takio K., Minami E., Shibuya N.** (2006) Plant cells recognize chitin fragments for defense signaling through a plasma membrane receptor. *Proc Natl Acad Sci USA* 103: 11086-11091
- Karimi M., De Meyer B., Hilson P.** (2005) Modular cloning in plant cells. *Trends Plant Sci* 10: 103-105
- Kawasaki T., Kawai T.** (2014) Toll-like receptor signaling pathways. *Front Immunol* 5: 461
- Kim T.W., Wang Z.Y.** (2010) Brassinosteroid signal transduction from receptor kinases to transcription factors. *Ann Rev Plant Biol* 61: 681-704
- Kobayashi K., Hernandez L.D., Galan J.E., Janeway C.A., Jr., Medzhitov R., Flavell R.A.** (2002) IRAK-M is a negative regulator of Toll-like receptor signaling. *Cell* 110: 191-202

- Kobayashi M., Ohura I., Kawakita K., Yokota N., Fujiwara M., Shimamoto K., Doke N., Yoshioka H.** (2007) Calcium-dependent protein kinases regulate the production of reactive oxygen species by potato NADPH oxidase. *Plant Cell* 19: 1065-1080
- Kondo T., Kawai T., Akira S.** (2012) Dissecting negative regulation of Toll-like receptor signaling. *Trends Immunol* 33: 449-458
- Kong Q., Qu N., Gao M., Zhang Z., Ding X., Yang F., Li Y., Dong O.X., Chen S., Li X., Zhang Y.** (2012) The MEKK1-MKK1/MKK2-MPK4 kinase cascade negatively regulates immunity mediated by a mitogen-activated protein kinase kinase kinase in *Arabidopsis*. *Plant Cell* 24: 2225-2236
- Korner C.J., Klauser D., Niehl A., Dominguez-Ferreras A., Chinchilla D., Boller T., Heinlein M., Hann D.R.** (2013) The immunity regulator BAK1 contributes to resistance against diverse RNA viruses. *Mol Plant Microbe Interact* 26: 1271-1280
- Krol E., Mentzel T., Chinchilla D., Boller T., Felix G., Kemmerling B., Postel S., Arents M., Jeworutzki E., Al-Rasheid K.A., Becker D., Hedrich R.** (2010) Perception of the *Arabidopsis* danger signal peptide 1 involves the pattern recognition receptor AtPEPR1 and its close homologue AtPEPR2. *J Biol Chem* 285: 13471-13479
- Laemmli U.K.** (1970) Cleavage of structural proteins during the assembly of the head of bacteriophage T4. *Nature* 227: 680-685
- Lai Z., Li Y., Wang F., Cheng Y., Fan B., Yu J.Q., Chen Z.** (2011) *Arabidopsis* sigma factor binding proteins are activators of the WRKY33 transcription factor in plant defense. *Plant Cell* 23: 3824-3841
- Laluk K., Luo H., Chai M., Dhawan R., Lai Z., Mengiste T.** (2011) Biochemical and genetic requirements for function of the immune response regulator BOTRYTIS-INDUCED KINASE1 in plant growth, ethylene signaling, and PAMP-triggered immunity in *Arabidopsis*. *Plant Cell* 23: 2831-2849
- Lee D., Bourdais G., Yu G., Robatzek S., Coaker G.** (2015) Phosphorylation of the Plant Immune Regulator RPM1-INTERACTING PROTEIN4 Enhances Plant Plasma Membrane H⁺-ATPase Activity and Inhibits Flagellin-Triggered Immune Responses in *Arabidopsis*. *Plant Cell* 27: 2042-2056
- Lee J.S., Ellis B.E.** (2007) *Arabidopsis* MAPK phosphatase 2 (MKP2) positively regulates oxidative stress tolerance and inactivates the MPK3 and MPK6 MAPKs. *J Biol Chem* 282: 25020-25029
- Lehti-Shiu M.D., Zou C., Hanada K., Shiu S.H.** (2009) Evolutionary history and stress regulation of plant receptor-like kinase/pelle genes. *Plant Physiol* 150: 12-26
- Li B., Jiang S., Yu X., Cheng C., Chen S., Cheng Y., Yuan J.S., Jiang D., He P., Shan L.** (2015) Phosphorylation of trihelix transcriptional repressor ASR3 by MAP KINASE4 negatively regulates *Arabidopsis* immunity. *Plant Cell* 27: 839-856
- Li F., Cheng C., Cui F., de Oliveira M.V., Yu X., Meng X., Intorne A.C., Babilonia K., Li M., Li B., Chen S., Ma X., Xiao S., Zheng Y., Fei Z., Metz R.P., Johnson C.D., Koiwa H., Sun W., Li Z., de Souza Filho G.A., Shan L., He P.** (2014a) Modulation of RNA polymerase II phosphorylation downstream of pathogen perception orchestrates plant immunity. *Cell Host Microbe* 16: 748-758
- Li L., Li M., Yu L., Zhou Z., Liang X., Liu Z., Cai G., Gao L., Zhang X., Wang Y., Chen S., Zhou J.M.** (2014b) The FLS2-associated kinase BIK1 directly phosphorylates the NADPH oxidase RbohD to control plant immunity. *Cell Host Microbe* 15: 329-338
- Li S.Y., Strelow A., Fontana E.J., Wesche H.** (2002) IRAK-4: A novel member of the IRAK family with the properties of an IRAK-kinase. *Proc Natl Acad Sci USA* 99: 5567-5572
- Li X.Y., Lin H.Q., Zhang W.G., Zou Y., Zhang J., Tang X.Y., Zhou J.M.** (2005) Flagellin induces innate immunity in nonhost interactions that is suppressed by *Pseudomonas syringae* effectors. *Proc Natl Acad Sci USA* 102: 12990-12995
- Liebrand T.W., van den Burg H.A., Joosten M.H.** (2014) Two for all: receptor-associated kinases SOBIR1 and BAK1. *Trends Plant Sci* 19: 123-132

- Lin W., Li B., Lu D., Chen S., Zhu N., He P., Shan L.** (2014) Tyrosine phosphorylation of protein kinase complex BAK1/BIK1 mediates *Arabidopsis* innate immunity. *Proc Natl Acad Sci USA* 111: 3632-3637
- Lin W., Lu D., Gao X., Jiang S., Ma X., Wang Z., Mengiste T., He P., Shan L.** (2013) Inverse modulation of plant immune and brassinosteroid signaling pathways by the receptor-like cytoplasmic kinase BIK1. *Proc Natl Acad Sci USA* 110: 12114-12119
- Lin Z.D., Liebrand T.W., Yadeta K.A., Coaker G.L.** (2015) PBL13 is a serine/threonine protein kinase that negatively regulates *Arabidopsis* immune responses. *Plant Physiol* 169: 2950-2962
- Liu B., Li J.F., Ao Y., Qu J., Li Z., Su J., Zhang Y., Liu J., Feng D., Qi K., He Y., Wang J., Wang H.B.** (2012a) Lysin motif-containing proteins LYP4 and LYP6 play dual roles in peptidoglycan and chitin perception in rice innate immunity. *Plant Cell* 24: 3406-3419
- Liu J., Elmore J.M., Lin Z.J.D., Coaker G.** (2011) A Receptor-like Cytoplasmic Kinase Phosphorylates the Host Target RIN4, Leading to the Activation of a Plant Innate Immune Receptor. *Cell Host Microbe* 9: 137-146
- Liu T., Liu Z., Song C., Hu Y., Han Z., She J., Fan F., Wang J., Jin C., Chang J., Zhou J.M., Chai J.** (2012b) Chitin-induced dimerization activates a plant immune receptor. *Science* 336: 1160-1164
- Liu Z., Wu Y., Yang F., Zhang Y., Chen S., Xie Q., Tian X., Zhou J.M.** (2013) BIK1 interacts with PEPRs to mediate ethylene-induced immunity. *Proc Natl Acad Sci USA* 110: 6205-6210
- Lozano-Duran R., Macho A.P., Boutrot F., Segonzac C., Somssich I.E., Zipfel C.** (2013) The transcriptional regulator BZR1 mediates trade-off between plant innate immunity and growth. *eLife* 2: e00983
- Lozano-Duran R., Zipfel C.** (2015) Trade-off between growth and immunity: role of brassinosteroids. *Trends Plant Sci* 20: 12-19
- Lu D., Lin W., Gao X., Wu S., Cheng C., Avila J., Heese A., Devarenne T.P., He P., Shan L.** (2011) Direct ubiquitination of pattern recognition receptor FLS2 attenuates plant innate immunity. *Science* 332: 1439-1442
- Lu D., Wu S., Gao X., Zhang Y., Shan L., He P.** (2010) A receptor-like cytoplasmic kinase, BIK1, associates with a flagellin receptor complex to initiate plant innate immunity. *Proc Natl Acad Sci USA* 107: 496-501
- Lumbreras V., Vilela B., Irar S., Sole M., Capellades M., Valls M., Coca M., Pages M.** (2010) MAPK phosphatase MKP2 mediates disease responses in *Arabidopsis* and functionally interacts with MPK3 and MPK6. *Plant J* 63: 1017-1030
- Macho A.P., Boutrot F., Rathjen J.P., Zipfel C.** (2012) Aspartate oxidase plays an important role in *Arabidopsis* stomatal immunity. *Plant Physiol* 159: 1845-1856
- Macho A.P., Lozano-Duran R., Zipfel C.** (2015) Importance of tyrosine phosphorylation in receptor kinase complexes. *Trends Plant Sci*
- Macho A.P., Schwessinger B., Ntoukakis V., Brutus A., Segonzac C., Roy S., Kadota Y., Oh M.H., Sklenar J., Derbyshire P., Lozano-Duran R., Malinovskiy F.G., Monaghan J., Menke F.L., Huber S.C., He S.Y., Zipfel C.** (2014) A bacterial tyrosine phosphatase inhibits plant pattern recognition receptor activation. *Science* 343: 1509-1512
- Macho A.P., Zipfel C.** (2014) Plant PRRs and the activation of innate immune signaling. *Mol cell* 54: 263-272
- Macho A.P., Zipfel C.** (2015) Targeting of plant pattern recognition receptor-triggered immunity by bacterial type-III secretion system effectors. *Curr Opin Microbiol* 23: 14-22
- Mackey D., Belkhadir Y., Alonso J.M., Ecker J.R., Dangl J.L.** (2003) *Arabidopsis* RIN4 is a target of the type III virulence effector AvrRpt2 and modulates RPS2-mediated resistance. *Cell* 112: 379-389
- Mackey D., Holt B.F., 3rd, Wiig A., Dangl J.L.** (2002) RIN4 interacts with *Pseudomonas syringae* type III effector molecules and is required for RPM1-mediated resistance in *Arabidopsis*. *Cell* 108: 743-754

- Maekawa T., Kufer T.A., Schulze-Lefert P.** (2011) NLR functions in plant and animal immune systems: so far and yet so close. *Nat Immunol* 12: 817-826
- Malinovsky F.G., Batoux M., Schwessinger B., Youn J.H., Stransfeld L., Win J., Kim S.K., Zipfel C.** (2014) Antagonistic Regulation of Growth and Immunity by the *Arabidopsis* Basic Helix-Loop-Helix Transcription Factor HOMOLOG OF BRASSINOSTEROID ENHANCED EXPRESSION2 INTERACTING WITH INCREASED LEAF INCLINATION1 BINDING bHLH1. *Plant Physiol* 164: 1443-1455
- Mao G., Meng X., Liu Y., Zheng Z., Chen Z., Zhang S.** (2011) Phosphorylation of a WRKY transcription factor by two pathogen-responsive MAPKs drives phytoalexin biosynthesis in *Arabidopsis*. *Plant Cell* 23: 1639-1653
- Medzhitov R.** (2001) Toll-like receptors and innate immunity. *Nat Rev Immunol* 1: 135-145
- Melotto M., Underwood W., He S.Y.** (2008) Role of stomata in plant innate immunity and foliar bacterial diseases. *Annual Rev Phytopathol* 46: 101-122
- Meng X., Zhang S.** (2013) MAPK cascades in plant disease resistance signaling. *Ann Rev Phytopathol* 51: 245-266
- Mersmann S., Bourdais G., Rietz S., Robatzek S.** (2010) Ethylene signaling regulates accumulation of the FLS2 receptor and is required for the oxidative burst contributing to plant immunity. *Plant Physiol* 154: 391-400
- Meszáros T., Helfer A., Hatzimasoura E., Magyar Z., Serazetdinova L., Rios G., Bardoczky V., Teige M., Koncz C., Peck S., Bogre L.** (2006) The *Arabidopsis* MAP kinase kinase MKK1 participates in defence responses to the bacterial elicitor flagellin. *Plant J* 48: 485-498
- Mishina T.E., Zeier J.** (2007) Pathogen-associated molecular pattern recognition rather than development of tissue necrosis contributes to bacterial induction of systemic acquired resistance in *Arabidopsis*. *Plant J* 50: 500-513
- Miya A., Albert P., Shinya T., Desaki Y., Ichimura K., Shirasu K., Narusaka Y., Kawakami N., Kaku H., Shibuya N.** (2007) CERK1, a LysM receptor kinase, is essential for chitin elicitor signaling in *Arabidopsis*. *Proc Natl Acad Sci USA* 104: 19613-19618
- Monaghan J., Matschi S., Romeis T., Zipfel C.** (2015) The calcium-dependent protein kinase CPK28 negatively regulates the BIK1-mediated PAMP-induced calcium burst. *Plant Sign Behav* 10: e1018497
- Monaghan J., Matschi S., Shorinola O., Rovenich H., Matei A., Segonzac C., Malinovsky F.G., Rathjen J.P., MacLean D., Romeis T., Zipfel C.** (2014) The calcium-dependent protein kinase CPK28 buffers plant immunity and regulates BIK1 turnover. *Cell Host Microbe* 16: 605-615
- Mosher S., Seybold H., Rodriguez P., Stahl M., Davies K.A., Dayaratne S., Morillo S.A., Wierzbka M., Favery B., Keller H., Tax F.E., Kemmerling B.** (2013) The tyrosine-sulfated peptide receptors PSKR1 and PSY1R modify the immunity of *Arabidopsis* to biotrophic and necrotrophic pathogens in an antagonistic manner. *Plant J* 73: 469-482
- Moynagh P.N.** (2014) The roles of Pellino E3 ubiquitin ligases in immunity. *Nat Rev Immunol* 14: 122-131
- Murray P.J.** (2005) The primary mechanism of the IL-10-regulated anti inflammatory response is to selectively inhibit transcription. *Proc Natl Acad Sci USA* 102: 8686-8691
- Murray P.J., Smale S.T.** (2012) Restraint of inflammatory signaling by interdependent strata of negative regulatory pathways. *Nat Immunol* 13: 916-924
- Nakagawa T., Suzuki T., Murata S., Nakamura S., Hino T., Maeo K., Tabata R., Kawai T., Tanaka K., Niwa Y., Watanabe Y., Nakamura K., Kimura T., Ishiguro S.** (2007) Improved gateway binary vectors: High-performance vectors for creation of fusion constructs in Transgenic analysis of plants. *Biosci Biotech Bioch* 71: 2095-2100
- Naseem M., Wolfling M., Dandekar T.** (2014) Cytokinins for immunity beyond growth, galls and green islands. *Trends Plant Sci* 19: 481-484

- Navarro L., Dunoyer P., Jay F., Arnold B., Dharmasiri N., Estelle M., Voinnet O., Jones J.D. (2006) A plant miRNA contributes to antibacterial resistance by repressing auxin signaling. *Science* 312: 436-439
- Nekrasov V., Li J., Batoux M., Roux M., Chu Z.H., Lacombe S., Rougon A., Bittel P., Kiss-Papp M., Chinchilla D., van Esse H.P., Jorda L., Schwessinger B., Nicaise V., Thomma B.P., Molina A., Jones J.D., Zipfel C. (2009) Control of the pattern-recognition receptor EFR by an ER protein complex in plant immunity. *EMBO J* 28: 3428-3438
- Nemeth K., Salchert K., Putnoky P., Bhalerao R., Koncz-Kalman Z., Stankovic-Stangeland B., Bako L., Mathur J., Okresz L., Stabel S., Geigenberger P., Stitt M., Redei G.P., Schell J., Koncz C. (1998) Pleiotropic control of glucose and hormone responses by PRL1, a nuclear WD protein, in *Arabidopsis*. *Genes Dev* 12: 3059-3073
- Ntoukakis V., Schwessinger B., Segonzac C., Zipfel C. (2011) Cautionary notes on the use of C-terminal BAK1 fusion proteins for functional studies. *Plant Cell* 23: 3871-3878
- O'Neill L.A., Bowie A.G. (2007) The family of five: TIR-domain-containing adaptors in Toll-like receptor signalling. *Nat Rev Immunol* 7: 353-364
- Oda T., Hashimoto H., Kuwabara N., Akashi S., Hayashi K., Kojima C., Wong H.L., Kawasaki T., Shimamoto K., Sato M., Shimizu T. (2010) Structure of the N-terminal regulatory domain of a plant NADPH oxidase and its functional implications. *J Biol Chem* 285: 1435-1445
- Ogasawara Y., Kaya H., Hiraoka G., Yumoto F., Kimura S., Kadota Y., Hishinuma H., Senzaki E., Yamagoe S., Nagata K., Nara M., Suzuki K., Tanokura M., Kuchitsu K. (2008) Synergistic activation of the *Arabidopsis* NADPH oxidase AtRbohD by Ca^{2+} and phosphorylation. *J Biol Chem* 283: 8885-8892
- Park C.J., Caddell D.F., Ronald P.C. (2012) Protein phosphorylation in plant immunity: insights into the regulation of pattern recognition receptor-mediated signaling. *Front Plant Sci* 3: 177
- Park C.J., Peng Y., Chen X., Dardick C., Ruan D., Bart R., Canlas P.E., Ronald P.C. (2008) Rice XB15, a protein phosphatase 2C, negatively regulates cell death and XA21-mediated innate immunity. *PLoS Biol* 6: e231
- Pecher P., Eschen-Lippold L., Herklotz S., Kuhle K., Naumann K., Bethke G., Uhrig J., Weyhe M., Scheel D., Lee J. (2014) The *Arabidopsis thaliana* mitogen-activated protein kinases MPK3 and MPK6 target a subclass of 'VQ-motif'-containing proteins to regulate immune responses. *New Phytol* 203: 592-606
- Peck S.C. (2006) Analysis of protein phosphorylation: methods and strategies for studying kinases and substrates. *Plant J* 45: 512-522
- Petersen M., Brodersen P., Naested H., Andreasson E., Lindhart U., Johansen B., Nielsen H.B., Lacy M., Austin M.J., Parker J.E., Sharma S.B., Klessig D.F., Martienssen R., Mattsson O., Jensen A.B., Mundy J. (2000) *Arabidopsis* MAP kinase 4 negatively regulates systemic acquired resistance. *Cell* 103: 1111-1120
- Petutschnig E.K., Jones A.M., Serazetdinova L., Lipka U., Lipka V. (2010) The lysin motif receptor-like kinase (LysM-RLK) CERK1 is a major chitin-binding protein in *Arabidopsis thaliana* and subject to chitin-induced phosphorylation. *J Biol Chem* 285: 28902-28911
- Pieterse C.M., Van der Does D., Zamioudis C., Leon-Reyes A., Van Wees S.C. (2012) Hormonal modulation of plant immunity. *Annu Rev Cell Dev Biol* 28: 489-521
- Postma J., Liebrand T.W.H., Bi G., Evrard A., Bye R.R., Mbengue M., Joosten M.H.A.J., Robatzek S. (2015) The Cf-4 receptor-like protein associates with the BAK1 receptor-like kinase to initiate receptor endocytosis and plant immunity. *bioRxiv*
- Promega (2009) Serine/Threonine Phosphatase Assay System Technical Bulletin. TB218
- Pruitt R.N., Schwessinger B., Joe A., Thomas N., Liu F., Albert M., Robinson M.R., Chan L.J.G., Luu D.D., Chen H., Bahar O., Daudi A., De Vleeschauwer D., Caddell D., Zhang W., Zhao X., Li X., Heazlewood J.L., Ruan D., Majumder D., Chern M., Kalbacher H., Midha S., Patil P.B., Sonti R.V., Petzold C.J., Liu C.C., Brodbelt J.S., Felix G., Ronald P.C. (2015) The rice immune

receptor XA21 recognizes a tyrosine-sulfated protein from a Gram-negative bacterium. *Science Advances* 1: e1500245

- Qiu J.L., Fiiil B.K., Petersen K., Nielsen H.B., Botanga C.J., Thorgrimsen S., Palma K., Suarez-Rodriguez M.C., Sandbech-Clausen S., Lichota J., Brodersen P., Grasser K.D., Mattsson O., Glazebrook J., Mundy J., Petersen M.** (2008) *Arabidopsis* MAP kinase 4 regulates gene expression through transcription factor release in the nucleus. *EMBO J* 27: 2214-2221
- Ranf S., Eschen-Lippold L., Frohlich K., Westphal L., Scheel D., Lee J.** (2014) Microbe-associated molecular pattern-induced calcium signaling requires the receptor-like cytoplasmic kinases, PBL1 and BIK1. *BMC Plant Biol* 14: 374
- Ranf S., Gisch N., Schaffer M., Illig T., Westphal L., Knirel Y.A., Sanchez-Carballo P.M., Zahringer U., Huckelhoven R., Lee J., Scheel D.** (2015) A lectin S-domain receptor kinase mediates lipopolysaccharide sensing in *Arabidopsis thaliana*. *Nat Immunol* 16: 426-433
- Rasmussen M.W., Roux M., Petersen M., Mundy J.** (2012) MAP Kinase Cascades in *Arabidopsis* Innate Immunity. *Front Plant Sci* 3: 169
- Robert-Seilaniantz A., Grant M., Jones J.D.** (2011a) Hormone crosstalk in plant disease and defense: more than just jasmonate-salicylate antagonism. *Annu Rev Phytopathol* 49: 317-343
- Robert-Seilaniantz A., MacLean D., Jikumaru Y., Hill L., Yamaguchi S., Kamiya Y., Jones J.D.** (2011b) The microRNA miR393 re-directs secondary metabolite biosynthesis away from camalexin and towards glucosinolates. *Plant J* 67: 218-231
- Ronald P.C., Beutler B.** (2010) Plant and animal sensors of conserved microbial signatures. *Science* 330: 1061-1064
- Roux M., Schwessinger B., Albrecht C., Chinchilla D., Jones A., Holton N., Malinovsky F.G., Tor M., de Vries S., Zipfel C.** (2011) The *Arabidopsis* leucine-rich repeat receptor-like kinases BAK1/SERK3 and BKK1/SERK4 are required for innate immunity to hemibiotrophic and biotrophic pathogens. *Plant Cell* 23: 2440-2455
- Roux M.E., Rasmussen M.W., Palma K., Lolle S., Regue A.M., Bethke G., Glazebrook J., Zhang W., Sieburth L., Larsen M.R., Mundy J., Petersen M.** (2015) The mRNA decay factor PAT1 functions in a pathway including MAP kinase 4 and immune receptor SUMM2. *EMBO J* 34: 593-608
- Santiago J., Henzler C., Hothorn M.** (2013) Molecular mechanism for plant steroid receptor activation by somatic embryogenesis co-receptor kinases. *Science* 341: 889-892
- Schulze B., Mentzel T., Jehle A.K., Mueller K., Beeler S., Boller T., Felix G., Chinchilla D.** (2010) Rapid heteromerization and phosphorylation of ligand-activated plant transmembrane receptors and their associated kinase BAK1. *J Biol Chem* 285: 9444-9451
- Schweighofer A., Kazanaviciute V., Scheikl E., Teige M., Doczi R., Hirt H., Schwanninger M., Kant M., Schuurink R., Mauch F., Buchala A., Cardinale F., Meskiene I.** (2007) The PP2C-type phosphatase AP2C1, which negatively regulates MPK4 and MPK6, modulates innate immunity, jasmonic acid, and ethylene levels in *Arabidopsis*. *Plant Cell* 19: 2213-2224
- Schwessinger B., Roux M., Kadota Y., Ntoukakis V., Sklenar J., Jones A., Zipfel C.** (2011) Phosphorylation-dependent differential regulation of plant growth, cell death, and innate immunity by the regulatory receptor-like kinase BAK1. *PLoS Gen* 7: e1002046
- Segonzac C., Macho A.P., Sanmartin M., Ntoukakis V., Sanchez-Serrano J.J., Zipfel C.** (2014) Negative control of BAK1 by protein phosphatase 2A during plant innate immunity. *EMBO J* 33: 2069-2079
- Shan L., He P., Li J., Heese A., Peck S.C., Nurnberger T., Martin G.B., Sheen J.** (2008) Bacterial effectors target the common signaling partner BAK1 to disrupt multiple MAMP receptor-signaling complexes and impede plant immunity. *Cell Host Microbe* 4: 17-27
- Shao F., Golstein C., Ade J., Stoutemyer M., Dixon J.E., Innes R.W.** (2003) Cleavage of i PBS1 by a bacterial type III effector. *Science* 301: 1230-1233
- Shaw A.S., Kornev A.P., Hu J., Ahuja L.G., Taylor S.S.** (2014) Kinases and pseudokinases: lessons from RAF. *Mol Cell Biol* 34: 1538-1546

- Shi H., Shen Q., Qi Y., Yan H., Nie H., Chen Y., Zhao T., Katagiri F., Tang D.** (2013) BR-SIGNALING KINASE1 physically associates with FLAGELLIN SENSING2 and regulates plant innate immunity in *Arabidopsis*. *Plant Cell* 25: 1143-1157
- Shimizu T., Nakano T., Takamizawa D., Desaki Y., Ishii-Minami N., Nishizawa Y., Minami E., Okada K., Yamane H., Kaku H., Shibuya N.** (2010) Two LysM receptor molecules, CEBiP and OsCERK1, cooperatively regulate chitin elicitor signaling in rice. *Plant J* 64: 204-214
- Shinya T., Yamaguchi K., Desaki Y., Yamada K., Narisawa T., Kobayashi Y., Maeda K., Suzuki M., Tanimoto T., Takeda J., Nakashima M., Funama R., Narusaka M., Narusaka Y., Kaku H., Kawasaki T., Shibuya N.** (2014) Selective regulation of the chitin-induced defense response by the *Arabidopsis* receptor-like cytoplasmic kinase PBL27. *Plant J* 79: 56-66
- Shiu S.H., Bleecker A.B.** (2001) Receptor-like kinases from *Arabidopsis* form a monophyletic gene family related to animal receptor kinases. *Proc Natl Acad Sci USA* 98: 10763-10768
- Smith J.M., Leslie M.E., Robinson S.J., Korasick D.A., Zhang T., Backues S.K., Cornish P.V., Koo A.J., Bednarek S.Y., Heese A.** (2014) Loss of *Arabidopsis thaliana* Dynamin-Related Protein 2B reveals separation of innate immune signaling pathways. *PLoS Pathog* 10: e1004578
- Soellick T.R., Uhrig J.F.** (2001) Development of an optimized interaction-mating protocol for large-scale yeast two-hybrid analyses. *Genome Biol* 2: research0052
- Somssich M., Ma Q., Weidtkamp-Peters S., Stahl Y., Felekyan S., Bleckmann A., Seidel C.A., Simon R.** (2015) Real-time dynamics of peptide ligand-dependent receptor complex formation in planta. *Sci Signal* 8: ra76
- Song J., Keppler B.D., Wise R.R., Bent A.F.** (2015) PARP2 Is the Predominant Poly(ADP-Ribose) Polymerase in *Arabidopsis* DNA Damage and Immune Responses. *PLoS Gen* 11: e1005200
- Spartz A.K., Ren H., Park M.Y., Grandt K.N., Lee S.H., Murphy A.S., Sussman M.R., Overvoorde P.J., Gray W.M.** (2014) SAUR Inhibition of PP2C-D Phosphatases Activates Plasma Membrane H⁺-ATPases to Promote Cell Expansion in *Arabidopsis*. *Plant Cell* 26: 2129-2142
- Sreekanta S., Bethke G., Hatsugai N., Tsuda K., Thao A., Wang L., Katagiri F., Glazebrook J.** (2015) The receptor-like cytoplasmic kinase PCRK1 contributes to pattern-triggered immunity against *Pseudomonas syringae* in *Arabidopsis thaliana*. *New Phytol* 207: 78-90
- Stegmann M., Anderson R.G., Ichimura K., Pecenkova T., Reuter P., Zarsky V., McDowell J.M., Shirasu K., Trujillo M.** (2012) The ubiquitin ligase PUB22 targets a subunit of the exocyst complex required for PAMP-triggered responses in *Arabidopsis*. *Plant Cell* 24: 4703-4716
- Suarez-Rodriguez M.C., Adams-Phillips L., Liu Y., Wang H., Su S.H., Jester P.J., Zhang S., Bent A.F., Krysan P.J.** (2007) MEKK1 is required for flg22-induced MPK4 activation in *Arabidopsis* plants. *Plant Physiol* 143: 661-669
- Sun W., Cao Y., Jansen Labby K., Bittel P., Boller T., Bent A.F.** (2012) Probing the *Arabidopsis* flagellin receptor: FLS2-FLS2 association and the contributions of specific domains to signaling function. *Plant Cell* 24: 1096-1113
- Sun Y., Han Z., Tang J., Hu Z., Chai C., Zhou B., Chai J.** (2013a) Structure reveals that BAK1 as a co-receptor recognizes the BRI1-bound brassinolide. *Cell Res* 23: 1326-1329
- Sun Y., Li L., Macho A.P., Han Z., Hu Z., Zipfel C., Zhou J.M., Chai J.** (2013b) Structural basis for flg22-induced activation of the *Arabidopsis* FLS2-BAK1 immune complex. *Science* 342: 624-628
- Tang J., Han Z., Sun Y., Zhang H., Gong X., Chai J.** (2015) Structural basis for recognition of an endogenous peptide by the plant receptor kinase PEPR1. *Cell Res* 25: 110-120
- Tateda C., Zhang Z., Shrestha J., Jelenska J., Chinchilla D., Greenberg J.T.** (2014) Salicylic acid regulates *Arabidopsis* microbial pattern receptor kinase levels and signaling. *Plant Cell* 26: 4171-4187
- Tintor N., Ross A., Kanehara K., Yamada K., Fan L., Kemmerling B., Nurnberger T., Tsuda K., Saijo Y.** (2013) Layered pattern receptor signaling via ethylene and endogenous elicitor peptides during *Arabidopsis* immunity to bacterial infection. *Proc Natl Acad Sci USA* 110: 6211-6216
- Tovar-Mendez A., Miernyk J.A., Hoyos E., Randall D.D.** (2014) A functional genomic analysis of *Arabidopsis thaliana* PP2C clade D. *Protoplasma* 251: 265-271

- Trujillo M., Ichimura K., Casais C., Shirasu K. (2008) Negative regulation of PAMP-triggered immunity by an E3 ubiquitin ligase triplet in *Arabidopsis*. *Curr Biol* 18: 1396-1401
- Tsuda K., Somssich I.E. (2015) Transcriptional networks in plant immunity. *New Phytol* 206: 932-947
- van der Hoorn R.A., Kamoun S. (2008) From Guard to Decoy: a new model for perception of plant pathogen effectors. *Plant Cell* 20: 2009-2017
- Wan J., Tanaka K., Zhang X.C., Son G.H., Brechenmacher L., Nguyen T.H., Stacey G. (2012) LYK4, a lysin motif receptor-like kinase, is important for chitin signaling and plant innate immunity in *Arabidopsis*. *Plant Physiol* 160: 396-406
- Wan J., Zhang X.C., Neece D., Ramonell K.M., Clough S., Kim S.Y., Stacey M.G., Stacey G. (2008) A LysM receptor-like kinase plays a critical role in chitin signaling and fungal resistance in *Arabidopsis*. *The Plant cell* 20: 471-481
- Wang G., Roux B., Feng F., Guy E., Li L., Li N., Zhang X., Lautier M., Jardinaud M.F., Chabannes M., Arlat M., Chen S., He C., Noel L.D., Zhou J.M. (2015a) The Decoy Substrate of a Pathogen Effector and a Pseudokinase Specify Pathogen-Induced Modified-Self Recognition and Immunity in Plants. *Cell Host Microbe* 18: 285-295
- Wang, H., Yang, C., Zhang, C., Wang, N., Lu, D., Wang, J., Shanshan Zhang¹, Wang, Z.X., Ma, H., Wang, X. (2011) Dual role of BKI1 and 14-3-3 s in brassinosteroid signaling to link receptor with transcription factors. *Dev Cell* 21, 825–834
- Wang J., Jiang J.J., Wang J., Chen L., Fan S.L., Wu J.W., Wang X.L., Wang Z.X. (2014) Structural insights into the negative regulation of BRI1 signaling by BRI1-interacting protein BKI1. *Cell Res* 24: 1328-1341
- Wang J., Li H., Han Z., Zhang H., Wang T., Lin G., Chang J., Yang W., Chai J. (2015b) Allosteric receptor activation by the plant peptide hormone phytosulfokine. *Nature* 525: 265-268
- Wang W.F., Wang Z.Y. (2014) At the Intersection of Plant Growth and Immunity. *Cell Host Microbe* 15: 401-403
- Wang X.L., Chory J. (2006) Brassinosteroids regulate dissociation of BKI1, a negative regulator of BRI1 signaling, from the plasma membrane. *Science* 313: 1118-1122
- Weyhe M., Eschen-Lippold L., Pecher P., Scheel D., Lee J. (2014) Ménage à trois. *Plant Sign Behav* 9: e29519
- Willmann R., Lajunen H.M., Erbs G., Newman M.A., Kolb D., Tsuda K., Katagiri F., Fliegmann J., Bono J.J., Cullimore J.V., Jehle A.K., Gotz F., Kulik A., Molinaro A., Lipka V., Gust A.A., Nurnberger T. (2011) *Arabidopsis* lysin-motif proteins LYM1 LYM3 CERK1 mediate bacterial peptidoglycan sensing and immunity to bacterial infection. *Proc Natl Acad Sci USA* 108: 19824-19829
- Wilton M., Subramaniam R., Elmore J., Felsensteiner C., Coker G., Desveaux D. (2010) The type III effector HopF2(Pto) targets *Arabidopsis* RIN4 protein to promote *Pseudomonas syringae* virulence. *Proc Natl Acad Sci USA* 107: 2349-2354
- Wong H.L., Pinontoan R., Hayashi K., Tabata R., Yaeno T., Hasegawa K., Kojima C., Yoshioka H., Iba K., Kawasaki T., Shimamoto K. (2007) Regulation of rice NADPH oxidase by binding of Rac GTPase to its N-terminal extension. *Plant Cell* 19: 4022-4034
- Wu C.-H., Krasileva K.V., Banfield M.J., Terauchi R., Kamoun S. (2015) The “sensor domains” of plant NLR proteins: more than decoys? *Fronts Plant Sci* 6
- Xiang T., Zong N., Zou Y., Wu Y., Zhang J., Xing W., Li Y., Tang X., Zhu L., Chai J., Zhou J.M. (2008) *Pseudomonas syringae* effector AvrPto blocks innate immunity by targeting receptor kinases. *Curr Biol* 18: 74-80
- Xu J., Wei X., Yan L., Liu D., Ma Y., Guo Y., Peng C., Zhou H., Yang C., Lou Z., Shui W. (2013) Identification and functional analysis of phosphorylation residues of the *Arabidopsis* BOTRYTIS-INDUCED KINASE1. *Protein Cell* 4: 771-781
- Xue T., Wang D., Zhang S., Ehltng J., Ni F., Jakab S., Zheng C., Zhong Y. (2008) Genome-wide and expression analysis of protein phosphatase 2C in rice and *Arabidopsis*. *BMC Genomics* 9: 550

- Yamaguchi K., Yamada K., Ishikawa K., Yoshimura S., Hayashi N., Uchihashi K., Ishihama N., Kishi-Kaboshi M., Takahashi A., Tsuge S., Ochiai H., Tada Y., Shimamoto K., Yoshioka H., Kawasaki T.** (2013) A receptor-like cytoplasmic kinase targeted by a plant pathogen effector is directly phosphorylated by the chitin receptor and mediates rice immunity. *Cell Host Microbe* 13: 347-357
- Yamaguchi Y., Huffaker A., Bryan A.C., Tax F.E., Ryan C.A.** (2010) PEPR2 is a second receptor for the Pep1 and Pep2 peptides and contributes to defense responses in *Arabidopsis*. *Plant Cell* 22: 508-522
- Yamaguchi Y., Pearce G., Ryan C.A.** (2006) The cell surface leucine-rich repeat receptor for AtPep1, an endogenous peptide elicitor in *Arabidopsis*, is functional in transgenic tobacco cells. *Proc Natl Acad Sci USA* 103: 10104-10109
- Yi S.Y., Shirasu K., Moon J.S., Lee S.G., Kwon S.Y.** (2014) The activated SA and JA signaling pathways have an influence on flg22-triggered oxidative burst and callose deposition. *PLoS One* 9: e88951
- Yuan J., He S.Y.** (1996) The *Pseudomonas syringae* Hrp regulation and secretion system controls the production and secretion of multiple extracellular proteins. *J Bacteriol* 178: 6399-6402
- Zeqiraj E., van Aalten D.M.F.** (2010) Pseudokinases-remnants of evolution or key allosteric regulators? *Curr Opin Struct Biol* 20: 772-781
- Zhang J., Li W., Xiang T., Liu Z., Laluk K., Ding X., Zou Y., Gao M., Zhang X., Chen S., Mengiste T., Zhang Y., Zhou J.M.** (2010) Receptor-like cytoplasmic kinases integrate signaling from multiple plant immune receptors and are targeted by a *Pseudomonas syringae* effector. *Cell Host Microbe* 7: 290-301
- Zhang J., Shao F., Li Y., Cui H., Chen L., Li H., Zou Y., Long C., Lan L., Chai J., Chen S., Tang X., Zhou J.M.** (2007) A *Pseudomonas syringae* effector inactivates MAPKs to suppress PAMP-induced immunity in plants. *Cell Host Microbe* 1: 175-185
- Zhang W., Fraiture M., Kolb D., Loeffelhardt B., Desaki Y., Boutrot F.F., Tor M., Zipfel C., Gust A.A., Brunner F.** (2013) *Arabidopsis* receptor-like protein30 and receptor-like kinase suppressor of BIR1-1/EVERSHED mediate innate immunity to necrotrophic fungi. *Plant Cell* 25: 4227-4241
- Zhang Z., Wu Y., Gao M., Zhang J., Kong Q., Liu Y., Ba H., Zhou J., Zhang Y.** (2012) Disruption of PAMP-induced MAP kinase cascade by a *Pseudomonas syringae* effector activates plant immunity mediated by the NB-LRR protein SUMM2. *Cell Host Microbe* 11: 253-263
- Zhou Z., Wu Y., Yang Y., Du M., Zhang X., Guo Y., Li C., Zhou J.M.** (2015) An *Arabidopsis* Plasma Membrane Proton ATPase Modulates JA Signaling and Is Exploited by the *Pseudomonas syringae* Effector Protein AvrB for Stomatal Invasion. *Plant Cell* 27: 2032-2041
- Zipfel C.** (2014) Plant pattern-recognition receptors. *Trends in immunology* 35: 345-351
- Zipfel C., Kunze G., Chinchilla D., Caniard A., Jones J.D., Boller T., Felix G.** (2006) Perception of the bacterial PAMP EF-Tu by the receptor EFR restricts *Agrobacterium*-mediated transformation. *Cell* 125: 749-760
- Zorzatto C., Machado J.P., Lopes K.V., Nascimento K.J., Pereira W.A., Brustolini O.J., Reis P.A., Calil I.P., Deguchi M., Sachetto-Martins G., Gouveia B.C., Loriato V.A., Silva M.A., Silva F.F., Santos A.A., Chory J., Fontes E.P.** (2015) NIK1-mediated translation suppression functions as a plant antiviral immunity mechanism. *Nature* 520: 679-682